

\OPTIMIZATION OF CAPILLARY GC-FTIR

FOR


COMPLEX SAMPLE ANALYSIS


by

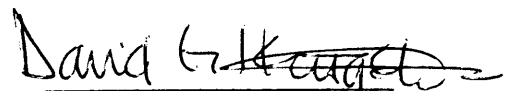
John Richard Cooper

Thesis submitted to the Graduate Faculty of the  
Virginia Polytechnic Institute and State University  
in partial fulfillment of the requirements for the degree of  
MASTER OF SCIENCE  
in  
Chemistry

APPROVED:

  
Larry T. Taylor, Chairman

  
T. C. Ward

  
D. G.I. Kingston

September, 1982

Blacksburg, Virginia

## ACKNOWLEDGEMENTS

The author would like to take this opportunity to thank the many people who have helped in my research and academic efforts. Special thanks goes to Dr. L. T. Taylor for his unending patience and support through the course of the past two years. I would also like to thank T. C. Ward and D. G. Kingston for proofreading of this manuscript and for helpful comments. Many thanks to R. S. Brown for his often extensive technical help concerning the operation and understanding of the FTIR instrumentation. In addition, each member of the immediate research group should be commended for their patience in regards to the sometimes hectic scheduling which was needed to pursue this project. Personal thanks also go to D. Perdue for the excellent typing provided.

The author gratefully acknowledges the financial support offered and the aviation fuel samples provided by Major D. D. Potter of the United States Air Force.

Thanks should also go to the Accuspec Corporation for the donation of chromatography and infrared accessories, and to S. Lowry and the Nicolet Instrument Corporation for the opportunity to use their state-of-the-art GC/FTIR instrumentation. Additional acknowledgements go to H. C. Dorn et al. for NMR data concerning the jet fuel samples and to the Biochemistry Department, VPI for use of the mass spectrometer facilities.

## TABLE OF CONTENTS

	<u>Page</u>
Title Page. . . . .	i
Acknowledgements. . . . .	ii
List of Tables. . . . .	iv
List of Figures . . . . .	v
Introduction. . . . .	1
Historical. . . . .	3
Experimental: Equipment. . . . .	8
Results and Discussion	
1) Column Selection and Interface Considerations . . . . .	13
2) Samples . . . . .	19
3) Instrument and Associated Parameters. . . . .	21
4) GC/FTIR Results . . . . .	17
5) GC-MS: Comparisons . . . . .	89
Conclusions . . . . .	107
References. . . . .	111
Vita. . . . .	114
Abstract	

LIST OF TABLES

<u>Table</u>		<u>Page</u>
1	Standard Mixture Used with Model 36 Lightpipe and Nicolet 6000 FTIR. . . . .	10
2	Standard Mixture Used with 40 cm Lightpipe and Nicolet 7199 FTIR. . . . .	11
3	Standard Mixture Used with Accuspec GC and Varian Mat Mass Spectrometer. . . . .	12
4	Parameter File Listing . . . . .	24
5	Figure 31 Spectral Results . . . . .	70
6	Figure 39 Spectral Results . . . . .	81

## LIST OF FIGURES

<u>Figure</u>		<u>Page</u>
1	Nicolet 6000 Optical Layout. . . . .	14
2	CHEMIGRAM for VN-77-11 with Model 26 IR Cell. . . . .	16
3	On-Column Injector (Exploded View) . . . . .	20
4	VN-77-11 Separation on 60 m DB-5 Fused Silica Column (TCD Only) . . . . .	22
5	CHEMIGRAM for VN-80-39 with Model 26 IR Cell and DB-5 Column . . . . .	28
6	TCD Trace After Model 26 IR Cell (VN-80-39). . . . .	30
7	VN-80-39 GSR and 2800-3000 $\text{cm}^{-1}$ RCN (Model 26 IR Cell) . . . . .	31
8	VN-80-39 3020-3200 $\text{cm}^{-1}$ and 650-950 $\text{cm}^{-1}$ RCN (Model 26 IR Cell) . . . . .	32
9	Single Beam Spectrum (Model 26 IR Cell). . . . .	34
10	File Spectrum #636 VN-80-39 (Model 26 IR Cell). . . . .	38
11	File Spectrum #700-707 VN-80-39 (Model 26 IR Cell) . . . . .	39
12	File Spectrum #636 (16 $\text{cm}^{-1}$ ) VN-80-39. . . . .	41
13	File Spectrum #700-707 (16 $\text{cm}^{-1}$ ) VN-80-39. . . . .	42
14	TCD Trace VN-80-39 after Model 36 IR Cell. . . . .	44
15	File Spectrum #251-255 VN-80-39 (Model 36 IR Cell) . . . . .	45
16	File Spectrum #334-340 VN-80-39 (Model 36 IR Cell) . . . . .	47
17	GSR VN-77-11 (Model 36 IR Cell). . . . .	48

LIST OF FIGURES (Cont'd)

<u>Figure</u>		<u>Page</u>
18	File Spectrum #136-130 VN-77-11 (Model 36 IR Cell) . . . . .	49
19	File Spectrum #224-218 VN-77-11 (Model 36 IR Cell) . . . . .	50
20	File Spectrum #461-455 VN-77-11 (Model 36 IR Cell) . . . . .	52
21	File Spectrum #691-684 Trans-decalin Standard (Model 36). . . . .	54
22	File Spectrum #478-550 M-xylene Standard (Model 36) . . . . .	55
23	File Spectrum #621-630 N-decane Standard (Model 36) . . . . .	56
24	Nicolet 7199 Optical Layout. . . . .	58
25	CHEMIGRAM of VN-77-11 Separated on DB-1 Fused Silica Column (7199 System). . . . .	60
26	RCN 2800-300 $\text{cm}^{-1}$ VN-77-11 (Nicolet 7199 System). . . . .	62
27	Single Beam Spectrum (7199 System) . . . . .	63
28	1/2 RCN 2800-3150 $\text{cm}^{-1}$ VN-77-11 (7199 System). . . .	64
29	File Spectrum #184-179 VN-77-11 (7199 System). . . .	65
30	File Spectrum #365-356 VN-77-11 (7199 System). . . .	67
31	File Spectrum #703-694, #703-698; #461-455 (Model 36) . . . . .	68
32	VN-80-39 GSR Model 36; 7199 System . . . . .	71
33	File Spectrum #313-324 VN-80-39 (7199 System). . . .	73
34	File Spectrum #420-405 VN-80-39 (7199 System). . . .	74

LIST OF FIGURES (Cont'd)

<u>Figure</u>		<u>Page</u>
35	GSR of Microgram Mixture (7199 System) . . . . .	75
36	File Spectrum #417-413 p-xylene Standard (7199 System). . . . .	76
37	File Spectrum #767-760 tetralin Standard (7199 System). . . . .	78
38	File Spectrum #718-713 cis-decalin Standard (7199 System). . . . .	79
39	File Spectrum #449-444 o-xylene; #414-410 m-xylene Standards . . . . .	80
40	RCN 3020-3200 $\text{cm}^{-1}$ VN-80-40 (7199 System). . . . .	83
41	File Spectrum #322-310 VN-80-40 (7199 System). . . . .	84
42	File Spectrum #892-876 VN-80-40 (7199 System). . . . .	85
43	File Spectrum #892-876; #862-813 VN-80-40. . . . .	86
44	File Spectrum #862-813 VN-80-40 (7199 System). . . . .	87
45	File Spectrum #645-542 VN-80-40 (7199 System). . . . .	88
46	GC-MS Total Ion Chromatogram VN-77-11. . . . .	91
47a	File Spectrum #1756 VN-77-11 (GC-MS) . . . . .	92
47b	File Spectrum #1921 VN-77-11 (GC-MS) . . . . .	92
48	File Spectrum #2266 VN-77-11 (GC-MS) . . . . .	93
49	GSR Section VN-77-11 Model 36; 7199 System . . . . .	95
50	File Spectra #2291; #2315 VN-77-11 (GC-MS) . . . . .	96
51	File Spectrum #3900 VN-80-40 (GC-MS) . . . . .	98
52a	GC-MS Total Ion Chromatogram (1) VN-80-40. . . . .	99
52b	GC-MS Total Ion Chromatogram (2) VN-80-40. . . . .	100

LIST OF FIGURES (Cont'd)

<u>Figure</u>		<u>Page</u>
53	File Spectrum #286-295 FTIR VN-80-40 (7199 System) . . . . .	101
54	File Spectrum #3922 VN-80-40 (GC-MS) . . . . .	103
55	File Spectra #4620, #4670 VN-80-40 (GC-MS). . . . .	104
56	File Spectra #8081, #7856 Standard Mixture (GC-MS). . . . .	106

## INTRODUCTION

The gas chromatography/infrared (GC-IR) method of analysis, while not new, has only recently improved to the point where complex, real world samples can effectively be studied. To perform such an analysis, a highly efficient separating mode (gas chromatography) must be interfaced to an infrared detection system which is capable of rapid scanning and computerized data handling.

The advent of modern Fourier transform infrared (FTIR) spectrometers offers improvements and advantages over conventional dispersive infrared spectrophotometers for detecting eluting components from a gas chromatograph<sup>1</sup>. Increased optical throughput, rapid-scanning of the IR region and dedicated high-speed computers make possible routine high-resolution infrared spectra. The effluent from a gas chromatographic separation can be directed through a heated lightpipe placed in the path of the infrared beam and FTIR spectra of GC fractions obtained as they elute from the GC column. Nitrogen-cooled Hg-Cd-Te (MCT) detectors and advanced lightpipe designs are particularly responsible for the improvement in IR sensitivity. Coupled with the recent development of highly efficient capillary columns as the separation mode, valuable gas phase spectra for even complex "real-world" samples should be obtainable. At present, narrow bore fused silica capillary columns give the most efficient separations in gas chromatography.

The major objectives of this research are the separation and

identification of components in aviation jet fuel samples by GC-FTIR. Optimum conditions and parameters will be established for proper capillary gas chromatography. The interfacing of capillary GC with FTIR presents some unique situations with respect to both chromatography and detection. Two Nicolet FTIR optical benches, with respective GC hardware, will be used in assessing those conditions/parameters needed for state-of-the-art GC-FTIR. In addition, gas chromatography-mass spectrometry data for the same jet fuel samples will be presented in an effort to compare directly information obtainable from both spectroscopic methods. A fused silica capillary column is used to achieve the maximum separation of components. Sensitivities from both GC-FTIR and GC-MS will be directly compared for the same sample components isolated using on-the-fly methods.

Characterization and identification of components in aviation jet fuels are of interest to the United States Air Force in that compounds may be present that are carcinogenic and/or have appreciable heteroatom (alcohols, ethers, etc.) character. Since concentration of highly branched alkanes can generally improve fuel performance (e.g. high octane number), the presence of such aliphatics should be significant. Finally, identification of decomposition products due to fuel instability would be of interest with respect to storage of such aviation products.

## HISTORICAL

Because of recent advances in both gas chromatography and FTIR, optimizing the GC-FTIR experiment has been of obvious concern to many researchers. A review of these developments and advances should give a better understanding of how the research reported here relates to other work and how the GC-FTIR technique could be applied to complex real-world samples.

While packed column gas chromatography offered reasonable separation of sample components, the development in 1957 of open tubular capillary columns<sup>2</sup> initiated the evolution of GC columns with higher efficiency and lower resistance to gas flow. The open tubular design consequently resulted in a lower pressure drop across the column. Another pioneer, D. H. Desty, (1958) applied "open tubulars" (so-called because a thin film of stationary phase is deposited on the walls of a thin open tube) to the separation of petroleum products<sup>3</sup>. Desty et al. also contributed to capillary column technology by suggesting a simple design for a machine which could draw and coil glass capillary tubing<sup>13</sup>.

Holasz and Horvath initiated the development of support coated open tubular (SCOT) columns<sup>4</sup> which were found to be more efficient than packed columns. Although the stationary phase is coated on a support (as in packed columns), the center of the tube is still open. L. V. Azarraga was one of the first to use SCOT columns with on-line FTIR detection for analysis of environmental samples<sup>5</sup>. SCOT columns, while

providing capillary efficiency, also afforded a sample loading compatible with the existing GC-FTIR sensitivity. D. M. Hembree, et al. resorted to GC separations using a SCOT column but used cryogenic trapping of fractions from the chromatographic run for final off-line FTIR analysis. Solvent refined coal (SRC) fractions were the "real, complex samples" used to illustrate GC-FTIR<sup>11</sup>. Such samples were commonly too complex for sufficient separation by SCOT columns followed by on-line FTIR detection.

Therefore, while SCOT columns offered needed sample loading and enhanced capillary efficiency, work resumed to develop what has come to be known as WCOT (Wall coated open tubular) capillary columns. These columns were found to have unmatched separating capability. Instead of a support, the stationary phase is coated on the smooth wall of the capillary, thus the name WCOT. Azarraga first presented preliminary WCOT capillary GC-FTIR results in 1976<sup>9</sup>.

K. M. Shafer boasts that "the first on-the-fly GC-FTIR spectra ever obtained using WCOT (glass) capillary columns"<sup>7</sup> was achieved in his laboratory. Shafer found the 0.5 mm i.d. x 40 m glass column gave better separations than a SCOT column, but not as good as other more narrow bore WCOT columns. Despite his claim, Shafer's separation of a wastewater sample provided only a small number of separated components. Shafer was not able to use columns less than 0.5 mm i.d. because of the comparably limited sample capacity, again relating back to FTIR detection limitations. Later, Shafer and Cooke et al. developed the methodology to compare GC-FTIR and GC-MS data directly, thereby

elucidating more effectively various components. Since WCOT columns were commonly used in GC-MS, a 0.5 mm i.d. glass WCOT with 0.8  $\mu\text{m}$  stationary film thickness was tested in the GC-FTIR experiment and favorable detection limits achieved.<sup>8</sup> Environmental sample data from both FTIR and MS could then be more readily compared due to similar chromatographic conditions. Finally, Rossiter has achieved an on-line spectrum of 20 ng of isobutylmethacrylate by using a short (6 cm) lightpipe<sup>12</sup>. In an effort to demonstrate on-line GC-FTIR with the short lightpipe, a jet fuel sample was separated by gas chromatography. The wide bore WCOT glass capillary column, however, provided only marginal separation of the complex fuel sample.

Although glass capillaries (WCOT) can be very useful for separating complex mixtures, the soda lime which is commonly used to manufacture these columns can be brittle and often difficult to work with. Column end straightening by a torch can cause a loss of column deactivation which can lead to tailing peaks.

Dandeneau and Zerenner have shown that capillary WCOT columns made from fused silica ( $\text{SiO}_2$ ) are not only easier to deactivate but are flexible enough to bend even though fused silica is inherently straight<sup>10</sup>. These workers found that fused silica was unexcelled in inertness to all functional groups tested. Flexible and rugged, fused silica columns can be inserted directly into injection ports, through transfer lines and detector fittings. Such columns are available with inner diameters of 0.35-0.2 mm. Film thicknesses for these columns can be as high as 1.2  $\mu\text{m}$  for maximum sample capacity (commonly 500 ng per component).

Using an OV-101 fused silica capillary of narrow bore (0.2 mm i.d. x 50 m), Azarraga in 1981 analyzed environmental samples by GC/FTIR prepared from waste effluents of the printing and ink industry<sup>6</sup>. Preconcentration using a SCOT capillary column combined with cold trapping was necessary, however, prior to separation on the fused silica column.

Recently, Griffiths has used wide bore fused silica (>0.3 mm i.d.) with 0.5  $\mu\text{m}$  film thickness in the further development of capillary GC-FTIR techniques<sup>14</sup>. His efforts have concentrated on the principal problem with capillary GC-FTIR, its "chemical dynamic range", i.e. the difference between the maximum quantity of any component able to be injected onto a column without degradation of GC performance to the minimum amount yielding an observable infrared spectrum. He has discussed the "problem" in terms of the choice between narrow-bore fused silica columns coated with thin (0.2-0.3  $\mu\text{m}$ ) layers of stationary phase to wider bore glass columns with much thicker (0.8-1.2  $\mu\text{m}$ ) layers of stationary phase. He has indicated, though, that few separations of truly complex samples using fused silica columns coupled with FTIR detection have been shown.

Garlock et al. have demonstrated the use of narrow as well as wide bore fused silica columns in separating coal derived products (SRC), perfumes, essential oils and a few jet fuels derived from kerosene. For less than 100 ng, narrow bore (0.25 mm i.d.) columns were usable. However, for maximum sample loading 0.3 mm i.d. columns with 1.0  $\mu\text{m}$  film thickness were required. A colleague has indicated that fused

silica columns handled overloading reasonably well<sup>15</sup>. A 36 cm x 1.4 mm diameter lightpipe was used in their experiments along with a narrow band MCT detector resulting in a sensitive on-the-fly GC-FTIR technique.

Shafer and Jakobsen have shown success in coupling a narrow bore fused silica column (0.25 mm i.d.) with FTIR and have achieved acceptable detection limits. They also have interfaced a mass spectrometer in series with the GC-FTIR<sup>16</sup>. (It should be noted that the last three references (14-16) have not appeared in publication at the time of this writing).

In light of the several methods and developments just cited, a combination of the best gas chromatographic separation available with optimal FTIR conditions should lead to a hyphenated method capable of producing quality infrared spectra on-the-fly for even very complex samples. The greater part of this research is an attempt to determine those parameters necessary to separate, characterize and identify components in aviation jet fuels. Emphasis will center around final quality IR spectra that can be identified by the EPA vapor phase library search routines available in the Nicolet FTIR data base. No prior pretreatment or preconcentration of samples is to be envisioned. Because the majority of components in jet fuels do not contain strong absorbing groups (i.e., like isobutylmethacrylate), proper optimization of all parameters will be critical. Two optimized GC-FTIR systems using different lightpipe designs and MCT detectors will be compared in light of the requirements necessary to analyze these complex samples.

In reference to the actual jet fuel samples to be analyzed, LC-NMR by Dorn, et al. has been used to characterize both qualitatively and quantitatively major classes of compounds present. Data showing percent alkanes, monoaromatics and dicyclic aromatics are presented. Their data also indicate the presence of alkenes in these Air Force jet fuels<sup>18</sup>. In general, no prior pretreatment was used before analysis.

## EXPERIMENTAL

### Equipment:

Two GC-FTIR configurations were used in assessing a "best system". In our laboratory we have a Nicolet series 6000 FTIR with a liquid nitrogen cooled Hg-Cd-Te detector capable of scanning the IR region 4000-400  $\text{cm}^{-1}$ . The Michelson interferometer has a maximum mirror velocity of 3.130  $\text{cm}/\text{sec}$  although 0.586  $\text{cm}/\text{sec}$  is the recommended value for MCT detectors. The Nicolet 6000 FTIR uses a single disc drive with 8-sector cartridges and is controlled by a Nicolet IR-80 data processor. Cylindrical lightpipe arrangements of both 2mm i.d. x 6 cm and 3 mm i.d. x 6 cm stainless steel were supplied by the Accuspec Corp. Each lightpipe was placed in the cell holder normally used for LC cells. An Accuspec Compact GC with auxillary microvolume thermal conductivity detector (TCD) fitted for capillary columns was used. Available columns included a 25 m wide-bore glass capillary (OV-101), a 0.32 mm i.d. x 25 m CP-sil 5 and a 0.35 mm i.d. x 60 m DB-5 fused silica capillary (the latter two columns being bonded phases). A home-made on-column injector was fitted to the Accuspec GC to make use

of the Carlo-Erba 0.23 mm o.d. syringe needle design. As general practice, the effluent from the column was transferred to the lightpipe via a heated transfer line and returned by narrow bore heated tubing to the TCD heated block in the GC. In the case where fused silica was used, the column was fed through the transfer line up to the IR lightpipe.

Also available was a dual-beam Nicolet 7199 system with GC 7000 external bench, 40 cm x 1 mm i.d. gold plated lightpipe, and narrow band (4000-700  $\text{cm}^{-1}$ ) MCT-A<sup>+</sup> detector. The GC employed in this study was from Hewlett Packard and was fitted with capillary split-splitless injectors. For data storage, dual disc drives (and a storage module capable of holding 5000 8  $\text{cm}^{-1}$  file spectra) were utilized. The capillary column available at Nicolet was a 60 m x 0.3 mm i.d. DB-1 bonded phase fused silica interfaced to the 40 cm lightpipe by 0.7 mm i.d. glass lined tubing.

The Nicolet 6000 in our laboratory had available nitrogen purging for the IR bench while only compressed "dried" air was available at Nicolet for the 7199 system.

A Varian MAT 112 Electron Impact mass spectrometer was interfaced to the Accuspec GC and DB-5 fused silica column. The source voltage was 70 eV and the operating temperature was 240°C. The Varian-MAT 620/L-100 computer uses 32 sector hard disk cartridges to store accumulated data. A ten inch heated transfer line brought the effluent directly into the mass spectrometer and no make-up gas was used (flow rate ~2 ml/min).

Jet fuel samples were provided by Major D. D. Potter from the Air Force Aero Propulsion Laboratory, Wright-Patterson Air Force Base, OH. Samples were received and stored in teflon-tape-sealed 100 mL glass bottles and resealed after each opening.

The standard mixtures used in these experiments were as follows:

TABLE 1  
STANDARD MIXTURE USED WITH MODEL 36  
LIGHTPIPE AND NICOLET 6000 FTIR

<u>Compound</u>	<u>bp(°C)</u>	<u>Quantity (μL)</u>
m-xylene	138	20
nonane	150	30
cumene	152	15
p-ethyl toluene	162	30
decane	174	15
indan	176	1
trans-decalin	185	30
undecane	195	10
1,2,3,4-tetra- methylbenzene	205	1
dodecane	216	15
tridecane	232	10

(Component mixture diluted to 3.0 ml with n-octane)

TABLE 2

STANDARD MIXTURE USED WITH 40cm  
LIGHTPIPE AND NICOLET 7199 FTIR

<u>Component</u>	<u>bp(°C)</u>	<u>Quantity (μL)</u>
methylcyclopentane	72	10
2,4-dimethylpentane	81	10
2,3-dimethylpentane	90	7.5
iso-octane	99	10
2,5-dimethylhexane	108	5
2-methylheptane	116	7
1,2-dimethylcyclohexane		
cis-	130	10
trans-	123	
p-xylene	138	1.5
m-xylene	139	5
o-xylene	144	10
nonane	150	10
m-ethyltoluene	159	5
p-ethyltoluene	162	2
o-ethyltoluene	164	5
tert-butylcyclohexane	171	5
indan	176	7
trans-decalin	185	5
cis-decalin	193	2
tetralin	207	4
isopropylcyclohexane	155	3

(Component mixture diluted to 10.0 mL with n-hexane)

TABLE 3  
STANDARD MIXTURE USED WITH  
ACCUSPEC GC AND VARIAN MAT MASS SPECTROMETER

<u>Component</u>	<u>Quantity (<math>\mu</math>L)</u>
hexane	10
methylcyclopentane	5
2,4-dimethylpentane	10
2,3-dimethylpentane	7
heptane	10
2,5-dimethylhexane	5
2-methylheptane	7
1,2-dimethylcyclohexane (cis and trans)	10
m-xylene	5
o-xylene	10
isopropylcyclohexane	3
m-ethyltoluene	5
p-ethyltoluene	2
o-ethyltoluene	5
tert-butylcyclohexane	5
indan	7
trans-decalin	5
cis-decalin	2
tetralin	4

(Component mixture diluted to 10.0 mL with tridecane)

## RESULTS AND DISCUSSION

### Column Selection and Interface Considerations:

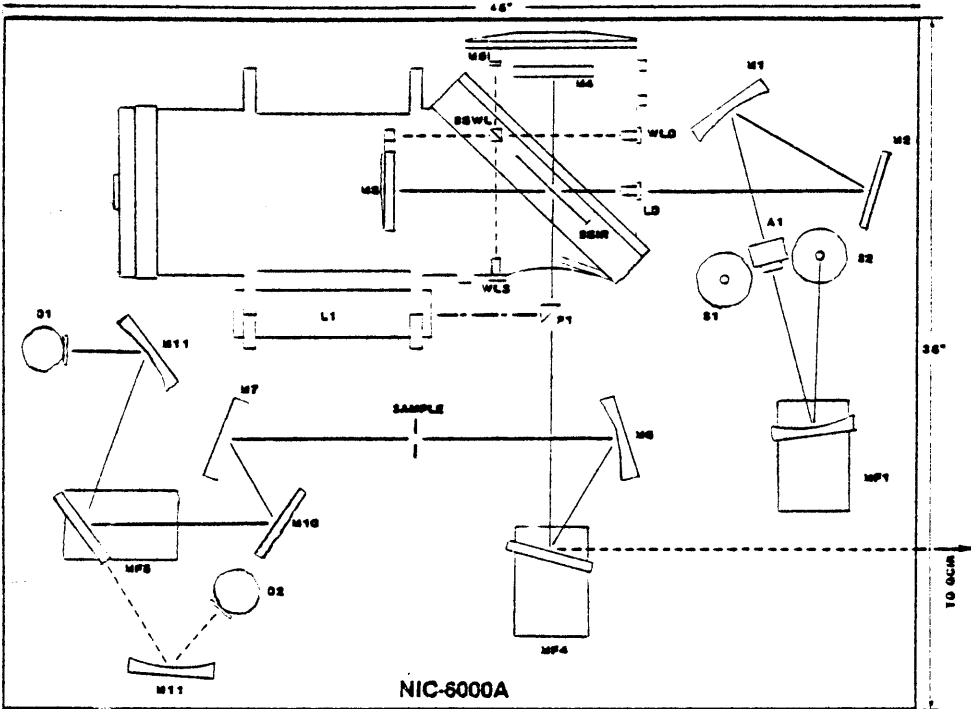
Historically, many kinds of gas chromatography columns have been used with FTIR. Packed column use is relatively straightforward since peaks are generally broad (relative to capillary columns). Sample loading and IR detection are generally not a problem. Several other columns have been tested for their separating power with reference to jet fuel samples.

Preliminary experiments used a twelve foot stainless steel Apiezon L packed column (2 mm i.d.) with an Accuspec polished stainless steel lightpipe (Model 36) of dimension 3 mm i.d. x 6 cm. An Accuspec Compact GC fitted with heated injectors designed for packed columns was used. The GC cell was placed in the sample compartment of the Nicolet 6000 bench which normally holds a 1 mm (or less) pathlength liquid chromatography cell (Figure 1). Using the adjusting screws of the IR cell, the Model 36 was optimized for the 3 mm infrared beam. To properly align the cell, the IR signal is monitored by observing an oscilloscope signal from the center burst of the interferogram as the instrument scans. The effects of the longer pathlength cell (relative to an LC cell) were soon realized as defocusing of the IR beam resulted in decreased throughput of infrared signal. It was also determined that for complex jet fuel samples, packed column efficiency was not adequate for the separation desired.

An OV-101 wide bore glass capillary column (25 meters) was then

## OPTICAL LAYOUTS

## NIC-6000A Single Beam FT-IR Spectrometer



## LEGEND

- S1, S2 Alternate source positions  
 MF1 Computer controlled source selection mirror, spherical 4.5" E.F.L.  
 A1 Computer controlled aperture  
 M1 Collimating off-axis parabolic mirror, 8.2" E.F.L.  
 M2 Flat mirror  
 M3 Moving mirror assembly  
 M4 Fixed mirror (I.R. beam and reference laser)  
 M5 Fixed mirror (white light)  
 BSWL White light beamsplitter  
 BSIR Infrared/reference laser beamsplitter  
 LD Centerline reference laser detector  
 WLD White light detector  
 WLS White light source  
 L1 Reference laser  
 P1 Centerline laser prism  
 MF4 2-position, computer controlled flat mirror  
 M6 Sample focusing mirror, off-axis parabola, 9.3" E.F.L.  
 M7 Sample collection mirror, off-axis parabola, 9.3" E.F.L.  
 M10 Flat mirror  
 MF5 2-position, computer controlled, detector selection mirror, flat  
 M11 Detector focusing mirror, off axis parabola, 3.5" E.F.L.  
 D1, D2 Alternate detector positions

FIGURE 1. Nicolet 6000 Optical Layout

made available by the Accuspec Corp. along with a compact GC fitted with split-splitless capillary injector and a heated lightpipe of dimensions 2 mm i.d. x 6 cm (to cut down on dead volume). Operating in the splitless mode, injections of less than 0.2  $\mu$ l of jet fuel were made. Separations were markedly improved relative to the packed column.

Optimization of the IR signal, however, now became more critical as less sample passed through the cell. Also, the smaller diameter of the lightpipe decreased the signal throughput considerably. As standard operating procedure, the cell was adjusted to an optimum position, the MCT-B detector then moved until maximum signal was achieved, and finally the interferometer mirrors were aligned for maximum final signal. Most of the time this alignment was done with the cell at room temperature to simplify the procedure. A jet fuel, VN77-11 JP-4, was selected and separated with the path of the effluent being column - IR cell - microvolume TCD. The column-IR-TCD route was chosen to minimize any band broadening which might occur due to the TCD dead volume.

The instrumental parameters and temperature program are given on the real-time CHEMIGRAM for the jet fuel separation carried-out on the 25 meter OV-101 glass capillary (Figure 2). Given the required amount of sample injected for IR detection, this separation was not considered adequate and a slight column overloading was observed. Since the objective of the separation was to isolate low concentration components, we considered the glass column to have too low a sample

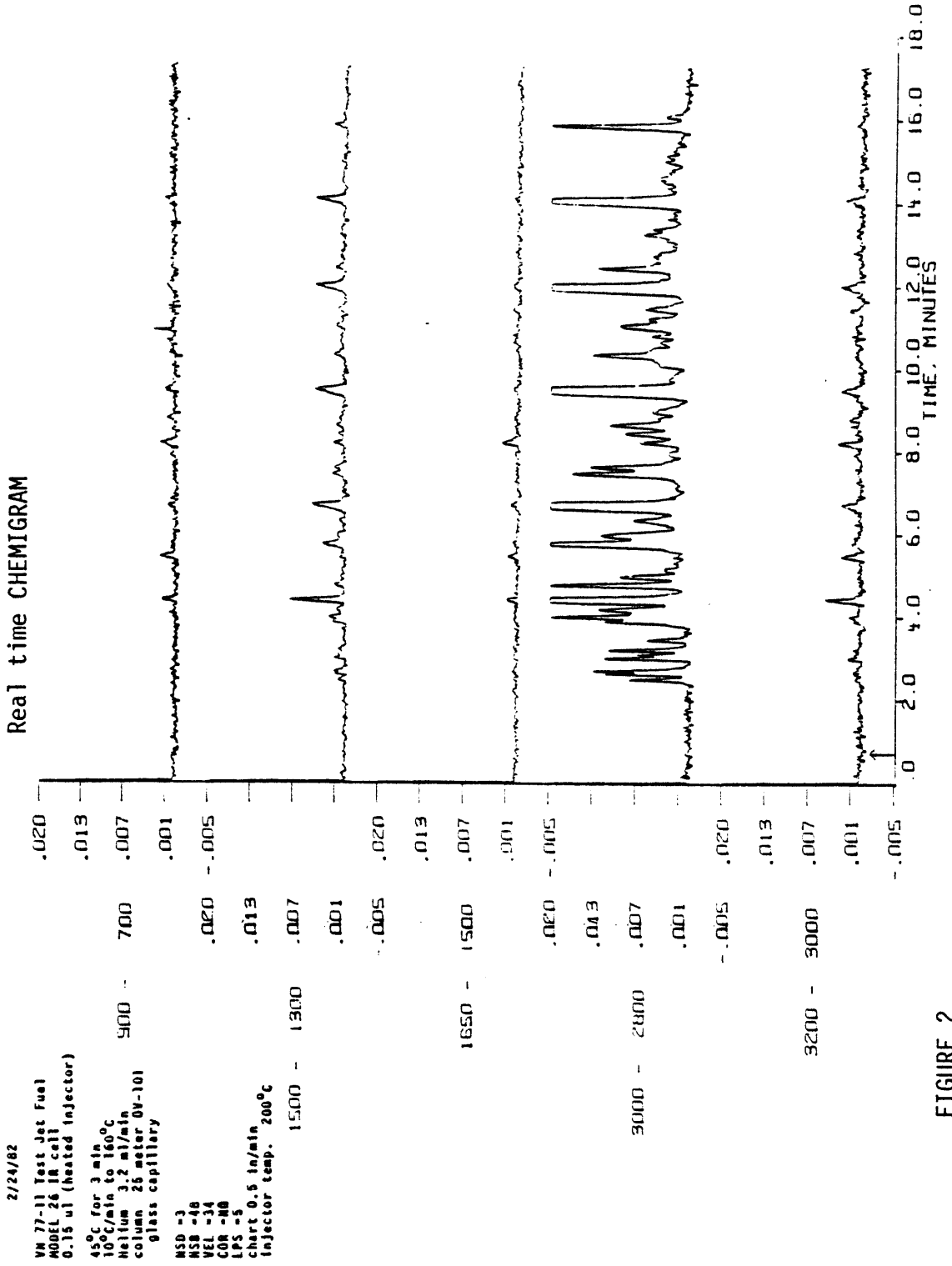


FIGURE 2

capacity and only fair chromatographic efficiency. Handling of the rigid glass column was also considered unnecessarily awkward, and the column connections were somewhat difficult. In addition, overlapping (coeluting) peaks meant that identification by spectral matching using the EPA vapor phase library could become tedious.

Upon reviewing the literature and chromatography supply catalogs, WCOT (Wall Coated Open Tubular) fused silica capillary columns seemed to provide the best separating efficiency. Fused silica was chosen over narrower bore glass because of the flexibility and durability of fused silica. Longer lengths of column would also be easier to handle. With fused silica, the column could be inserted through the heated transfer line up to or very near the IR cell thus minimizing dead volume (critical in capillary chromatography). Although fused silica is durable, sharp right angle bends are not feasible without threat of breakage. Construction, therefore, of a curved, heated, 15 inch transfer line (exiting through the top of the GC) was needed to reach the Model 26 cell.

After experimenting with a 25 m x 0.32 mm i.d. CP-SIL-5 (methylsiloxane) bonded phase fused silica capillary column, it was decided to go to a longer (60 meter) column for a maximum separation. The 60 m x 0.35 mm i.d. DB-5 column proved to be adequate for separating selected jet fuels. A column any longer than 60 meters might have caused handling problems in the GC oven, and the cost of such an extremely long column would have been prohibitive. The DB-5

column from J & W Scientific is capable of generating over 175,000 theoretical plates. With its 1.0 micron film thickness, column sample capacity was about 500 ng per component (recommended). The methyl-phenyl-vinylsiloxane character of the DB-5 column also offered possible functional group interaction leading to further discriminatory separation. An additional advantage of the bonded phase was that relatively large amounts of solvent(s) could be injected without damage to the stationary phase. Upper temperature limits of 325 to 350°C made the bonded phase with fused silica a prime choice.

One important consequence of switching to fused silica over glass columns was that a make-up gas (helium) had to be used to retain chromatographic separation as the effluent passes through the relatively large dead volume of the lightpipe. For the Model 26 this dead volume was about 190  $\mu$ l. The wide bore glass column used previously was run with a helium flow rate of about 3.2 ml/min and no make-up gas. Because narrower fused silica columns are rarely used with flow rates above 2 ml/min and because the eluting peaks may be very close together, a total flow of 5 ml/min including make-up helium was used through the lightpipe. The make-up gas was supplied by a tee at the exit of the column from the oven. The gas was passed through the same transfer line as the column effluent, thus forcing the eluting components through the cell. A heated return line from the lightpipe brought the effluent back to the microvolume thermal conductivity detector in the GC.

Finally, an adequate injection technique was required for the capillary column. The idea of "on-column" injection, whether cold or heated, was considered to be the most reliable and reproducible method. Sample discrimination (i.e. relating to inconsistent vaporization of high boiling components) could be eliminated by switching from standard vaporizing injection methods to on-column. S. Trestianu and Carlo Erba Instruments have presented valuable information on this injection technique<sup>20</sup>. For jet fuel samples, instant vaporization may become a major problem in higher boiling fractions. Since no commercial on-column injector would fit the Accuspec GC, one was designed based on the use of the Carlo Erba (0.23 mm o.d.) syringe needle (See Figure 3). This homemade injector design required an extra-long syringe needle (11.5 cm), but the assembly has been successfully used with wide bore (>0.3 mm i.d.) as well as narrow bore (0.25 mm i.d.) fused silica columns. Injection is made at a point inside the oven while retaining an unimpaired helium carrier gas flow rate. Because a mass-flow sensitive microvolume TCD was used, any changes in flow would be immediately apparent. In summary, on-column injection was chosen in order that a more quantitative and higher sample loading could be employed.

#### Samples:

As a preliminary screening, 10 jet fuels were separated with the fused silica column to determine their complexity and boiling point ranges. The microvolume (~20  $\mu$ L) TCD was directly connected to

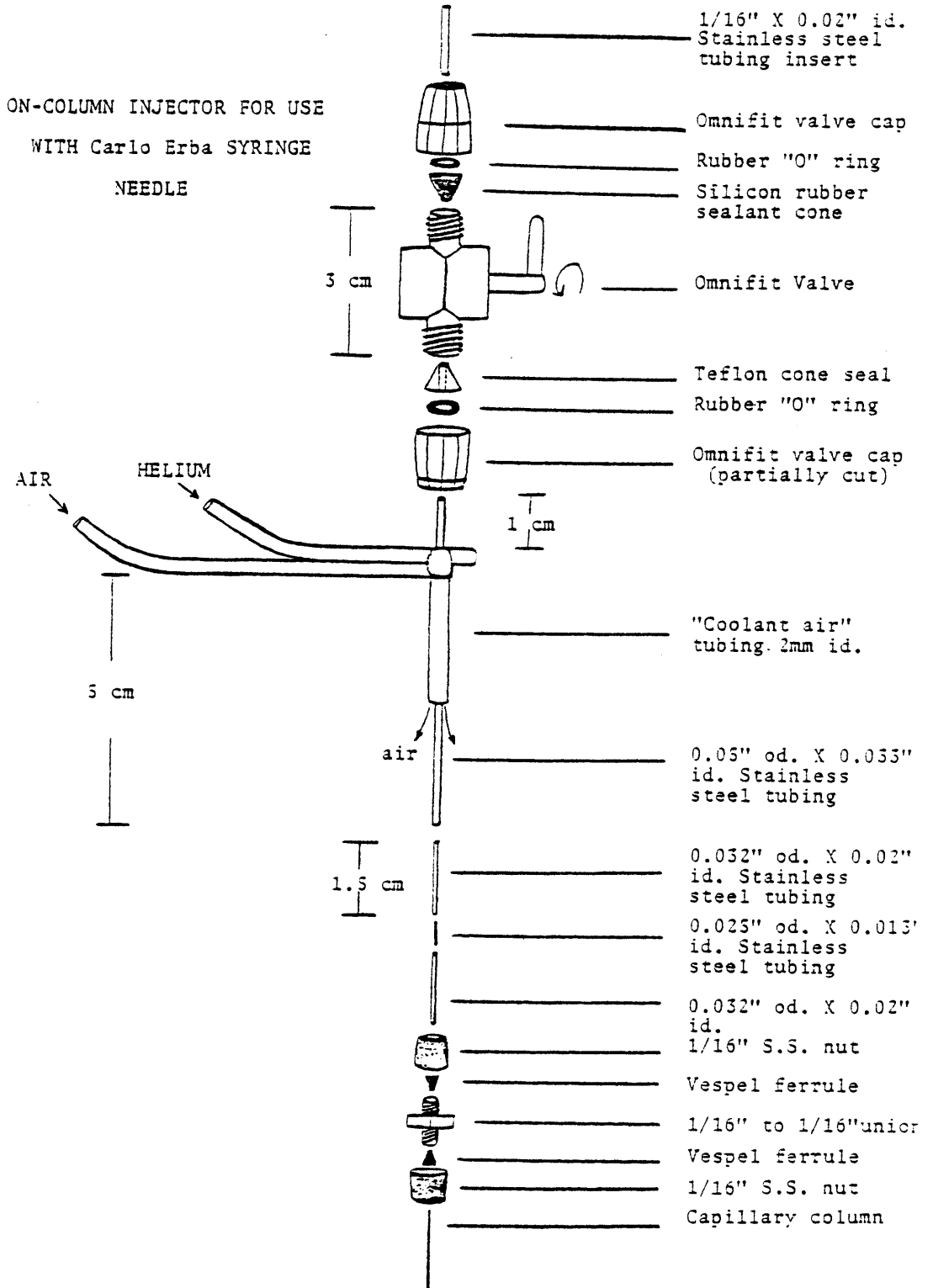


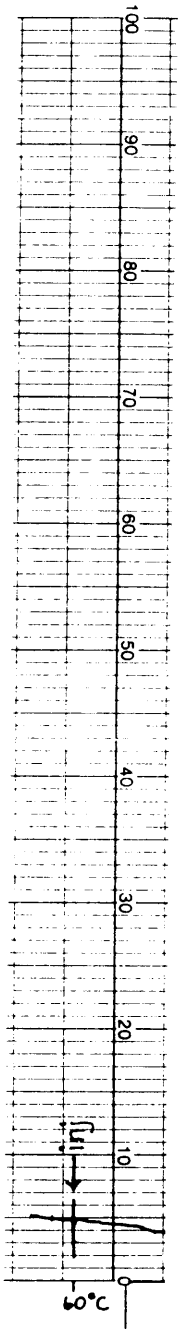
FIGURE 3

the column outlet to monitor these "ideal, no dead volume" separations. Figure 4 illustrates such a separation on the 60 meter DB-5 fused silica column. More information on these fuels was made available by Dorn et al.<sup>8</sup> who previously employed <sup>1</sup>H and <sup>13</sup>C LC-NMR to characterize these jet fuels. The alkane, monoaromatic, polyaromatic and (possible) alkene content reported by Dorn was considered in selecting a few samples for GC-FTIR analysis. Three of the ten fuel samples were chosen for GC-FTIR analysis. One test jet fuel (VN-77-11 JP-4 from shale oil) contained mostly alkanes, a second (VN-80-39 Aromatic Blend) contained mostly monoaromatics, and a third (VN-80-40 Aromatic Blending Stock) was 68% polyaromatic in character.

The fused silica capillary column provided the necessary efficiency for separating these samples. The on-column injector allowed more sample to be injected onto the column (as compared to the heated injector) with minimal overloading characteristics. Also, dilutions could be made of the sample to lower sample loading thereby increasing chromatographic resolution. A phenomena called the "solvent effect" could invariably be utilized in which peaks are sharpened due to the slow-moving plug of low boiling solvent<sup>22,23</sup>.

#### Instrument and Associated Parameters:

Having delineated the mode of chromatography, injection technique and pertinent samples, attention is now turned to the FTIR instrument and associated parameters. In capillary GC-FTIR, aside from chromatography, the two major considerations to be faced are those of optical



throughput and detector sensitivity. Throughput relates to the intensity of the infrared beam which is allowed to pass through the heated lightpipe to the MCT detector. Sensitivity relates to the detector response for a given amount of sample vapor. Lightpipe length and diameter affect throughput and sensitivity since a long, narrow lightpipe will allow less IR radiation through, but because of the longer pathlength sensitivity may be increased. For long, narrow lightpipes a reflective (but inert) surface is required for maximum throughput. Azarraga has described the requirements and method for attaining higher reflective lightpipes using a gold coating<sup>17</sup>.

For our Nicolet 6000 setup, the Accuspec IR cells were considered short enough that the absence of gold coating would not result in an appreciable loss in throughput. For work using the 60 meter fused silica capillary, the 2 mm i.d. x 6 cm Model 26 lightpipe was chosen initially to reduce dead volume (190  $\mu$ l instead of 400  $\mu$ l for the Model 36).

As stated previously, the procedure for achieving the best throughput was to 1) align the cell, 2) modify the position of the MCT detector and 3) tune (align) the interferometer mirrors. However, before such alignments can be pursued certain FTIR instrument parameters must be established. These parameters are collected in a specified PARAMETER FILE which is stored in the computer (See Table 4).

TABLE 4

GC-FTIR  
INSTRUMENT PARAMETERS

## PRF

AFN	=	HG	
APT	=	FL	
BDL	=		10
COR	=	MD	
DFN	=		20
FIT	=	YS	
FSZ	=		2816
GAN	=		1
HPS	=		1
LPS	=		6
MIR	=	SB	
NDP	=		2048
NPD	=		200
NPT	=		1024
NSB	=		40
NSD	=		10
NSS	=		10
NSK	=		0
NTP	=		4096
PTS	=		3
SGH	=		8
SGL	=		1
SMO	=	NO	
SSP	=		2
VEL	=		50

.

One of these important parameters, mirror velocity, (VEL) was set to 50. At VEL=50, a rapid-scan mode is employed where rapid acquisition of interferograms occurs. For fused silica capillary GC, rapid data collection is essential because of narrow peak widths and closely spaced peaks. Using VEL=50 (or higher), however, creates a source of noise due to instrumental vibration. Although the FTIR bench has a very heavy base plate and vibration damping feet, vibration patterns can cause problems in data collection. COR (correlation) is the parameter used to circumvent excessively noisy conditions. By a more or less trial and error method, the COR is set to different values until enough "bad data collects" are thrown out to achieve a smooth flowing scan rate. Values of COR include NO (no correlation; all scans collected) up to a correlation factor of 32 (HI). Care must be taken when setting COR, as excessively noisy conditions can affect the overall data collect time frame which may simulate a slower scan rate altogether. Under such conditions pertinent information on unresolved peaks may be lost. As a consequence of the rapid scan mode only 2048 data points are normally collected per scan, corresponding to an 8  $\text{cm}^{-1}$  resolution spectra. Therefore, a file size (FSZ) of 2816 is needed to contain those points.

To achieve the best possible signal to noise ratio, a maximum number of scans must be coadded and ratioed to a series of coadded background scans. Experimentally, ten scans coadded (NSD) into a data file would take about 1 second when ratioed to 40 coadded background scans (NSB). The real time CHEMIGRAM is the limiting factor when

wanting to collect and ratio data because of computer data-acquisition and storage limitations. The absolute maximum number of background scans capable of being ratioed to one-half that value of sample scans is 54 (e.g. 27 sample scans). Since NSD must be a factor of 2, 4, 8, etc. less than NSB (by design), then this maximum would not be useful for rapid data file collect situations (i.e. 27/2 does not exist for the CHEMIGRAM program since it is not a whole number). Ideally, in the rapid scan mode, several data files can be collected per second. However, the S/N would suffer due to a minimum of scans being coadded.

Data collection can be manipulated, therefore, according to what the complexity of the sample happens to be. As always, peak width will affect the scan rate in that more than one file shall define a component peak. For less complex samples, either a slower scan rate can be used or more scans can be coadded for better S/N. Both procedures will save on storage space on the computer disk. Also, instead of saving every file, a threshold value (absorbance) can be entered in the computer where only those files which contain absorbing compounds will be stored (barring excessive random noise).

Finally, the aperture (APT) of the infrared beam can be stepped-down depending on how much throughput is needed. Typically, a full aperture is used for maximum signal throughput. One other fine-tune parameter is the use of low pass and high pass 4-pole Butterworth noise filters. Since optimal LPS and HPS filter settings are a function of mirror VEL, the manufacturer's values are normally used (Table 4). A

consequence of using such filters is usually less signal throughput, however. After the velocity, aperture and associated parameters have been set, the signal throughput can be fully optimized with an oscilloscope as described previously at the beginning of Column Selection and Interface Considerations.

Using the Model 26 lightpipe, MCT-B detector and a nitrogen gas purge for the IR bench, no more than 6 volts throughput was possible for an IR cell temperature of 270°C. As a point of reference, 25 volts throughput is possible when no lightpipe is in the path of the infrared beam. The 270°C lightpipe temperature was chosen since it is the highest recommended temperature possible for the cell (before the teflon seals begin to soften) and because gas chromatographic comparisons were desired when using higher boiling mixtures.

#### GC/FTIR Results:

Preliminary screening of the jet fuels using the 60 meter DB-5 column and Accuspec GC with microvolume TCD, directly, indicated that Aromatic Blending Stock VN-80-39 was a relatively simple fuel. Also, due to its previously suggested overall monoaromatic character<sup>18</sup>, this sample was considered to be an interesting fuel to examine. Five infrared windows were chosen in obtaining the real time CHEMIGRAM. Regions 3200-3030, 1650-1500 and 950-650  $\text{cm}^{-1}$  give characteristic aromatic absorbances while regions 3000-2800 and 1500-1300  $\text{cm}^{-1}$  give information regarding aliphatic C-H stretching and bending vibrations (See Figure 5). Instrument parameters are given on the CHEMIGRAM, and the information from each selected IR window region confirms

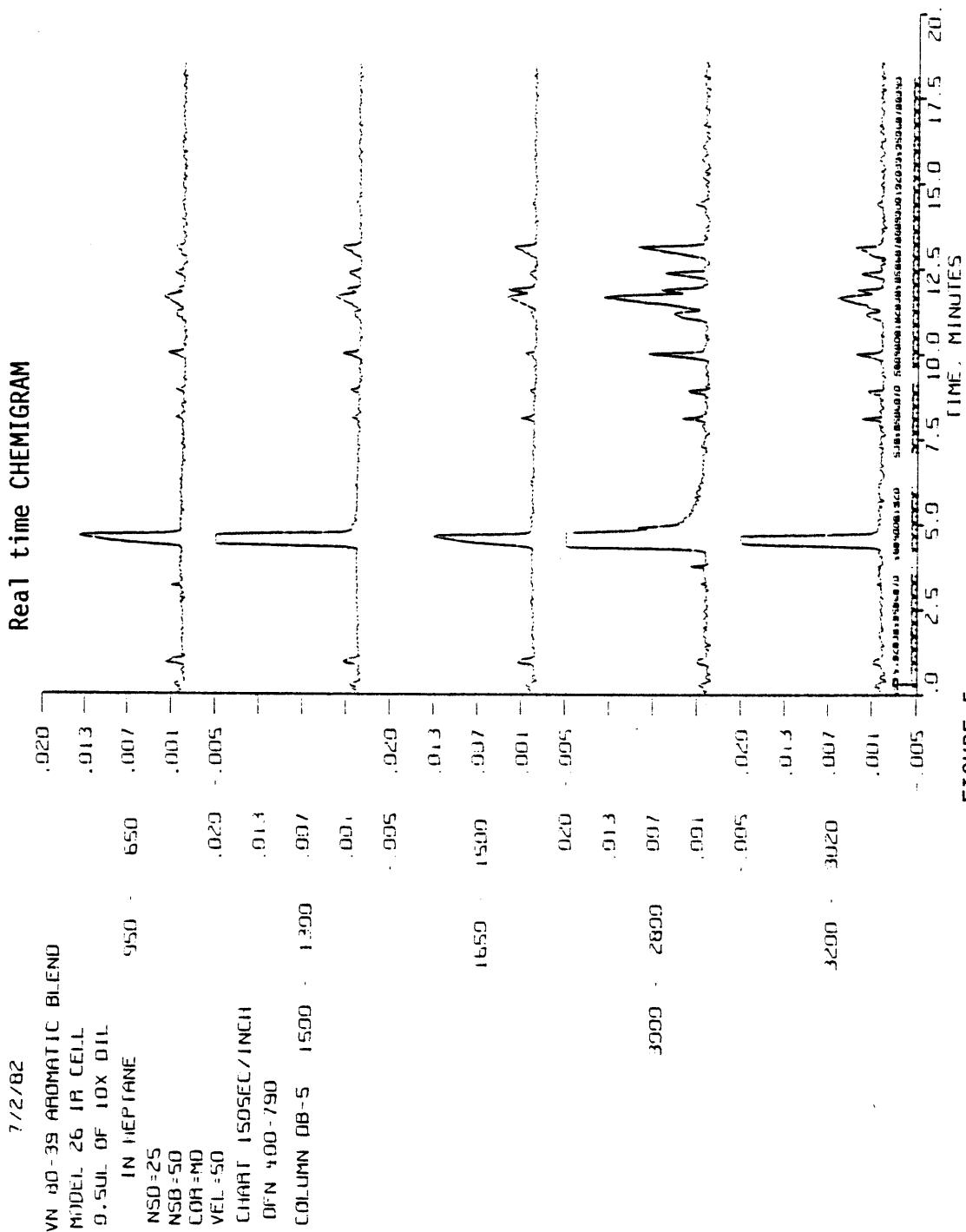


FIGURE 5

immediately the expected aromatic character. All window regions show a very strong absorbance for the heptane solvent because of the relatively large amount present. The TCD trace of this same separation indicates similar chromatography and relative peak intensities (Figure 6). The first three peaks in the TCD trace are assigned to air, freon (syringe cleaning fluid) and a hexane impurity, respectively.

Before Fourier transforming the jet fuel data to absorbance spectra, a chromatographic reconstruction based on this infrared information can be generated. Infrared window regions can be specified, whereby the resulting reconstruction is functional group specific, or the entire region  $4000\text{-}400\text{ cm}^{-1}$  may be chosen, most often done using the Gram-Schmidt orthogonalization<sup>21</sup> (See Figures 7-8).

✓ An extensive mathematical explanation pertaining to the generation of reconstructed chromatograms has been given by Hohne, et al.<sup>24</sup>. Briefly, the Gram-Schmidt reconstruction is a collection of orthogonal distances from a set of basis files (taken while no absorbing compounds are present) to each successive scan in the GC run. Compounds absorbing light (infrared) in the lightpipe change the shape of the interferogram. The change in shape increases the distance from the interferogram segment to the basis set. A plot of these distances appears as a set of peaks in the reconstruction. Whereas the Gram-Schmidt reconstruction uses infrared information from  $4000\text{-}400\text{ cm}^{-1}$ , specified IR window region reconstructs may give more useful information. Although the specified reconstructed chromatogram gives a reconstruct based on chemical class, this classification is not 100%

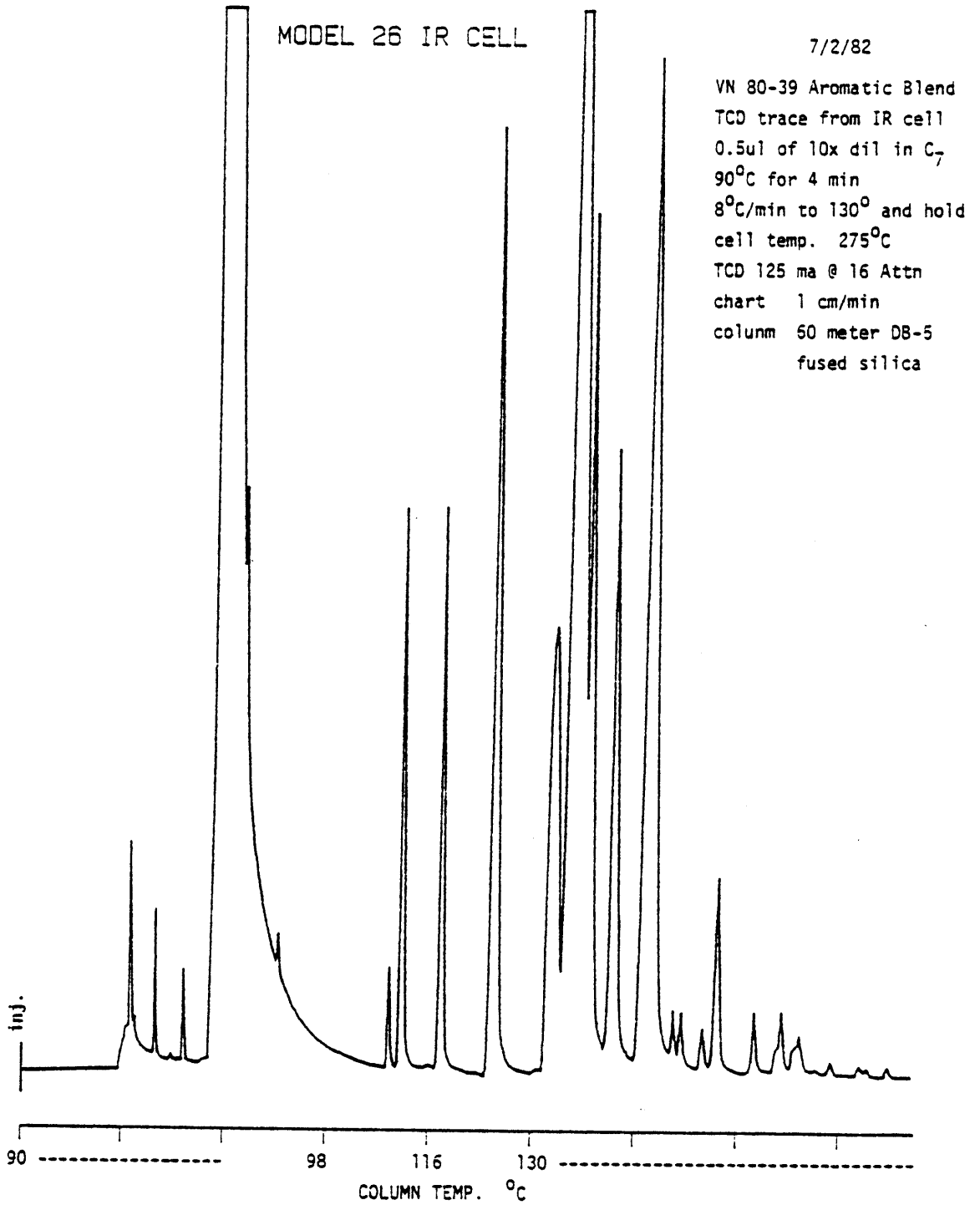
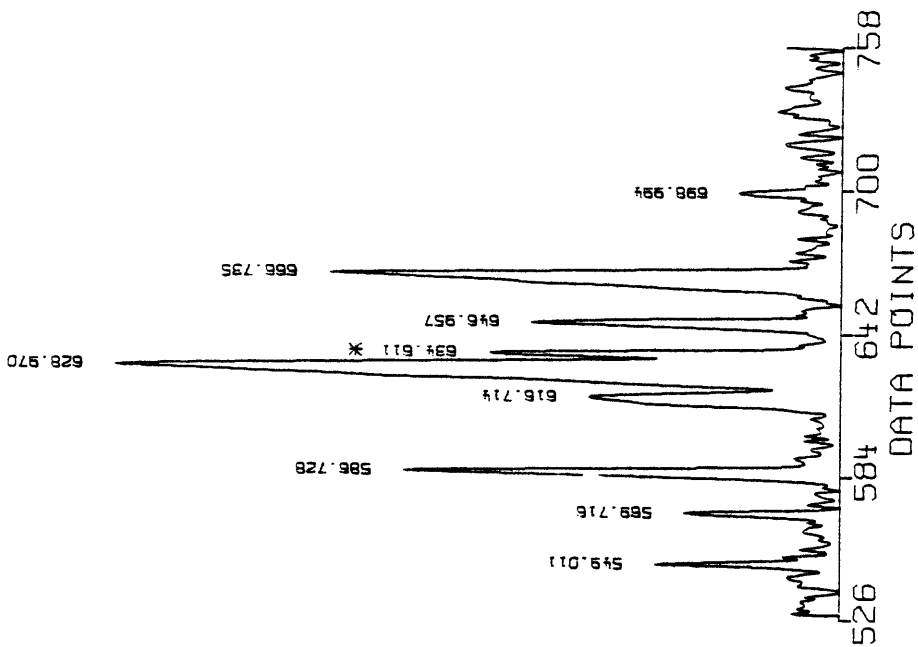


FIGURE 6

VN 80-39 (2800-3000 CM<sup>-1</sup>)  
W/ MODEL 26 IR CELL  
PPK



VN 80-39 GRAM-SCHMIDT  
RECONSTRUCTION MODEL 26 IR CELL  
PPK

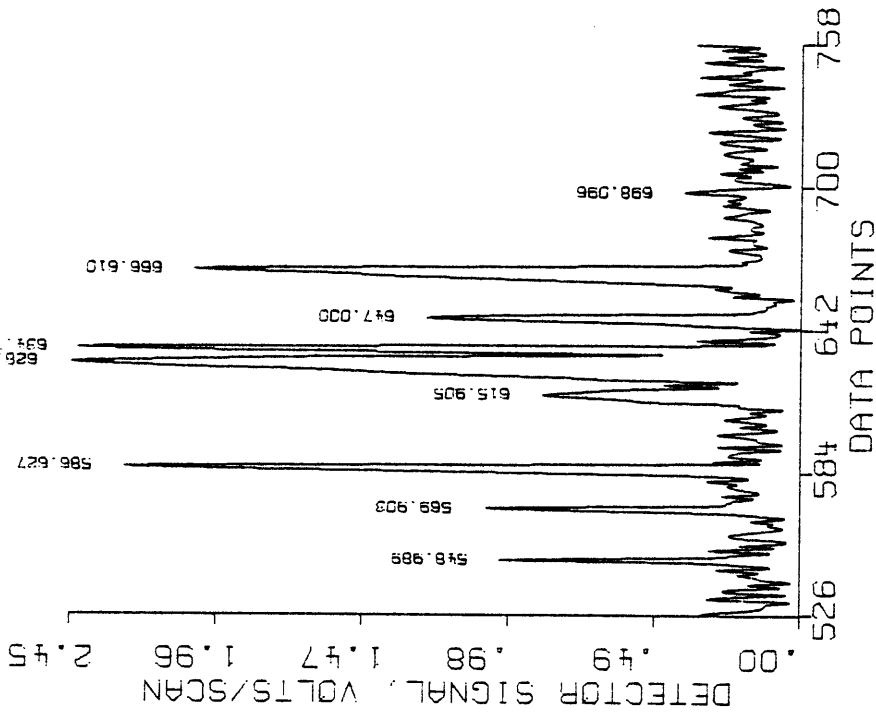


FIGURE 7

VN 80-39 (3020-3200 CM<sup>-1</sup>)  
PPK MODEL 26 IR CELL

VN 80-39 (650-950 CM<sup>-1</sup>) PPK  
MODEL 26 IR CELL

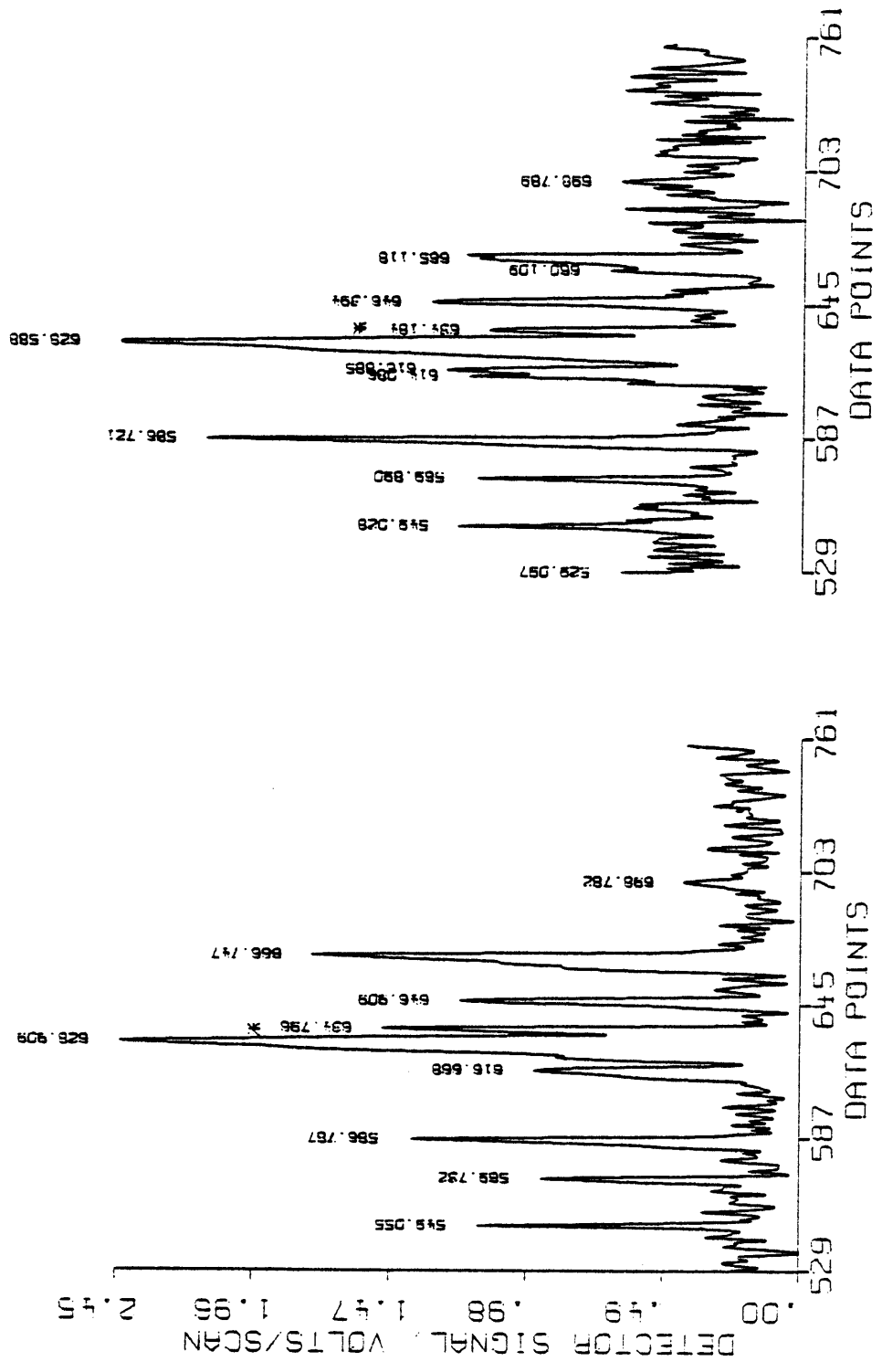
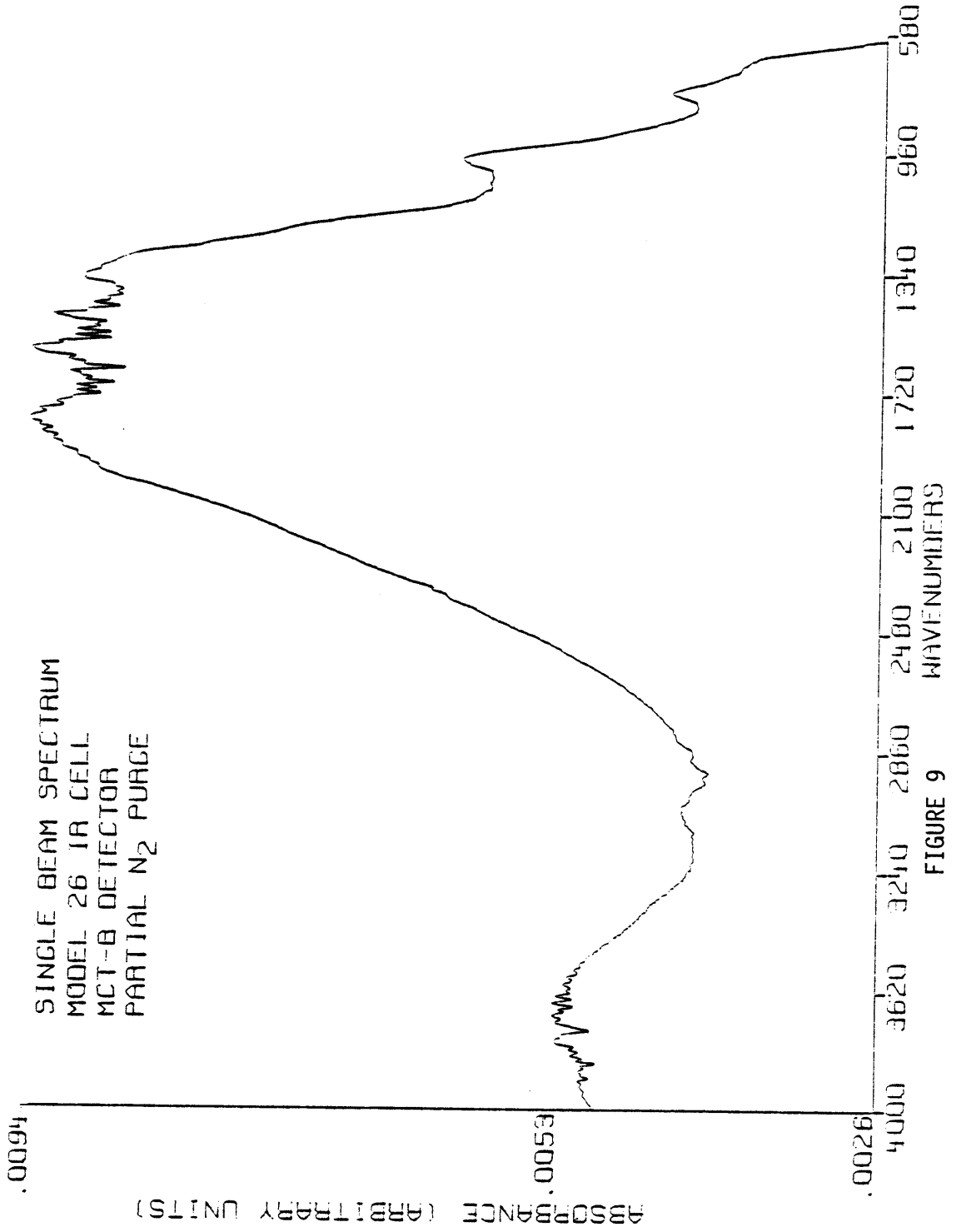


FIGURE 8

accurate. The inconsistency present is that no IR frequency exists where all compounds in a particular class absorb and no compounds not belonging to that class do not absorb. For this reason, class-specific reconstructions are only used as an aid in interpretation.

Comparison of the specified reconstructed chromatograms obtained from the interferometric data of VN-80-39 indicate a range of noise levels, particularly in the aromatic window regions 3200-3020 and 950-650  $\text{cm}^{-1}$ . The region 3200-3020  $\text{cm}^{-1}$  represents aromatic ring C-H stretching bands, and the 950-650  $\text{cm}^{-1}$  region contains information concerning out-of-plane C-H bending vibrations. Problems with S/N may be partially explained by reviewing the response curve for the MCT detector over the 4000-400  $\text{cm}^{-1}$  region. The overall response of the detector is found to be nonlinear in nature, where maximum throughput and S/N are achieved around 1600  $\text{cm}^{-1}$ . A single beam spectrum of the infrared background (Figure 9) can illustrate this nonlinear response where at lower areas in the spectrum S/N is generally decreased. As an example, the loss of sensitivity in the IR for aromatic compounds can be due partially to this response curve. In reviewing the response curve, one can see that the typical aromatic absorption regions (3200-3020  $\text{cm}^{-1}$  and 950-650  $\text{cm}^{-1}$ ) are at relative low points. Even though moderate IR absorption may occur in these regions, overall sensitivity is hindered by a low signal response. In spite of the low response for the region 3000-2800  $\text{cm}^{-1}$ , aliphatic C-H stretching vibrations (indicative of alkanes) still give good signal-to-noise since these infrared bands are so stable and intense. Problems with



signal-to-noise and throughput are therefore dependent on the overall absorbance characteristics of the species being examined. Of course, loss of throughput and signal-to-noise can also be related back to the short, narrow 2 mm i.d. x 6 cm lightpipe. The narrow bore (relative to the IR beam diameter) will cut down on throughput, and the short length may not provide the optimal cell pathlength necessary for sufficient sensitivity. Also, from looking at Figure 9 one can see that spectral interference from background CO<sub>2</sub> and water at around 1600 and 3600 cm<sup>-1</sup>, respectively, may occur. Although a constant nitrogen purge (transparent in the IR) of the optical bench is provided, changes in trace CO<sub>2</sub> and water levels remain a problem. Spectral subtractions would appear to alleviate such lingering background absorptions except that these levels may change significantly from the beginning to the end of a long gas chromatographic run.

After generating reconstructs of the chromatographic run (including the Gram-Schmidt reconstruct) the data are transformed to absorbance spectra using 4096 transformed points (NTP) ratioed to a transformed background file. Use of 4096 transform points ensures that the data file is zero filled from the end of the interferogram (NDP) to the end of the transform block. The 8 cm<sup>-1</sup> resolution spectra from such a transform can then be spectrally compared to the EPA (Environmental Protection Agency) vapor phase library for tentative identification.

Using the Nicolet computer, selected absorbance file spectra from VN-80-39 (Aromatic Blend) were software matched to EPA library file

spectra. A major peak at file #636 taken during the separation was used to illustrate the search and retrieval system. The location of this chromatographic peak is starred (\*) in each of the four reconstructs (Figures 7-8).

A description and understanding of the search and retrieval software is needed to fully appreciate its capabilities. Lowry et al. have fully described the search software and function for the Nicolet FTIR<sup>19</sup>. Briefly, the search routine uses any one of four algorithms and involves actual comparison of the sample spectrum with each member of the EPA search file. The EPA file contains 3300 component spectra of 16  $\text{cm}^{-1}$  resolution. Two algorithms, AB and SQ, use absolute difference and least squares approaches, respectively. The least squares metric (SQ) tends to weigh large differences in the spectra more than the absolute value calculation. In other words, one large difference between the sample and a reference spectrum is worse than an equivalent number of small ones. Two other algorithms, AD and SD, utilize the first derivatives of the sample spectrum and EPA file spectrum. The first derivative can use absolute or least squares metrics also. Advantages of the first derivative searches are to minimize the effects of sloping base line and/or excessive noise.

In operation, the search routine normalizes the sample spectrum to one absorbance unit and reduces it to 16  $\text{cm}^{-1}$  resolution, although the original spectrum is not destroyed (i.e. 8  $\text{cm}^{-1}$ ). The search may cover the entire range 4000-400  $\text{cm}^{-1}$  or it may be selectively specified by

blanking out certain regions of the spectrum where excessive noise or background compounds (such as carbon dioxide and water) may occur. Typically, the region 650-400  $\text{cm}^{-1}$  is blanked where little or no information is expected for that region. This region also has the worst S/N ratio of the entire IR spectrum due to low throughput. One should realize, however, that blanking too many regions can lead to inaccurate searches since vital information may not be entered. Usually, when excessive blanking is done, several compounds having a variety of functional groups may be retrieved because of the limited spectral range available. For instance, blanking of the amine absorption region may still give amines as possible matches since other wavenumber regions may be similar. In the search "RESULTS", the possible compound names (HITS) are given with each HIT location number in the EPA vapor phase library. The number below and to the right of the EPA file number indicates the match similarity (Figure 10). A smaller number coincides with a better match where zero (0) is a perfect match. Typical "match values" range from 50 to 3000 depending on the noise level of the sample spectrum. Each match listed beneath the first is the second, third, fourth, etc. "best match". Up to 32 "best matches" can be listed. The general rule adopted is that if the first "match value" is one half of the second "match value" (for the SQ algorithm in particular) then a reasonable amount of certainty can be expected. A spectral search for a minor component, file spectrum #700, from VN-80-39 gives a high match value due to the low S/N (Figure 11).

EPA VAPOR PHASE  
 BENZENE, 1,3,5-TRIMETHYL-

MODEL 26 IR CELL

.SRQ  
 ENTER SKIP REGIONS, NEGATIVE NO. IF DONE  
 LOW LIMIT 400  
 HIGH LIMIT 650  
 LOW LIMIT 3500  
 HIGH LIMIT 4000  
 LOW LIMIT -1  
 MAX FOR SCALING, NEG IF AUTO -1

EPA VAPOR PHASE  
 POSSIBLE HITS  
 799 BENZENE, 1,3,5-TRIMETHYL-,  
 295 IR C E  
 2498 BENZENE, 1,2,3,5-TETRAMETHYL-,  
 1763 IR B C E  
 75 BENZENE, 1,2,4-TRIMETHYL-,  
 2247 IR B D  
 914 BENZENE, 1,2,3,4-TETRAMETHYL-,  
 2650 IR B C D  
 222 3,5-LUTIDINE  
 2672 T6NJ C E  
 1190 BENZENE, HEXAMETHYL-,  
 2722 U 6-R  
 1107 BENZENE, 1,2,4,5-TETRAMETHYL-,  
 2731 IR B D E  
 457 2-BUTENE, 2,3-DIMETHYL-,  
 2602 1Y&UY  
 2476 BENZENE, 1-ETHYL-3-METHYL-,  
 2865 2R C  
 1600 CUMENE, 3,5-DIMETHYL-,  
 3017 1YR C E

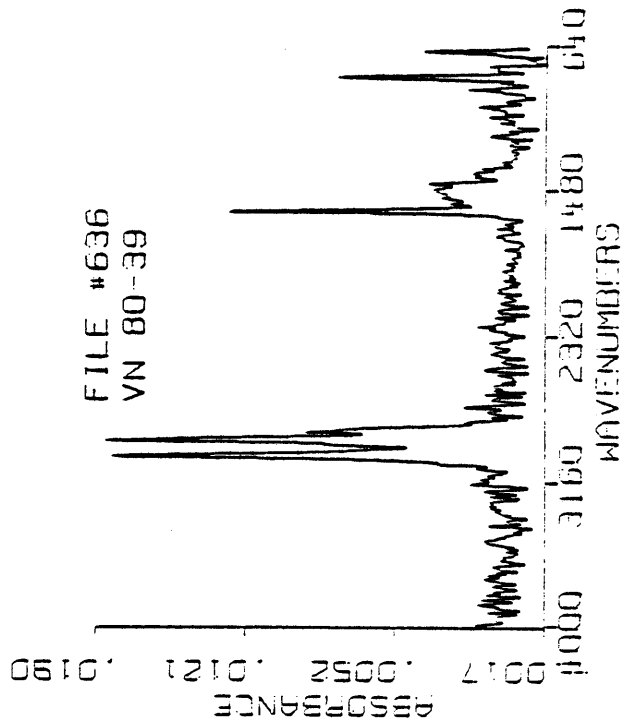
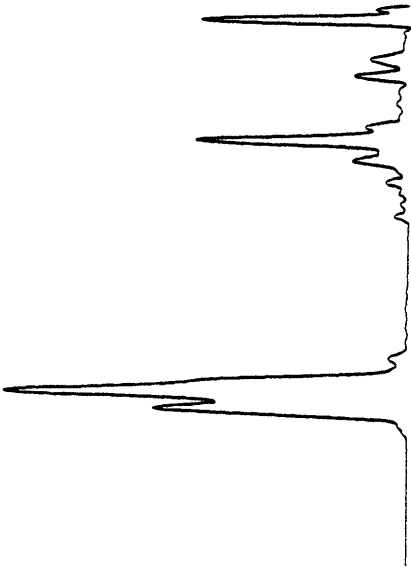


FIGURE 10

EPA VAPOR PHASE  
 BENZENE, 1,2,3-TRIMETHYL-

MODEL 26 IR CELL



SRQ  
 ENTER SKIP REGIONS, NEGATIVE NO. IF DONE  
 LOW LIMIT 400  
 HIGH LIMIT 670  
 LOW LIMIT 3500  
 HIGH LIMIT 4000  
 LOW LIMIT -1  
 MAX FOR SCALING, NEG IF AUTO -1

EPA VAPOR PHASE  
 POSSIBLE HITS  
 923 BENZENE, 1,2,3-TRIMETHYL-,  
 2533 IR B C  
 2476 BENZENE, 1-ETHYL-3-METHYL-,  
 3188 2R C  
 914 BENZENE, 1,2,3,4-TETRAMETHYL-,  
 3475 IR B C D  
 1190 BENZENE, HEXAMETHYL-,  
 3865 U 6-R  
 2498 BENZENE, 1,2,3,5-TETRAMETHYL-,  
 3927 IR B C E  
 2666 OCTANE, 3,6-DIPHENYL-,  
 4137 2YR&2YR&2  
 41 2-BUTENE, 2-METHYL-,  
 4178 YD2  
 75 BENZENE, 1,2,4-TRIMETHYL-,  
 4187 IR B D  
 902 BENZENE, BUTYL-,  
 4324 4R  
 2489 TOLUENE, O-ETHYL-,  
 4329 2R D

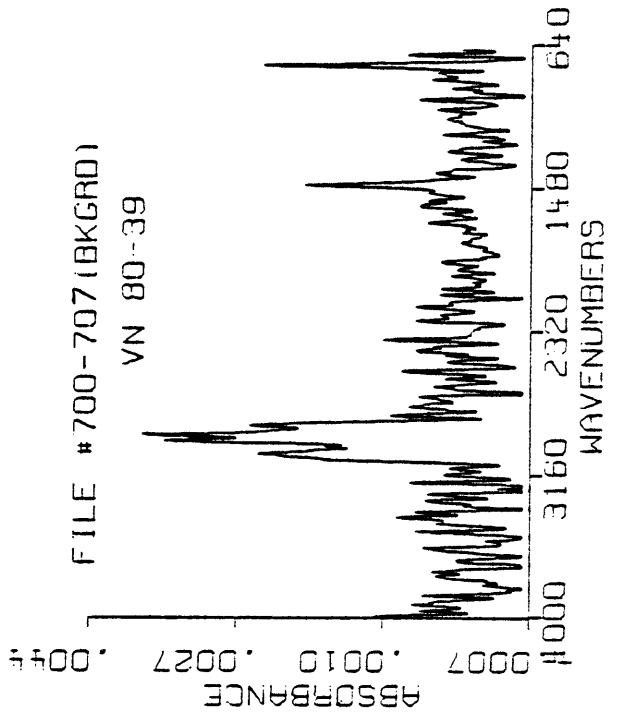


FIGURE 11

Even so, most of the other choices listed indicate a substituted benzene compound. An SQ algorithm was used in the search and a spectral subtraction done prior to the search. The background file spectrum #707 is subtracted from file spectrum #700 to eliminate CO<sub>2</sub> and water. The presence of these background compounds do affect the search results. A search of a major component, file spectrum #636, gives a more certain match with the other choices again being very similar, i.e. substituted benzenes (Figure 10). It is evident that different substitution on benzene does give rise to different absorption patterns.

Recalling that the search routine reduces the sample file spectrum from 8 cm<sup>-1</sup> to 16 cm<sup>-1</sup>, temporarily, Figures 12 and 13 illustrate the actual 16 cm<sup>-1</sup> spectra which were being matched. An obvious shortcoming of the present search system is that the same signal-to-noise ratios are not shared by both sample and EPA files. In addition, although normalized to an absorbance of 1.0, the actual spectrometer conditions under which the EPA library was formulated are not known. Most likely, a maximum number of scans was taken and coadded to produce a relatively noise-free spectrum. Also, overtone IR bands indicate that the EPA standards were concentrated to some extent. Both of these procedures can lead to library spectra which may not represent on-the-fly conditions, making spectral matching ambiguous when low S/N and overlapping GC peaks are encountered. Problems arise particularly when searching alkanes because of limited infrared information. One advantage of the present search system, however, is that additional

RTN = EPA VAPOR PHASE  
799 BENZENE, 1,3,5-TRIMETHYL-,  
16 CM-1

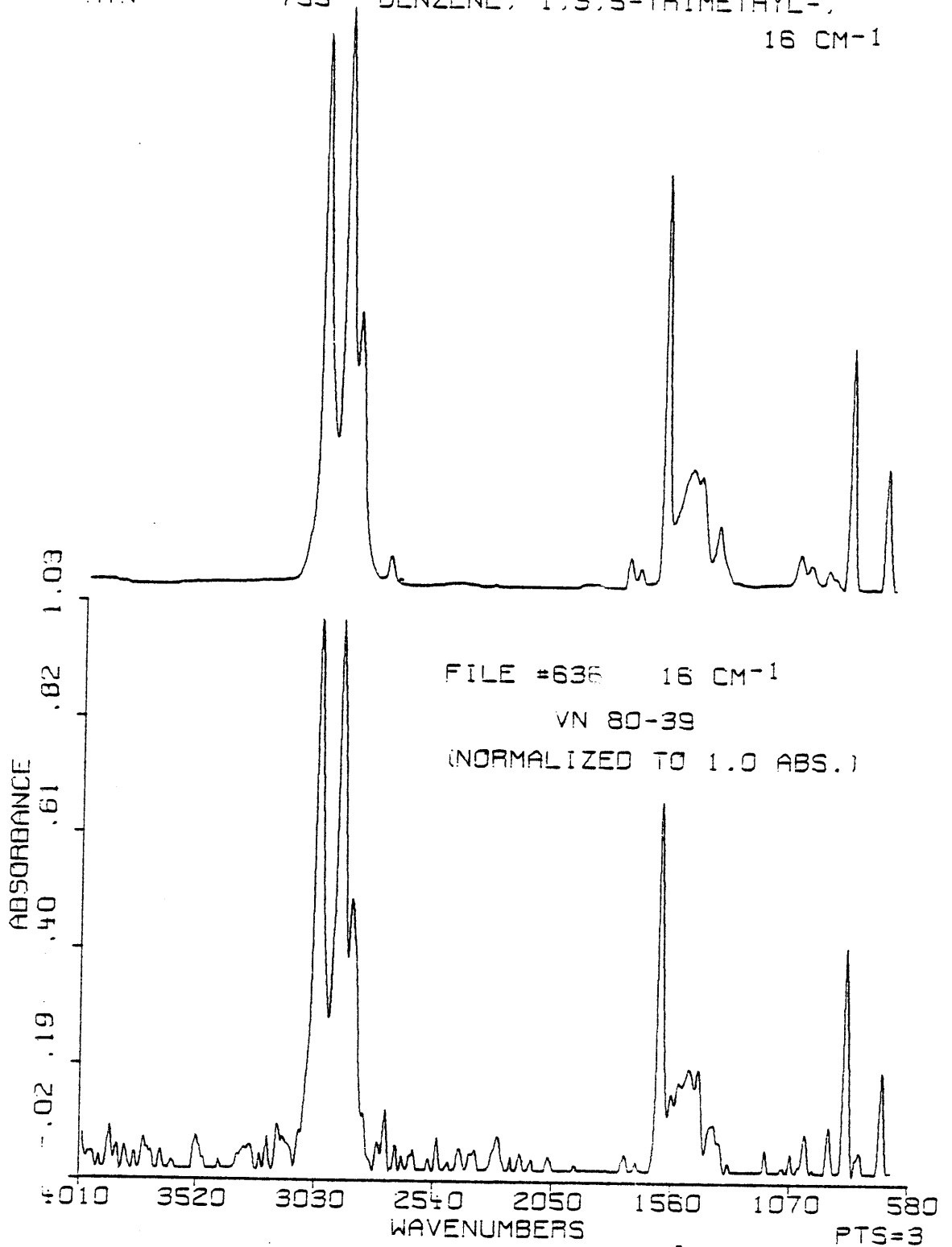


FIGURE 12. File Spectrum #636 (16cm<sup>-1</sup>) VN80-39

EPA VAPOR PHASE  
RTN = 923 BENZENE, 1,2,3-TRIMETHYL-

16 CM<sup>-1</sup>

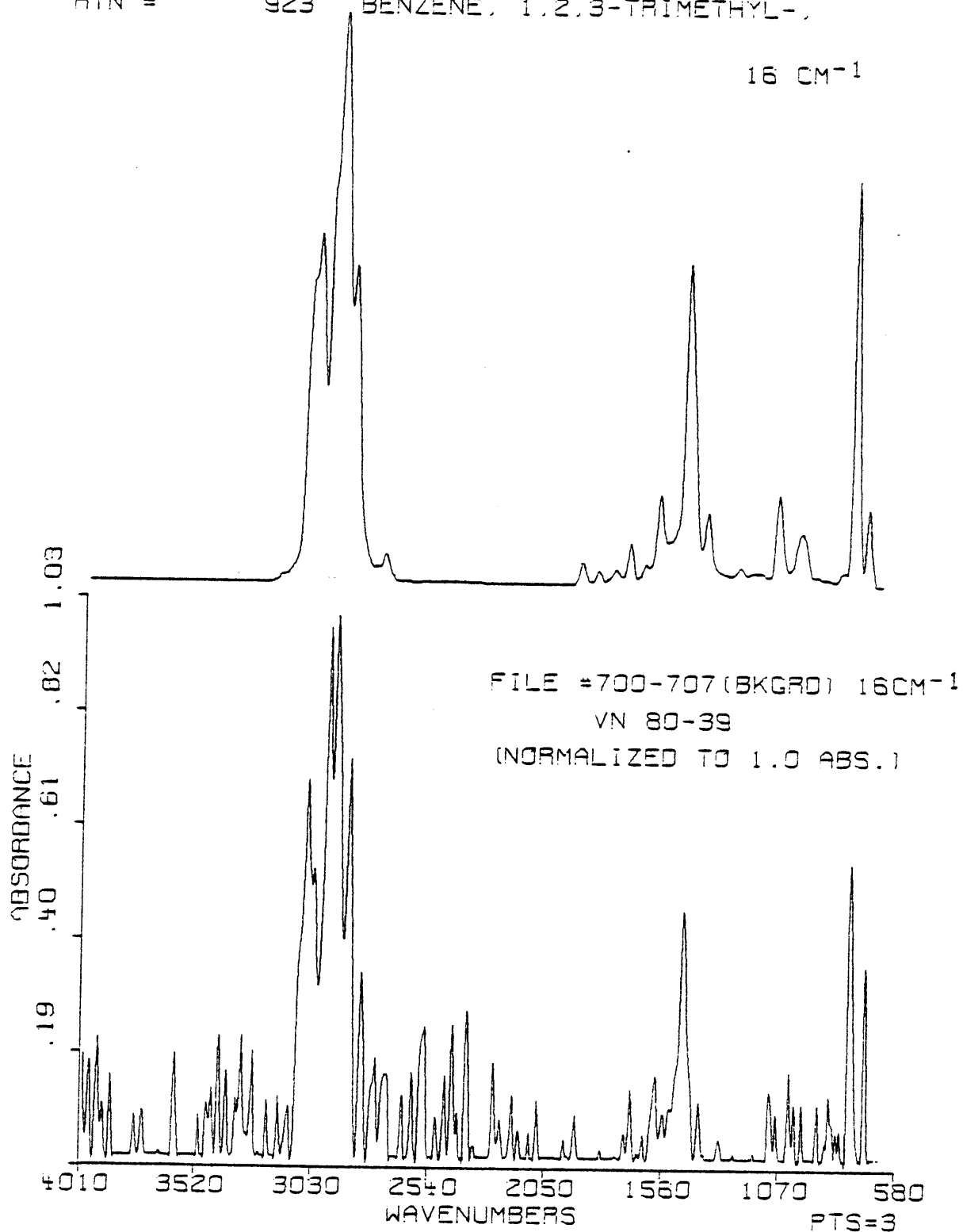


FIGURE 13. File Spectrum #700-707 (16cm<sup>-1</sup>)

spectra may be added to the library (for instance straight chain alkanes) which may more closely mimic on-the-fly conditions. From an examination of the infrared file spectra taken during the separation of VN-80-39 with the Model 26 IR cell, it appears that better infrared detection is needed if truly complex samples composed of a wide concentration range of individual components are to be analyzed. The spectral matching results from the library searches confirm the need for a more optimum system. One idea was to increase the throughput of IR signal by increasing the lightpipe inner diameter from 2 mm to 3 mm (Model 36). A consequence of this change was a doubling of dead volume from 0.2 ml to 0.4 ml. Use of the same make-up gas (He) at 5 ml/min, however, was found to cause not much more band broadening than the Model 26 cell. For example, a thermal conductivity trace (positioned after IR cell) using the 60 meter DB-5 column and Model 36 lightpipe of VN-80-39 indicates little additional band broadening over the Model 26 (Figure 14). Figure 15 illustrates the spectrum and search results for a major peak in the VN-80-39 separation using the wider bore lightpipe with the same sample volume injected. This spectrum corresponds to the same component peak searched using the Model 26 cell, (compare Figure 10 with 15). Slightly lower noise levels are seen with the Model 36 cell although overall S/N is about the same with both cells. A dilution effect is most likely occurring when using the Model 36 due to its relatively large dead volume and swift 5 ml/min make-up helium gas. Although the component absorbance is less with the Model 36 cell, the

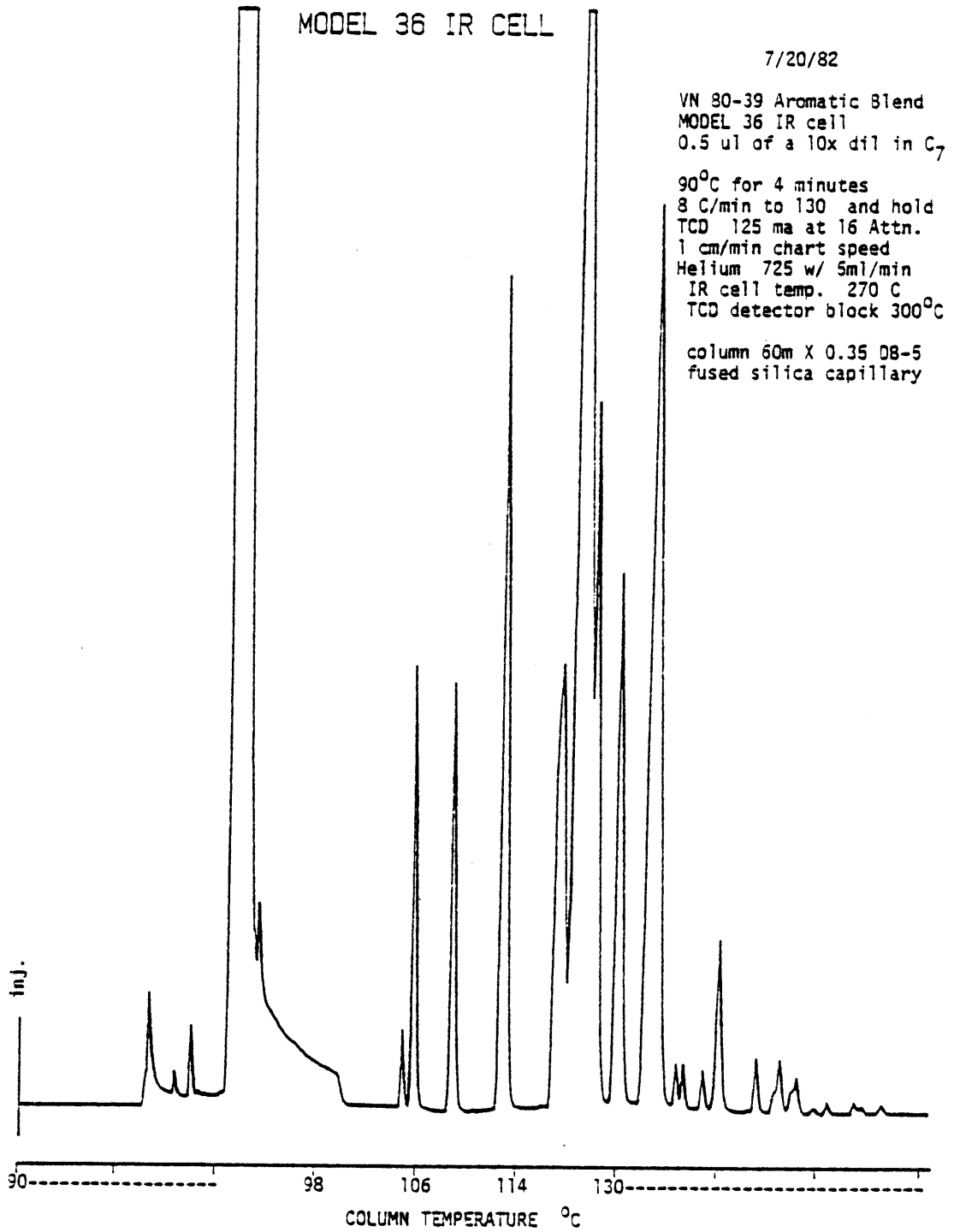
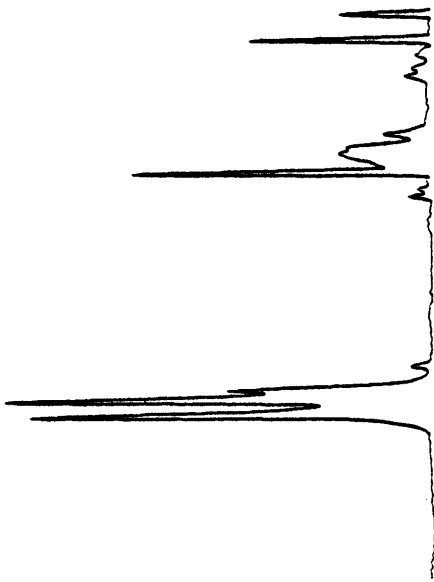


FIGURE 14. TCD trace

MODEL 36 IR CELL

EPA VAPOR PHASE  
BENZENE, 1,3,5-TRIMETHYL-



•SKG  
 ENTER SKIP REGIONS, NEGATIVE NO. IF DONE  
 LOW LIMIT 400  
 HIGH LIMIT 650  
 LOW LIMIT 3500  
 HIGH LIMIT 4000  
 LOW LIMIT -1  
 MAX FOR SCALING, NEG IF AUTO -1

EPA VAPOR PHASE  
 POSSIBLE HITS  
 799 BENZENE, 1,3,5-TRIMETHYL-,  
 IR C E  
 274  
 2498 BENZENE, 1,2,3,5-TETRAMETHYL-,  
 IR B C E  
 1807  
 75 BENZENE, 1,2,4-TRIMETHYL-,  
 IR B D  
 2306  
 457 2-BUTENE, 2,3-DIMETHYL-,  
 1Y&UY  
 2718  
 1190 BENZENE, HEXAMETHYL-,  
 U 6-R  
 2740  
 222 3,5-LUTIDINE  
 T6NJ C E  
 2756  
 1107 BENZENE, 1,2,4,5-TETRAMETHYL-,  
 IR B D E  
 2763  
 914 BENZENE, 1,2,3,4-TETRAMETHYL-,  
 IR B C D  
 2820  
 103 2,4-HEXADIENE, 2,5-DIMETHYL-,  
 1Y&UZUY  
 2874  
 41 2-BUTENE, 2-METHYL-,  
 YU2

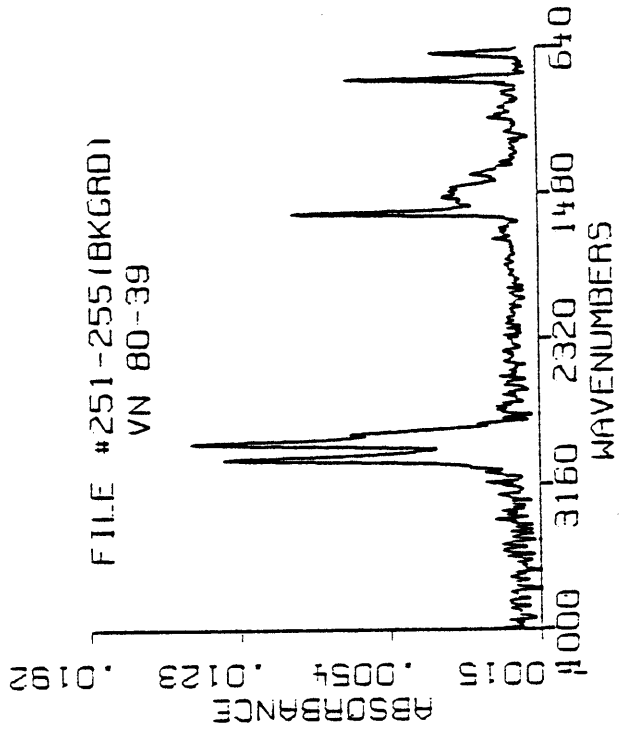


FIGURE 15

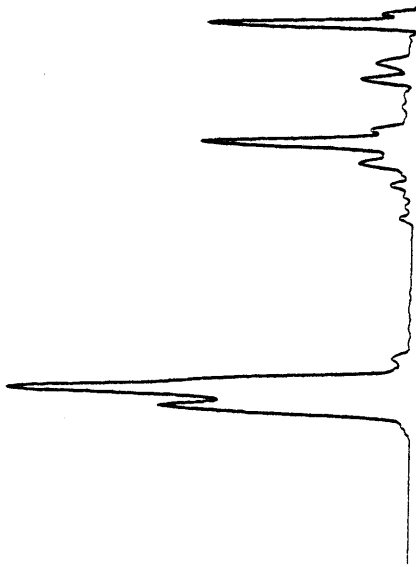
reduction in random noise benefits library search efforts. The same type of phenomena is seen for a minor component in the separation at file spectrum #334 using the Model 36 (Figure 16). The corresponding peak spectrum from using the Model 26 lightpipe (Figure 11) is much noisier than its Model 36 counterpart although S/N is roughly equivalent. Therefore, with very low concentration components, overall noise levels will greatly affect the reliability of the library search.

One other advantage of the Model 36 is that manipulation of the IR lightpipe for optimization of the infrared signal is easier than for the Model 26, due to its wider inner bore. In addition, twice the throughput (13 volts at 270°C) was attainable using the wider 3 mm x 6 cm lightpipe (Model 36) over the 2 mm i.d. cell.

To pursue a more complex sample, a test Jet Fuel derived from shale oil (VN-77-11) was separated on the 60 meter DB-5 fused silica column with FTIR detection through the Model 36 IR cell. A Gram-Schmidt reconstruction for VN-77-11 (Figure 17) indicates good separation despite the additional IR cell dead volume. A good signal to noise ratio is achieved with only 0.25  $\mu$ l of jet fuel sample injected. An EPA library search of one minor component, file spectrum #136, illustrates a good match followed by very similar second and fourth choices (Figure 18). Another search, file spectrum #224, gives excellent S/N and a confident search listing for the larger alkane peak (Figure 19). Good signal to noise for these components of the sample may be explained by the strong absorption character of alkanes (in

EPA VAPOR PHASE  
 BENZENE, 1,2,3-TRIMETHYL-,

MODEL 36 IR CELL



.SRQ  
 ENTER SKIP REGIONS, NEGATIVE NO. IF DONE  
 LOW LIMIT 400  
 HIGH LIMIT 650  
 LOW LIMIT 3500  
 HIGH LIMIT 4000  
 LOW LIMIT -1  
 MAX FOR SCALING, NEG IF AUTO -1

EPA VAPOR PHASE  
 POSSIBLE HITS  
 929 BENZENE, 1,2,3-TRIMETHYL-,  
 1R B C  
 2145 BENZENE, 1-ETHYL-3-METHYL-,  
 2476 2R C  
 3508 M-XYLENE  
 78 1R C  
 3656 1R C  
 914 BENZENE, 1,2,3,4-TETRAMETHYL-,  
 1R B C D  
 3920 BENZENE, 1,2,3,5-TETRAMETHYL-,  
 2498 1R B C E  
 4111 1R B D  
 75 BENZENE, 1,2,4-TRIMETHYL-,  
 4401 BENZENE, HEXAMETHYL-,  
 1150 U 6-R  
 4489 TOLUENE, O-ETHYL-,  
 2489 2R B  
 4497 PYRIDINE, 2-PENTYL-,  
 1549 TGHJ R5  
 4552 OCTANE, 3,6-DIPHENYL-,  
 2666 2YR&2YR&2  
 4586

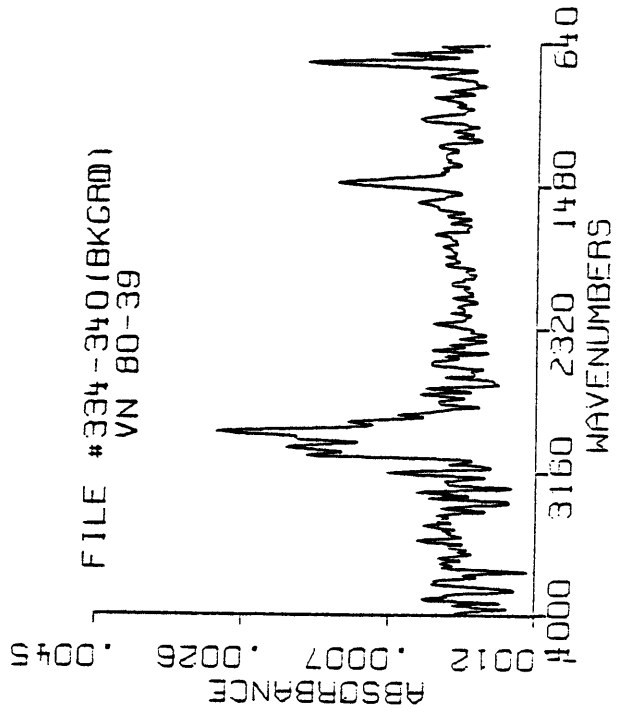


FIGURE 16

VN 77-11 TEST JET FUEL  
MODEL 36 IR CELL  
GRAM-SCHMIDT RECONSTRUCTION  
60 METER DB-5 FUSED SILICA  
CAPILLARY COLUMN  
MCT-B DETECTOR

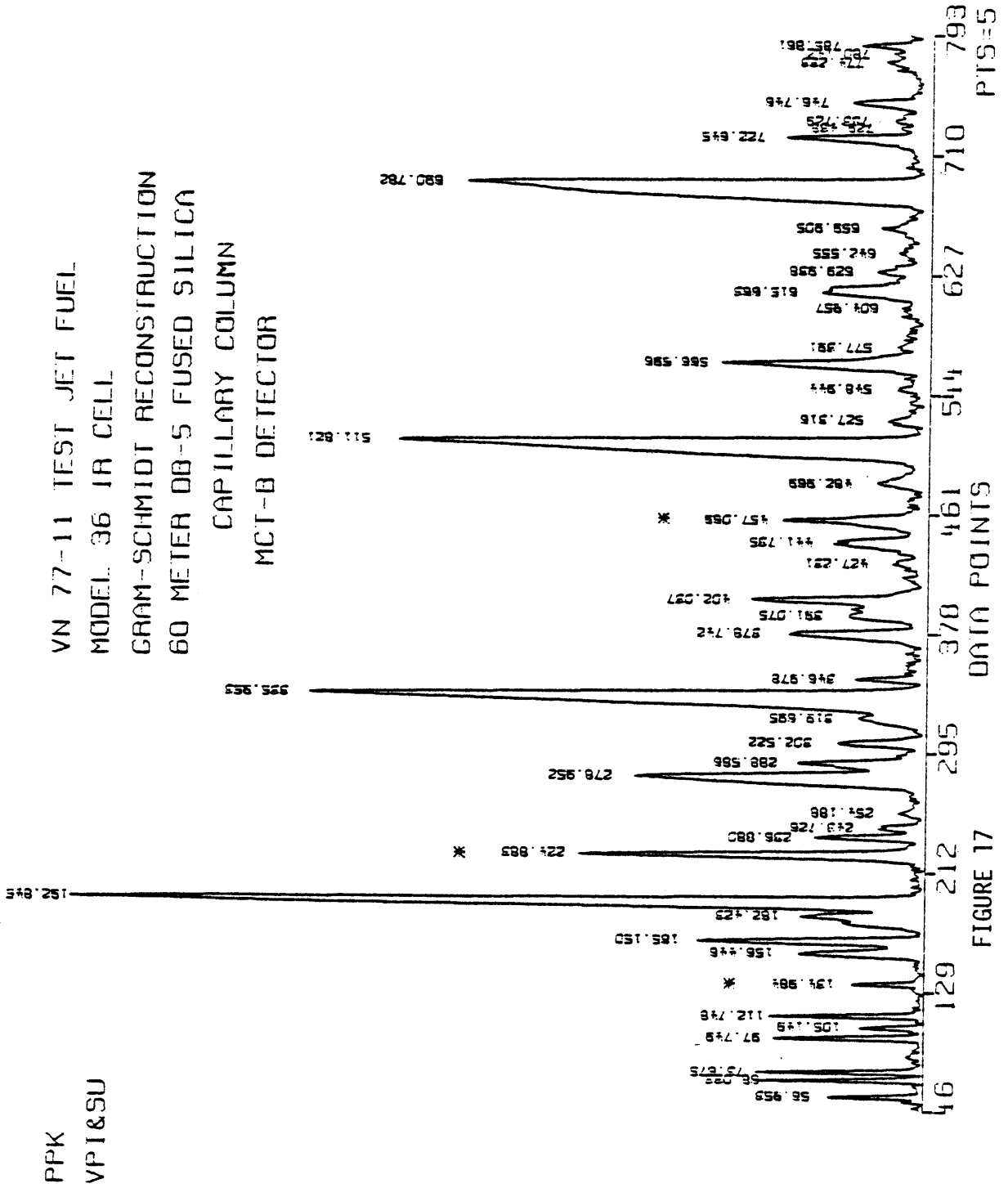


FIGURE 17

PPK  
VPI&SU

EPA VAPOR PHASE  
CYCLOPENTANE, METHYL-

MODEL 36 IR CELL

.SRQ  
ENTER SKIP REGIONS, NEGATIVE NO. IF DONE  
LOW LIMIT 400  
HIGH LIMIT 650  
LOW LIMIT 3600  
HIGH LIMIT 4000  
LOW LIMIT -1  
MAX FOR SCALING, NEG IF AUTO -1

EPA VAPOR PHASE  
POSSIBLE HITS  
45 CYCLOPENTANE, METHYL-,  
101 LSTJ A  
2480 CYCLOPENTANE  
173 LSTJ  
2494 HEPTANE, 2,2-DIMETHYL-,  
183 5X  
2583 CYCLOPENTANE, BUTYL-,  
244 LSTJ A4  
922 HEPTANE, 3,3-DIMETHYL-,  
254 4X2  
47 BUTANE, 2-METHYL-,  
291 2Y  
2930 ISOBUTANE  
292 1Y  
2907 BUTANE  
328 4H  
43 HEXANE, 2,2,5-TRIMETHYL-,  
346 1Y&2X  
802 HEXANE, 2,2,4-TRIMETHYL-,  
367 2Y&1X

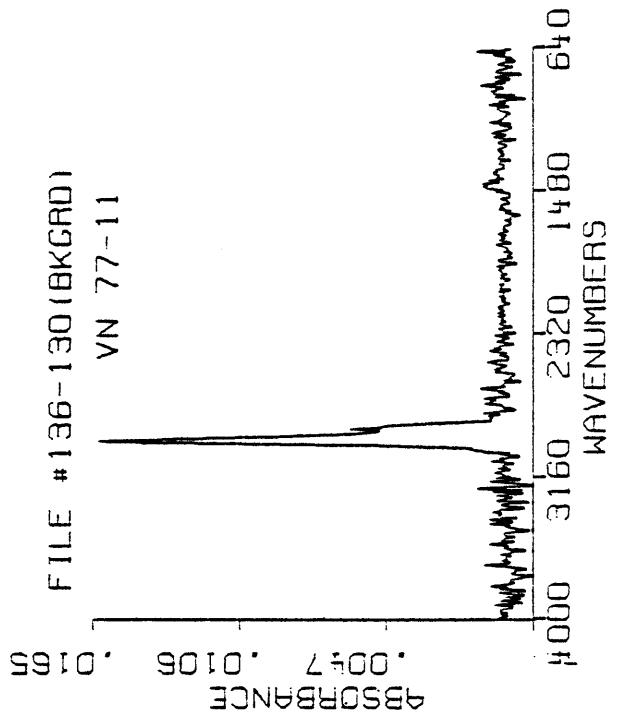
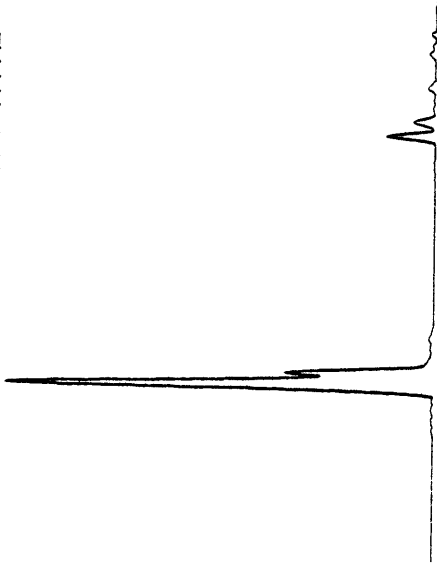


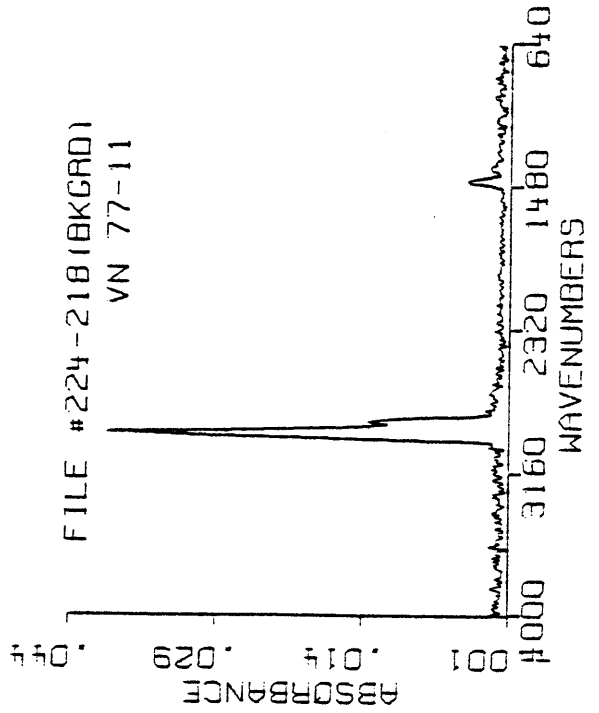
FIGURE 18

EPA VAPOR PHASE  
CYCLOHEXANE, 1,1-DIMETHYL-, C

MODEL 36 IR CELL



FILE #224-218(BKGRD)  
VN 77-11



.SRQ  
ENTER SKIP REGIONS, NEGATIVE NO. IF DONE  
LOW LIMIT 400  
HIGH LIMIT 700  
LOW LIMIT -1  
MAX FOR SCALING, NEG IF AUTO -1

EPA VAPOR PHASE

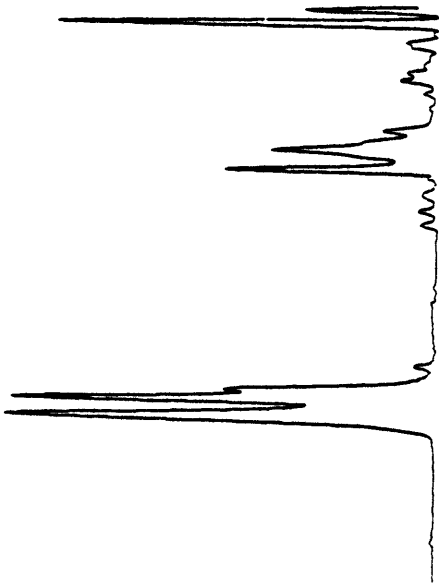
POSSIBLE HITS

- |      |                                 |
|------|---------------------------------|
| 646  | CYCLOHEXANE, 1,1-DIMETHYL-, C   |
| 48   | L6J A A                         |
| 2553 | HEPTADECANE, 6,9,12-TRIPROPYL-, |
| 155  | SY382 2Y3                       |
| 121  | CYCLOHEXANE, CIS-1,3-DIMETHYL-, |
| 173  | L67J A C -C                     |
| 2206 | UNDECANENITRILE                 |
| 176  | NC10                            |
| 2554 | HEPTADECANE, 6,12-DIETHYL-9-    |
| 176  | SY282 2Y5                       |
| 2155 | OCTYL DISULFIDE                 |
| 178  | 8338                            |
| 887  | NONANE                          |
| 179  | 9H                              |
| 2555 | HEXADECANE, 6,11-DIPENTYL-,     |
| 179  | SY382 2                         |
| 895  | OCTANE                          |
| 181  | 8H                              |
| 1768 | CYCLOHEXANE, 1-METHYL-,         |
| 193  | L607J A                         |

FIGURE 19

particular the C-H stretching vibrations) coupled with better throughput of the Model 36 cell. A third component showing absorbance in all five monitored IR window regions of the CHEMIGRAM (i.e. 3200-3020, 3000-2800, 1650-1500, 1500-1300 and 950-700  $\text{cm}^{-1}$ ) appears to be the co-elution of an aromatic and an aliphatic material. Subtraction of file spectrum #455 from #461 yields the spectrum shown in Figure 20. A spectral search using the SQ algorithm and select blanking identified the component tentatively as m-xylene. Here-in lies a true advantage of FTIR when coeluting peaks occur. The subtraction technique can subtract the absorbances of one spectrum from another. The actual subtraction can be performed so that 100% of one file spectrum is subtracted out of another. In addition, different percentages of spectrum A can be subtracted from spectrum B. The software allows increments of about 1% to be subtracted either plus or minus. With such a capability, co-eluting peaks (which may be present in different concentrations) can be subtracted in such a manner as to give a final spectrum conducive to library searching. While the subtraction of one component from another may lead to some arbitrary spectrum, this result should always be viewed with caution. Ambiguous and sometimes faulty conclusions can occur. For the subtracted peak in question, however, further evidence to be given later will support the present hypothesis. This test jet fuel was found to be a good example of a predominantly alkane-type mixture which agrees with the 85% alkane content previously determined by Dorn et al. with LC-NMR18.

EPA VAPOR PHASE  
M-XYLENE



MODEL 36 IR CELL

.SRQ  
ENTER SKIP REGIONS, NEGATIVE NO. IF DONE  
LOW LIMIT 400  
HIGH LIMIT 660  
LOW LIMIT 3600  
HIGH LIMIT 4000  
LOW LIMIT -1  
MAX FOR SCALING, NEG IF AUTO -1

EPA VAPOR PHASE  
POSSIBLE HITS

78	M-XYLENE
1655	IR C
923	BENZENE, 1,2,3-TRIMETHYL-,
3212	IR B C
871	P-XYLENE
3279	IR D
2476	BENZENE, 1-ETHYL-3-METHYL-,
3824	IR C
2222	BENZYLAMINE, 2,5-DIMETHYL-,
3941	ZIR B E
75	BENZENE, 1,2,4-TRIMETHYL-,
3964	IR B D
799	BENZENE, 1,3,5-TRIMETHYL-,
4157	IR C E
342	BITOLYL, M,MPR-,
4368	IR CR C
2200	ETHANETHIOL, 2-/BENZYLAMINO/-,
4387	SHENIR
2470	2,4-HEXADIENE
4408	20202

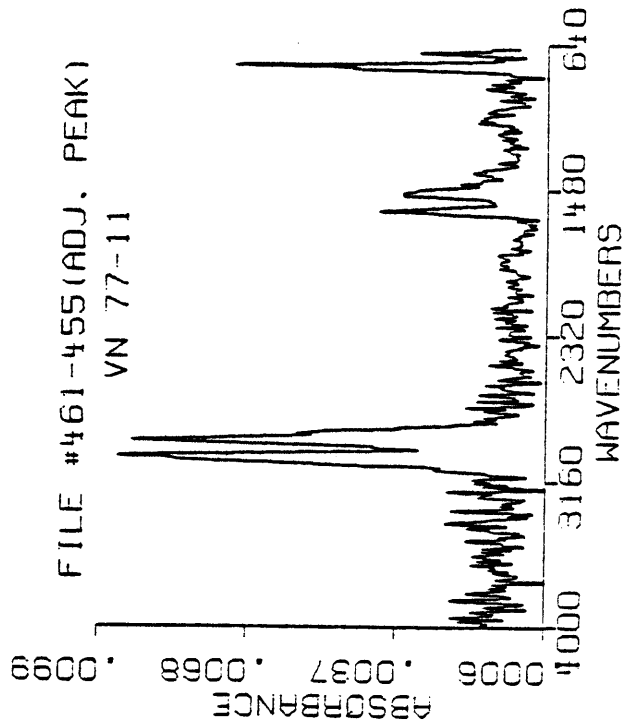


FIGURE 20

To get an idea of the detection limits possible for this GC-FTIR configuration, a twelve component mixture of alkanes, cyclic aliphatics and aromatics was separated chromatographically using the DB-5 column and Model 36 cell. Concentration ranges varied from 1.7  $\mu\text{g}$  injected of trans-decalin down to about 60 ng of indan. The indan was invariably lost in the background noise but decane (730 ng), trans-decalin (1.7  $\mu\text{g}$ ) and m-xylene (1.15  $\mu\text{g}$ ) gave reasonable S/N spectra. The spectrum (Figure 21), taken at the peak maximum, gave good response and a "confident" match for trans-decalin (note the position of cis-decalin isomer in the listing). The m-xylene component, however, showed considerably less IR response due to weaker aromatic-type absorbance. The high (1108) "match value" demonstrates a low S/N although 1.15  $\mu\text{g}$  had been injected (Figure 22). Injection of 730 ng of decane shows strong absorbance around  $2900\text{ cm}^{-1}$  but the library search is not very reliable due to so little infrared information (Figure 23). In the decane search results, the number one and two matches are standard spectra taken on-the-fly from previous chromatographic runs and then added to the library. Here, an example of the need for spectra representing real on-the-fly conditions is shown. Such representative library spectra are needed more for straight-chain hydrocarbons than for perhaps any other class of compounds. Spectral matching for these straight-chain aliphatics demands the most from the search software. Low S/N conditions often result in ambiguous matching in which reliable identification becomes impossible.

EPA VAPOR PHASE  
BICYCLO/4.4.0/DECANE

MODEL 36 IR CELL

SRR  
ENTER SKIP REGIONS, NEGATIVE NO. IF NONE  
LOW LIMIT 400  
HIGH LIMIT 750  
LOW LIMIT 3600  
HIGH LIMIT 4000  
LOW LIMIT -1  
MAX FOR SCALING, NEG IF AUTO -1

EPA VAPOR PHASE

POSSIBLE HITS

- 241 BICYCLO/4.4.0/DECANE
- 66 L66TJ
- 446 CYCLOOCTANE
- 137 L8TJ
- 2576 METHYLAMINE, 1-CYCLOHEPTYL-
- 149 L7TJ A12
- 1312 FENTACOSANE
- 161 25H
- 2314 HDRIADECYLAMINE
- 165 219
- 1038 NAPHTHALENE, DECAHYDRO-, CIS-
- 184 L66TJ
- 137 CYCLOHEXANE, PENTYL-, C
- 197 L6TJ A5
- 1276 TRICOSANE
- 198 23H
- 2316 PENTADECYLAMINE
- 208 215
- 417 CYCLOHEXANE, ETHYL-,
- 210 L6TJ A2

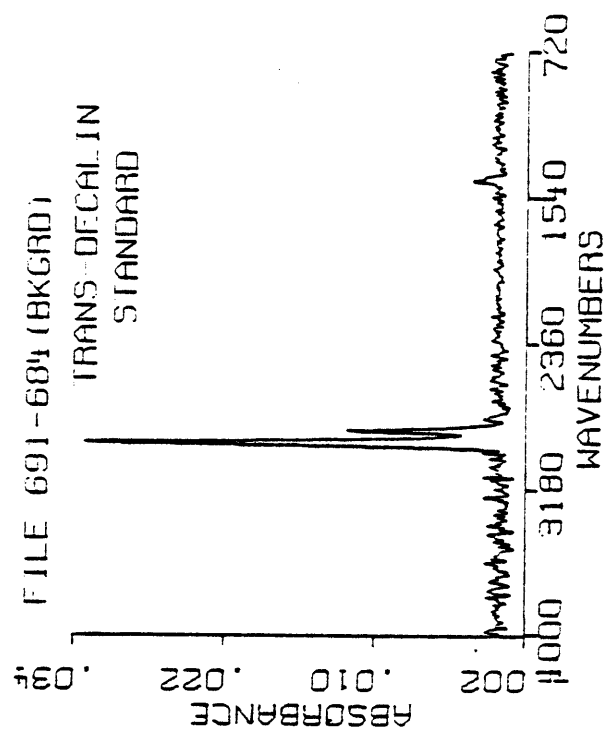
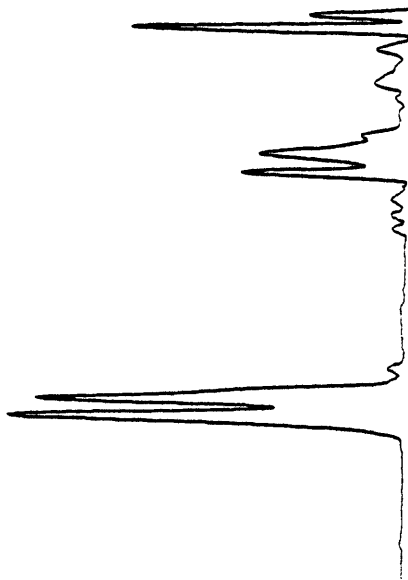


FIGURE 21

EPA VAPOR PHASE  
M-XYLENE

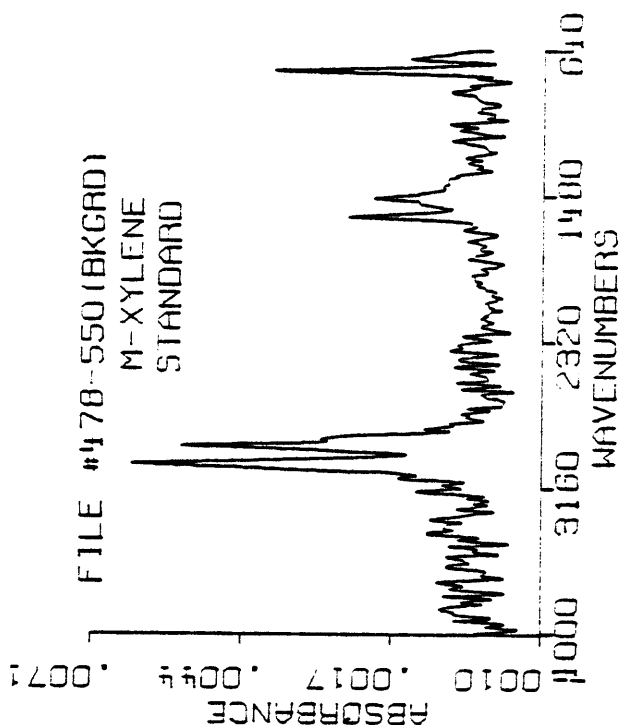
MODEL 36 IR CELL



.SRQ  
ENTER SKIP REGIONS, NEGATIVE NO. IF NONE  
LOW LIMIT 400  
HIGH LIMIT 640  
LOW LIMIT 3600  
HIGH LIMIT 4000  
LOW LIMIT -1  
MAX FOR SCALING, NEG IF AUTO -1

EPA VAPOR PHASE  
POSSIBLE HITS

- 78 M-XYLENE IR C
- 1108 IR C
- 342 BITOLYL, M,NPR-, IR CR C
- 2447 IR CR C
- 923 BENZENE, 1,2,3-TRIMETHYL-, IR B C
- 2915 IR B C
- 2988 IR C
- 799 BENZENE, 1,3,5-TRIMETHYL-, IR C E
- 3069 IR C E
- 871 P-XYLENE IR D
- 3430 IR D
- 75 BENZENE, 1,2,4-TRIMETHYL-, IR B D
- 3491 IR B D
- 222 3,5-LUTIDINE T6HJ C E
- 3589 IR B C E
- 2498 BENZENE, 1,2,3,5-TETRAMETHYL-, IR B C E
- 3678 IR B C E
- 2610 HEXANE, 1,3,5-TRIPHENYL-, IR%1YR&R
- 3708 IR%1YR&R



FILE #178-550 (BKGRD)  
M-XYLENE  
STANDARD

FIGURE 22

EPA VAPOR PHASE  
N-DECANE (JRC:6/10/82)

MODEL 36 IR CELL

.SRQ  
ENTER SKIP REGIONS, NEGATIVE NO. IF DONE  
LOW LIMIT 400  
HIGH LIMIT 750  
LOW LIMIT 3700  
HIGH LIMIT 4000  
LOW LIMIT -1  
MAX FOR SCALING, NEG IF AUTO -1

EPA VAPOR PHASE  
POSSIBLE HITS  
3301 120 N-DECANE (JRC:6/10/82)  
3302 137 N-UNDECANE (JRC:6/10/82)  
887 160 NONANE  
2554 160 HEPTADECANE, 6,12-DIETHYL-9-  
5Y2&2 2Y5  
2553 161 HEPTADECANE, 6,9,12-TRIPROPYL-,  
5Y3&2 2Y3  
895 169 OCTANE  
2555 184 HEXADECANE, 6,11-DIPENTYL-,  
5Y5&2 2  
415 186 DECAHE  
2155 187 OCTYL DISULFIDE  
2343 188 AMMONIUM BROMIDE, TETRAHEPTYL-,  
7 4K 8E & 4/7

.SRQ = 30

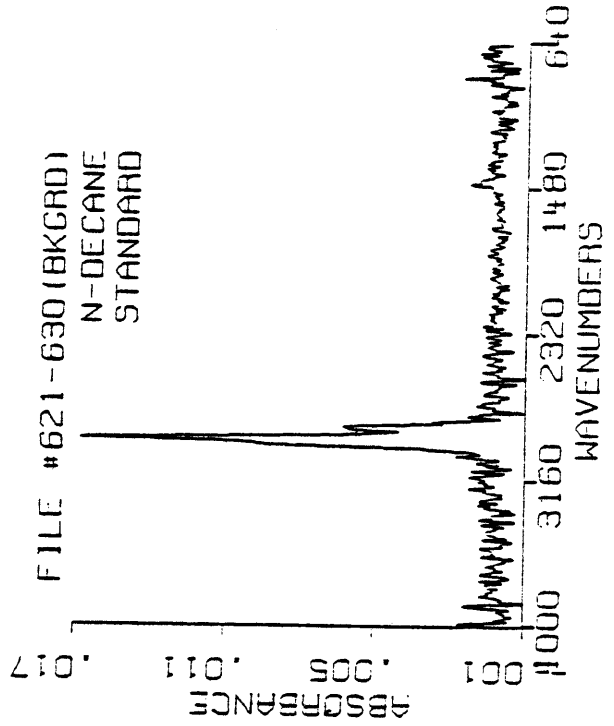


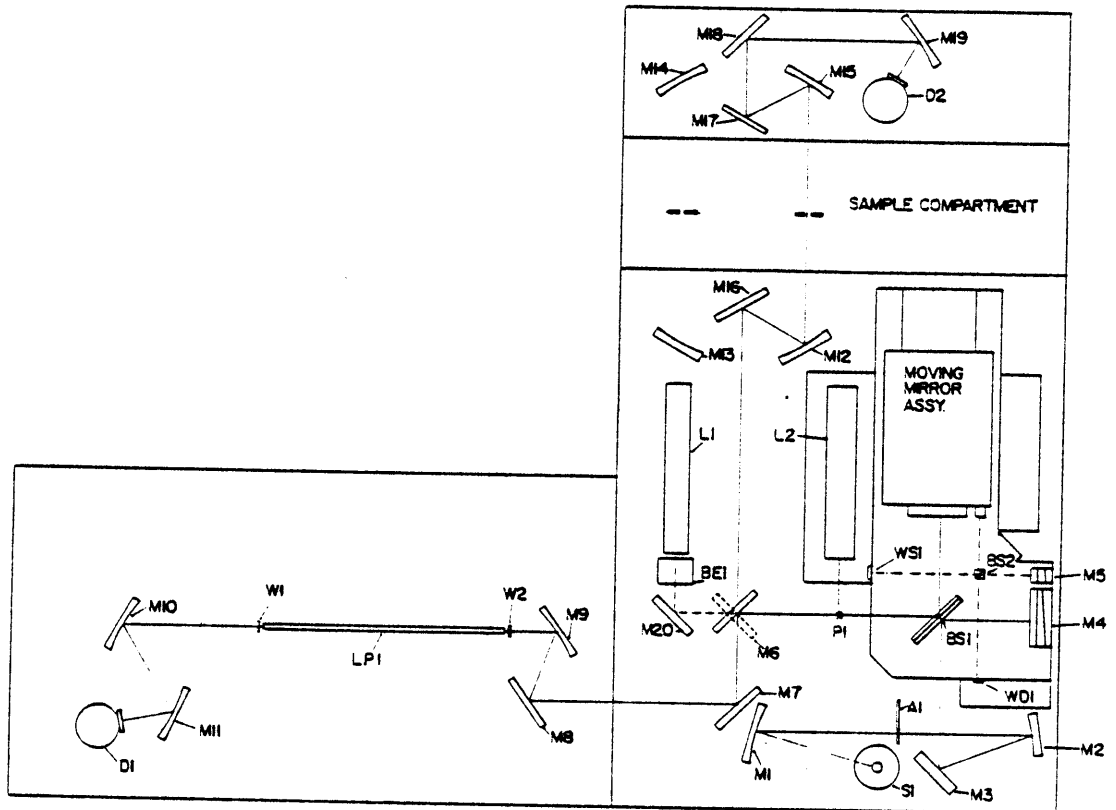
FIGURE 23

Thus far, the overall data indicate that a 3 mm x 6 cm lightpipe combined with a MCT-B detector (4000-400  $\text{cm}^{-1}$ ) can provide reasonable capillary GC-FTIR data for complex mixtures. The interfacing of fused silica capillary columns to such a system is feasible and sample loadings of over 1 microgram appear to be handled well by such a narrow bore column. A 0.5  $\mu\text{g}$  detection limit can be envisioned for weakly absorbing aromatics although a point is reached where low S/N can lead to ambiguous and often inaccurate library search results. A somewhat lower limit, around 200 ng, is possible for branched and cyclic aliphatics, although lack of infrared spectral information may lead to unreliable search results.

Although our Nicolet 6000 arrangement could achieve reasonable capillary GC-FTIR, a more sensitive system was made available for testing at the Nicolet Instrument Corporation, Madison, WI.

The system, a Nicolet 7199 dual-beam FTIR, was interfaced to an external GC lightpipe and detector bench which included a 40 cm x 1 mm i.d. lightpipe and narrow range MCT-A<sup>+</sup> liquid nitrogen cooled detector (4000-700  $\text{cm}^{-1}$ ) (See Figure 24). A Hewlett-Packard gas chromatograph with split injection was fitted with a DB-1 0.35 mm i.d. x 60 meter fused silica capillary column.

In an effort to compare the overall performance of both 6000 and 7199 Nicolet GC-FTIR systems, test jet fuel VN-77-11 was again used and a similar temperature program run. For this fuel, the effects of the DB-1 column vs. the DB-5 on retention time were considered minimal since VN-77-11 is mainly of aliphatic character. (The DB-5 is actually



### LEGEND

S1	- Source
M1	- Spherical Mirror. 4.5" E.F.L.
A1	- Aperture and Chopper
M2	- Spherical Mirror. 9.0" E.F.L.
M3	- Flat Mirror
BS1	- Beamsplitter and Compensator
BS2	- White Light Beamsplitter
M4	- Fixed Mirror
M5	- White Light Mirror
P1	- Centerline Laser Prism
M6	- 4-Position, Computer-Controlled Flat Mirror
M7, M8	- Flat Mirror
M9, M11	- Off-Axis Parabolic Mirror. 3.5" E.F.L.
W1, W2	- KBr windows
LPI	- 3.0 x 420 mm Gold-lined Pyrex Light Pipe

M10	- Off-Axis Parabolic Mirror. 9.3" E.F.L.
D1	- HgCdTe Detector and Dewar
M16, M17	- 2-Position, Computer-Controlled Flat Mirrors
M12, M13, M14, M15	- Off-Axis Parabolic Mirror. 9.3" E.F.L.
M18	- Flat Mirror
M19	- Off-Axis Parabolic Mirror. 3.5" E.F.L.
D2	- IR Detector
L2	- Centerline Laser
L1	- Alignment Laser
BE1	- Beam Expander
M20	- Flat Mirror
WS1	- White Light Source
WD1	- White Light Detector

White Light Beam	-----
Infrared Beam	=====
Laser Beam	-----

FIGURE 24. Nicolet 7199 Optical Layout

a methyl-phenyl-vinyl polysiloxane (bonded phase) while the DB-1 has only methyl character). The splitter was set to 30 ml/min helium making the split-ratio approximately 1:15. A make-up gas (He) was used to bring the total flow rate through the lightpipe to 4 ml/min. The flame ionization detector was not used due to the problems of re-directing the helium gas to a make-up tee.

The major operating parameters for this experiment are given below:

VEL = 50	injector temperature 260°C
COR = IN	lightpipe temperature 270°C
NSD = 10	
NSB = 40	
APT = FL	
GAN = 1	

The amount of fuel injected was 0.2  $\mu$ l, with the amount actually going to the column being approximately 0.013  $\mu$ l. The dual computer disc drive for this system made available almost 1600 8  $\text{cm}^{-1}$  data files to store the IR scans. No files are lost as a result of automatically switching to the second data disk cartridge. The throughput for this system was about 7.7 volts with a GAN=1. This throughput is only slightly more than achieved with the Model 26 lightpipe with MCT-B detector, although in terms of sensitivity the longer lightpipe and short range (4000-700  $\text{cm}^{-1}$ ) detector should give better response. The chromatographic parameters and IR windows monitored are given on the CHEMIGRAM and again the data indicate mostly aliphatic character (Figure 25). A reconstructed chromatogram of the infrared region 2800-3000  $\text{cm}^{-1}$  (aliphatic C-H) illustrates the separation possible

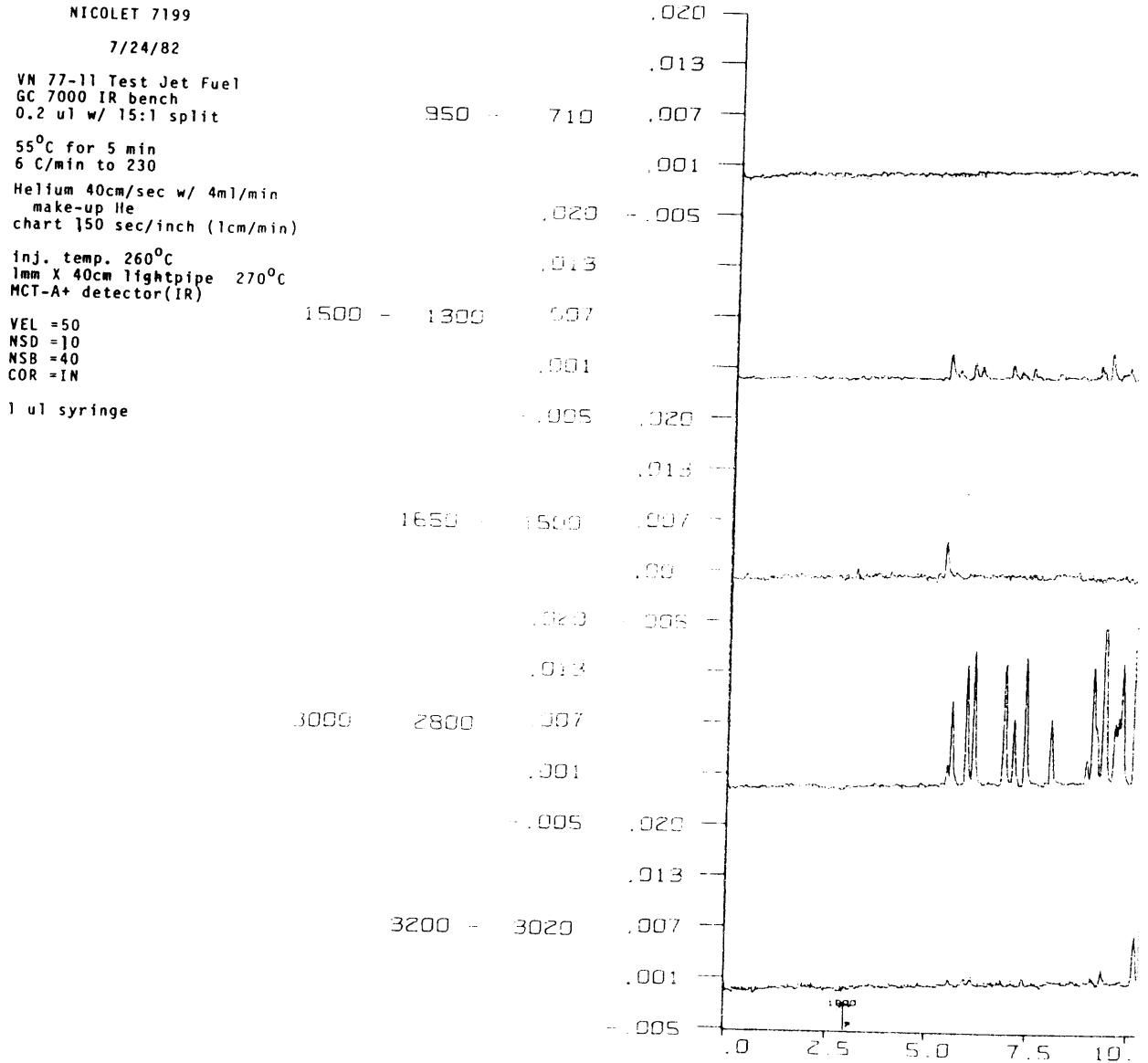
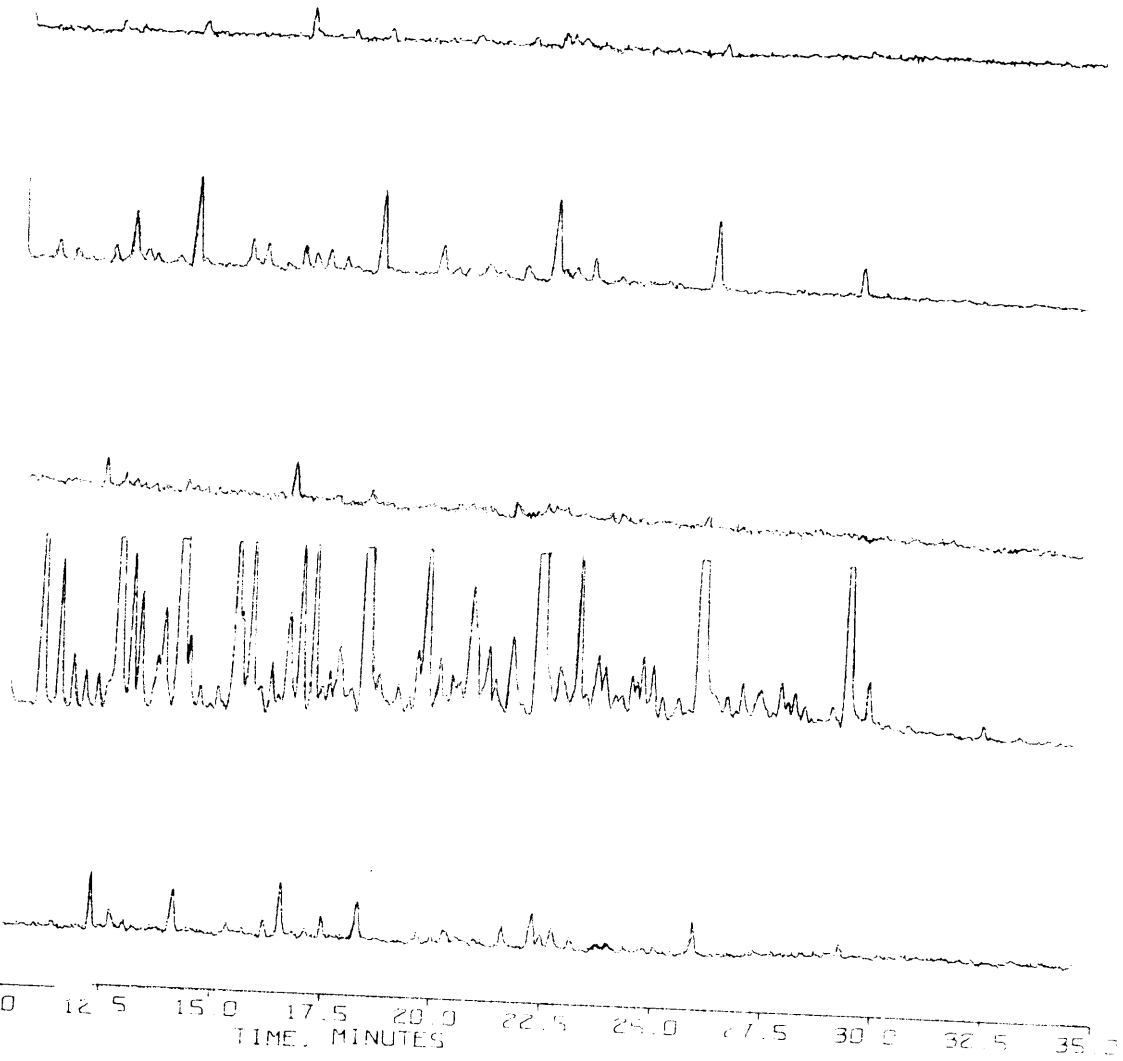


FIGURE 25. CHEMIGRAM of VN-77-11 Separated on DB-1 fused silica column (7199 System)



on fused silica columns with FTIR detection when no overloading is caused and when the infrared response is enhanced (Figure 26).

Figure 27 is a single beam spectrum showing the response curve and, in particular, the IR cutoff at  $700\text{ cm}^{-1}$  for the MCT-A<sup>+</sup> detector. For this highly sensitive system, CO<sub>2</sub> is easily distinguishable in light of the "dried air" used as the purge.

Figure 28 shows again the aliphatic region reconstructed chromatogram for VN-77-11 with a peak-picking routine used to locate components on the data disk. Only half of the total run is shown in order that a less confusing plot may be presented. Each peak picked by this routine is chosen according to a y-axis threshold value set by the user. The "starred" peaks will be spectrally matched and interpreted using the EPA library system.

A minor peak giving rise to file spectrum #184 was spectrally searched using the least squares algorithm SQ. This specific peak corresponds to the one previously searched when the Accuspec Model 36 lightpipe and Nicolet 6000 FTIR were used (Figure 18). Because of the excessive CO<sub>2</sub> and water vapor present (and because of the sensitivity now available) the regions  $2300\text{-}2400\text{ cm}^{-1}$  and  $3700\text{-}4000\text{ cm}^{-1}$  were blanked out. Also, the region below  $700\text{ cm}^{-1}$  was, of course, blanked corresponding to the detector cut-off. The library search identifies the peak component as methyl cyclopentane (Figure 29) with a moderate certainty. This finding confirms the earlier analysis although the actual amount being detected is much smaller in the current 7199 system experiment.

VN 77-11 JET FUEL  
NICOLET 7199 GC 7000  
1 MM X 40 CM LIGHTPIPE  
MCT-A<sup>+</sup> DETECTOR

2800-3000 CM<sup>-1</sup>  
RCN

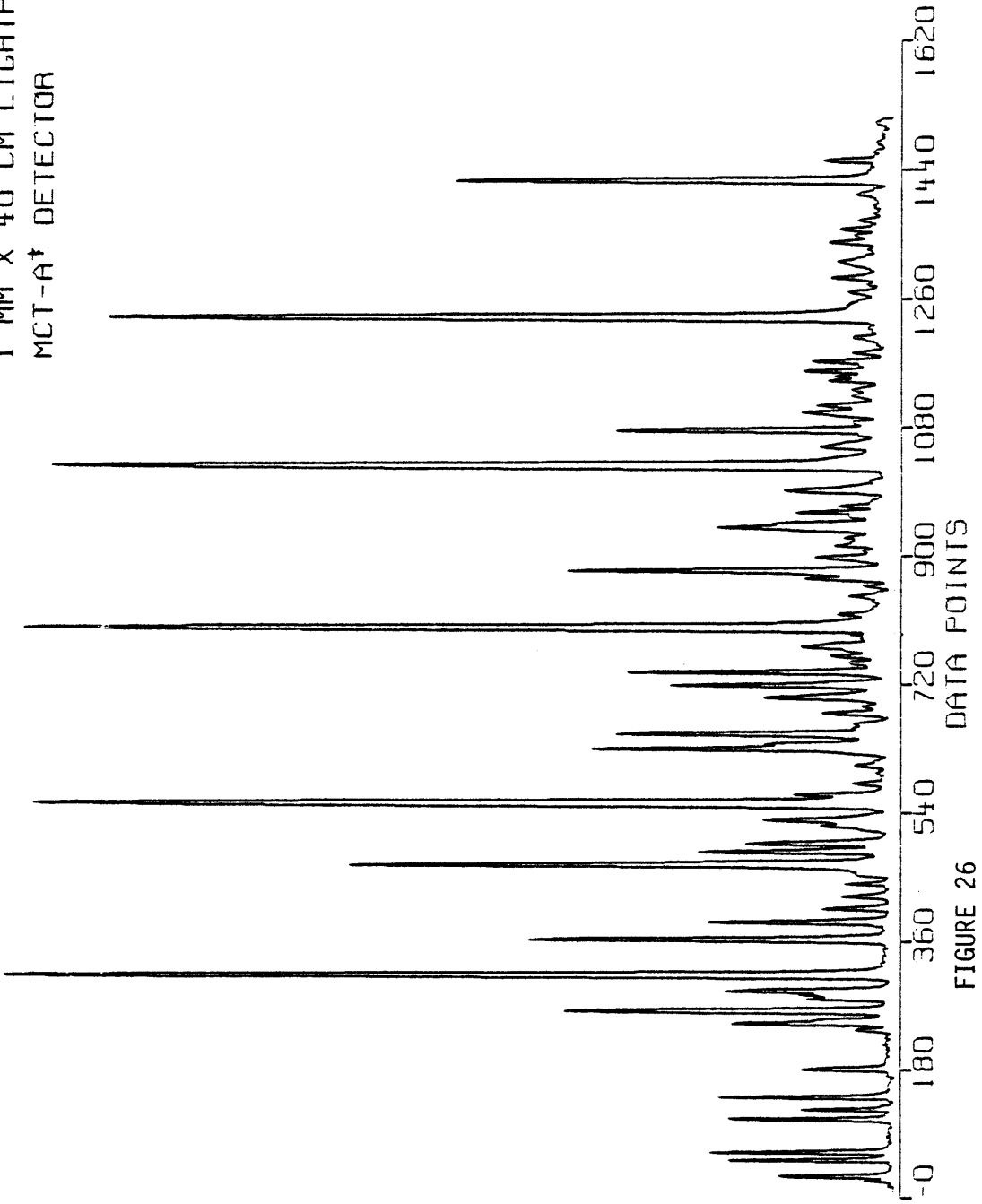
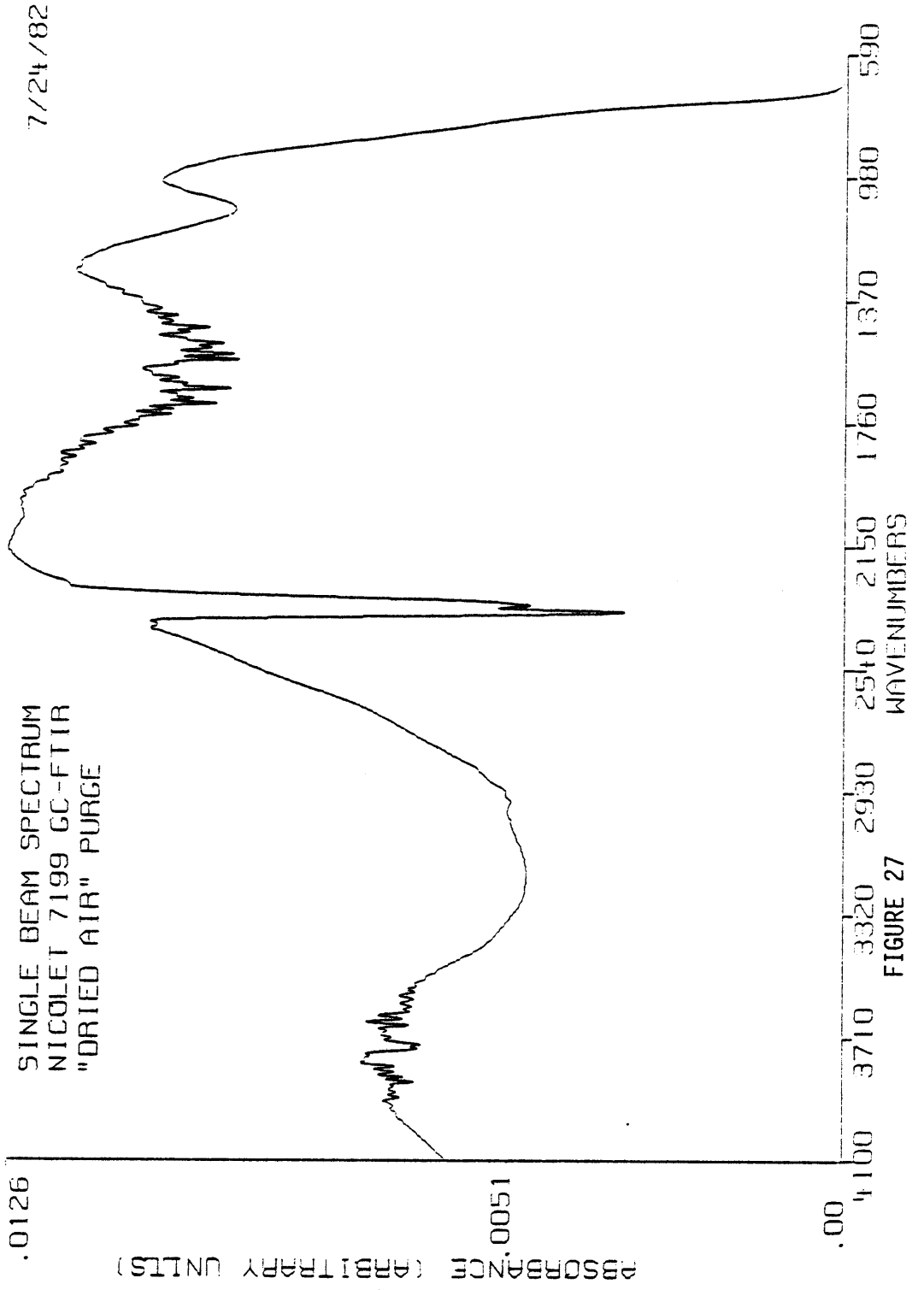


FIGURE 26



2800-3150  $\text{cm}^{-1}$  RCN  
 NICOLET 7199 SYSTEM  
 VN 77-11 JET FUEL (1)

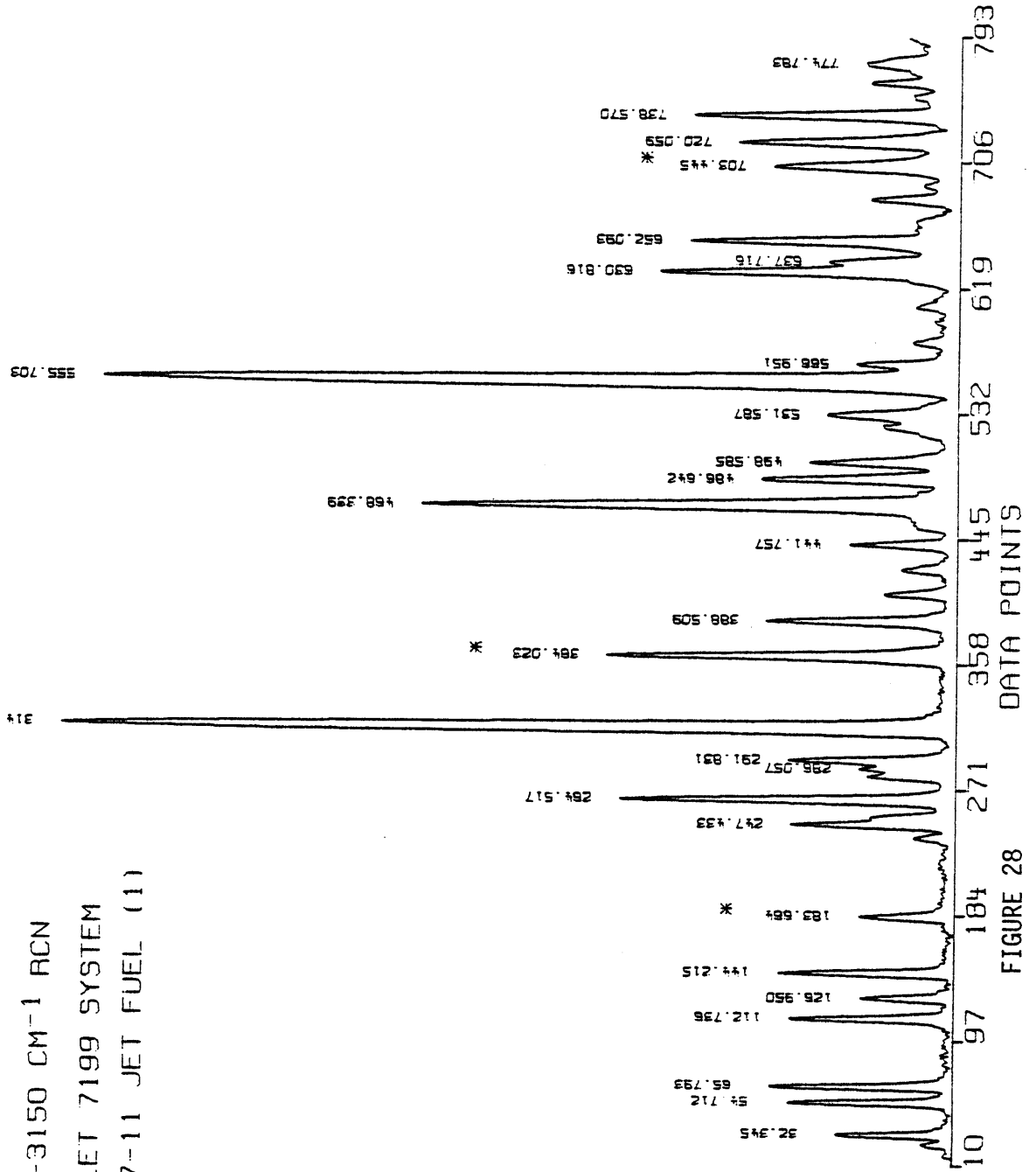


FIGURE 28

EPA VAPOR PHASE  
CYCLOPENTANE, METHYL-,

NICOLET 7199 SYSTEM

.SRQ  
ENTER SKIP REGIONS, NEGATIVE NO. IF DONE  
LOW LIMIT 400  
HIGH LIMIT 750  
LOW LIMIT 2300  
HIGH LIMIT 2400  
LOW LIMIT 3600  
HIGH LIMIT 4000  
LOW LIMIT -1  
MAX FOR SCALING, NEG IF AUTO -1

EPA VAPOR PHASE  
POSSIBLE HITS  
45 CYCLOPENTANE, METHYL-,  
LSTJ A  
2494 HEPTANE, 2,2-DIMETHYL-,  
5X  
43 HEXANE, 2,2,5-TRIMETHYL-,  
1Y&2X  
802 HEXANE, 2,2,4-TRIMETHYL-,  
2Y&1X  
922 HEPTANE, 3,3-DIMETHYL-,  
4X2  
2480 CYCLOPENTANE  
193 LSTJ  
2491 HEXANE, 2,5-DIMETHYL-,  
1Y2Y  
381 ISOOCTANE /30-CALLED,  
1Y&1X  
2930 ISOBUTANE  
1Y  
38 PENTANE, 2,4-DIMETHYL-,  
1Y&1Y  
226

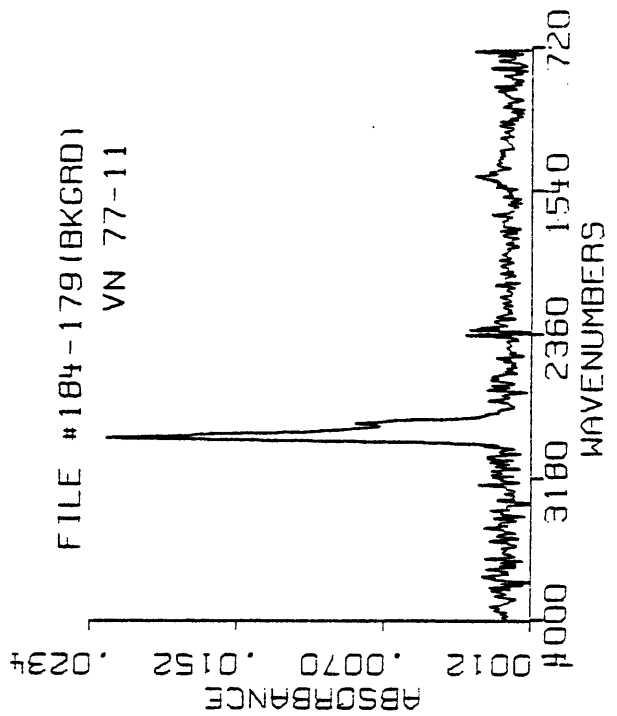


FIGURE 29

The superior sensitivity of the Nicolet 7199 (40 cm lightpipe) system is realized when one considers that a 1.4x increase in total absorbance is being seen for approximately 20 times less sample when compared with the best Nicolet 6000 (6 cm lightpipe) system. Numerically, the library search results with the 7199 system are roughly the same as the previous analysis, which may be due to baseline problems caused by an inconsistent "dried air" purge or fluctuations in the long 40 cm lightpipe temperature.

A search of file spectrum #365 corresponding to the same peak component as Figure 19 yields a match this time differing only by one methyl group (Figure 30). For this component the IR response is over 2 times that of the previous analysis (for 20 times less sample), and the library search match value of 21 is very convincing. Coeluting peaks may account for the discrepancy in identification between the "best" 6000 and 7199 systems, since the latter configuration gives a more resolved separation.

This greater sensitivity is manifested for the third "starred" peak in the reconstruction. File spectrum #703 (after subtracting out background water and CO<sub>2</sub> (i.e. file spectrum #694) was spectrally searched and found to closely resemble m-xylene (Figure 31). An indepth file by file inspection of the entire peak centered around file #703 revealed that two and possibly three classes of compounds were co-eluting in this peak. In an effort to isolate the aromatic component in this peak, file spectrum #703 had subtracted from it file spectrum #698 which was still within the peak envelope. This subtraction, while

NICOLET 7199 SYSTEM

EPA VAPOR PHASE  
CYCLOHEXANE, METHYL-

.SRQ  
ENTER SKIP REGIONS, NEGATIVE NO. IF DONE  
LOW LIMIT 400  
HIGH LIMIT 750  
LOW LIMIT -1  
MAX FOR SCALING, NEG IF AUTO -1

EPA VAPOR PHASE  
POSSIBLE HITS

12	CYCLOHEXANE, METHYL-
21	L67J A
3128	CYCLODODECANE
54	L-12-TJ
647	CYCLOHEXANE, ISOBUTYL-, C
74	L6J AY
646	CYCLOHEXANE, 1,1-DIMETHYL-, C
80	L6J A A
733	THIOPYRAN, TETRAHYDR-
99	T63TJ
2556	HEXADECANE, 6-,5,6,7,8-TETRAHYDR
103	L66&7J CY10K5
136	CYCLOHEXANE, PROPYL-, C
110	L67J A3
982	CYCLODODECENE
115	L12 A07J
417	CYCLOHEXANE, ETHYL-
118	L67J A2
234	CYCLOHEXANE, TRANS-1,2-DIMETHYL-,
119	L67J A B -7

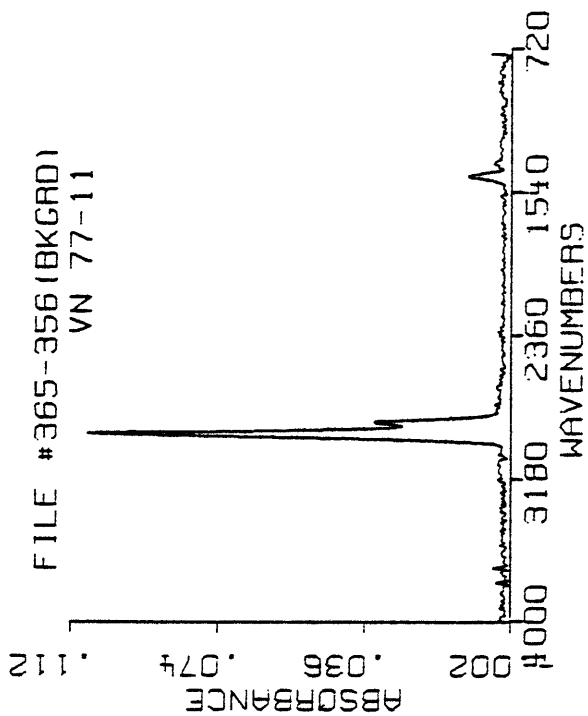


FIGURE 30

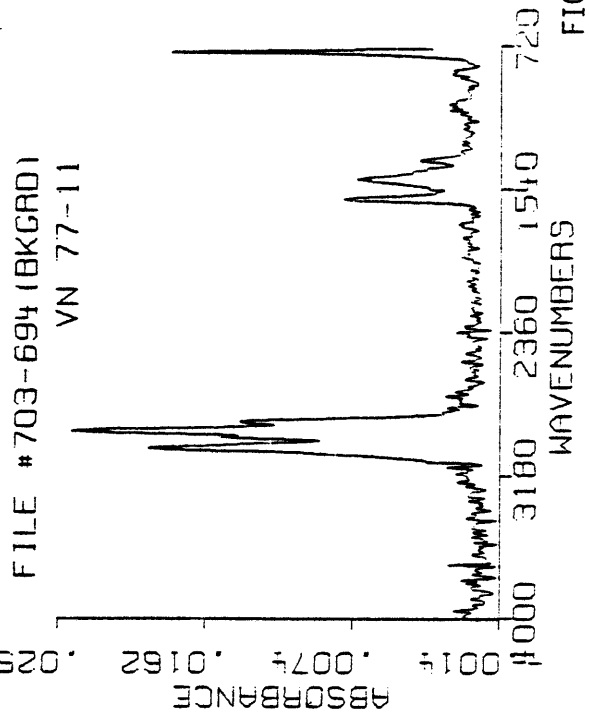
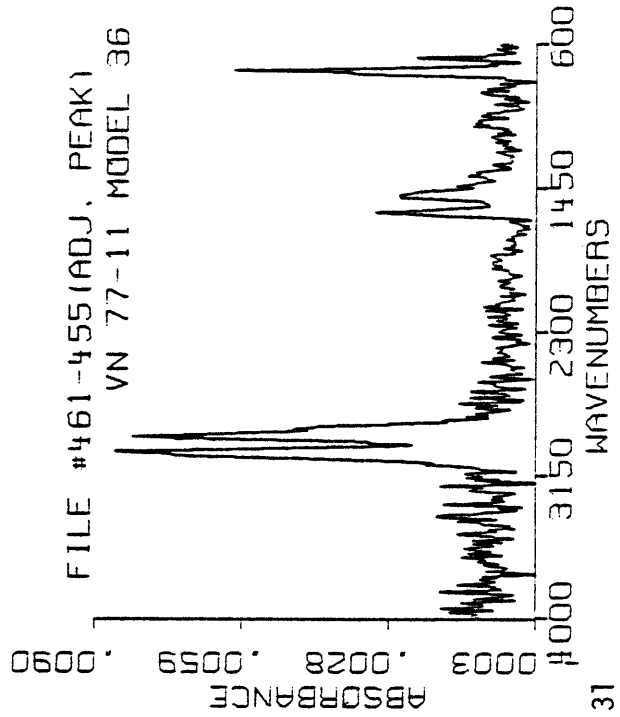
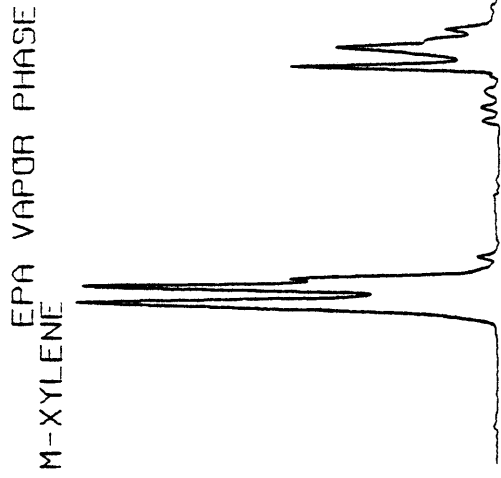
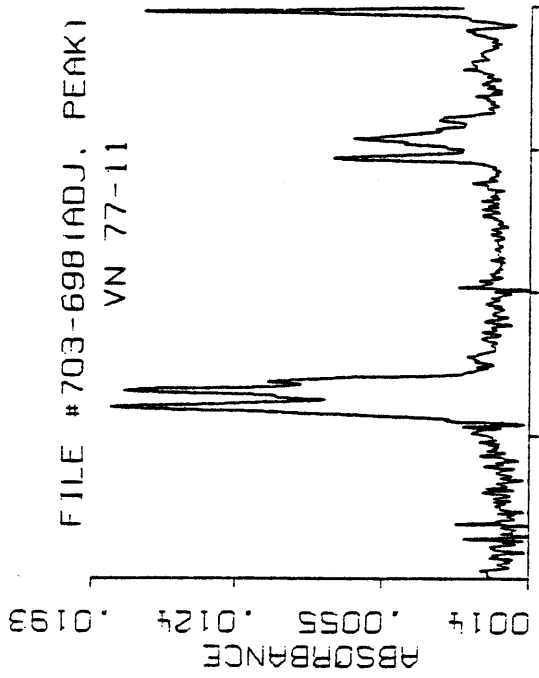


FIGURE 31

not as straight-forward as a simple background subtraction yielded a spectrum more closely matching (visually) the EPA library file spectrum of m-xylene. Particular attention is drawn to relative IR band heights in Figure 31. Comparison of the relative infrared band heights from these subtractions to the EPA file spectrum of m-xylene (Figure 31) confirms the assumption of co-eluting components. Further confirmation for the presence of m-xylene in VN-77-11 is shown in Figure 31, using the data collected when using the Nicolet 6000 (Model 36 lightpipe) system. A subtraction of file spectrum #455 from file spectrum #461 (both within the peak envelope) resulted in a spectrum and search results (Table 5) identifying m-xylene as present.

An important point to be made concerning spectral subtractions in complex mixture separations is that even though fused silica capillaries have a high degree of separating power, coeluting compounds are still very possible. CHEMIGRAM interpretation and specified IR window reconstructs, however, can help in determining the presence of underlying components.

The aromatic blend VN-80-39 jet fuel was next separated chromatographically employing the Nicolet 7199 system, and data was compared with the results from work with our Nicolet 6000 system. Figure 32 shows the Gram-Schmidt reconstruction for both GC-FTIR systems using the same temperature program and linear gas velocity. One difference between the two analyses was that 5 times less sample was injected into the 7199 GC-FTIR system. From a comparison of the reconstructed chromatograms, more information can be retrieved from the

TABLE 5

.SRQ  
 ENTER SKIP REGIONS, NEGATIVE NO. IF DONE  
 LOW LIMIT 400  
 HIGH LIMIT 735  
 LOW LIMIT 3600  
 HIGH LIMIT 4000  
 LOW LIMIT -1  
 MAX FOR SCALING, NEG IF AUTO -1

a) File #703-698(Adj.Peak)  
 VN 77-11 Nicolet 7199

EPA VAPOR PHASE  
 POSSIBLE HITS  
 78 M-XYLENE  
 371 1R C  
 923 BENZENE, 1,2,3-TRIMETHYL-,  
 1499 1R B C  
 2476 BENZENE, 1-ETHYL-3-METHYL-,  
 2388 2R C  
 2668 BUTANE, 1,3-DIPHENYL-, /PLUS/,-  
 2985 1YR&2R  
 342 BITOLYL, M,MPR-,  
 2998 1R CR C  
 2669 BUTANE, 1,3-DIPHENYL-, /MINUS/,-  
 3060 1YR&2R  
 871 P-XYLENE  
 3136 1R D  
 75 BENZENE, 1,2,4-TRIMETHYL-,  
 3200 1R B D  
 2610 HEXANE, 1,3,5-TRIPHENYL-,  
 3235 1YR&1YR&2R  
 2222 BENZYLAMINE, 2,5-DIMETHYL-,  
 3337 21R B E

SPECTRAL SEARCH LISTINGS  
 (SQ ALGORITHM)

b) File #703-694(Bkgrd)  
 VN 77-11 Nicolet 7199

c) File #461-455(Adj.Peak)  
 Model 36 IR cell

.SRQ  
 ENTER SKIP REGIONS, NEGATIVE NO. IF DONE  
 LOW LIMIT 400  
 HIGH LIMIT 745  
 LOW LIMIT 3600  
 HIGH LIMIT 4000  
 LOW LIMIT -1  
 MAX FOR SCALING, NEG IF AUTO -1

.SRQ  
 ENTER SKIP REGIONS, NEGATIVE NO. IF DONE  
 LOW LIMIT 400  
 HIGH LIMIT 650  
 LOW LIMIT 3600  
 HIGH LIMIT 4000  
 LOW LIMIT -1  
 MAX FOR SCALING, NEG IF AUTO -1

EPA VAPOR PHASE  
 POSSIBLE HITS  
 78 M-XYLENE  
 583 1R C  
 923 BENZENE, 1,2,3-TRIMETHYL-,  
 881 1R B C  
 2476 BENZENE, 1-ETHYL-3-METHYL-,  
 1372 2R C  
 75 BENZENE, 1,2,4-TRIMETHYL-,  
 1954 1R B D  
 2668 BUTANE, 1,3-DIPHENYL-, /PLUS/,-  
 1966 1YR&2R  
 914 BENZENE, 1,2,3,4-TETRAMETHYL-,  
 1998 1R B C D  
 2669 BUTANE, 1,3-DIPHENYL-, /MINUS/,-  
 2063 1YR&2R  
 806 O-XYLENE  
 2094 1R B  
 1190 BENZENE, HEXAMETHYL-,  
 2127 U 6-R  
 2610 HEXANE, 1,3,5-TRIPHENYL-,  
 2148 1YR&1YR&2R

EPA VAPOR PHASE  
 POSSIBLE HITS  
 78 M-XYLENE  
 1646 1R C  
 923 BENZENE, 1,2,3-TRIMETHYL-,  
 3222 1R B C  
 871 P-XYLENE  
 3275 1R D  
 2476 BENZENE, 1-ETHYL-3-METHYL-,  
 3826 2R C  
 2222 BENZYLAMINE, 2,5-DIMETHYL-,  
 3946 21R B E  
 75 BENZENE, 1,2,4-TRIMETHYL-,  
 3966 1R B D  
 799 BENZENE, 1,3,5-TRIMETHYL-,  
 4148 1R C E  
 342 BITOLYL, M,MPR-,  
 4334 1R CR C  
 2200 ETHANETHIOL, 2-/BENZYLAMINO/  
 4392 SH2M1R  
 2470 2,4-HEXADIENE  
 4409 2U2U2

VN 80-39 AROMATIC BLEND  
GRAM-SCHMIDT RECONSTRUCTION  
60 METER DB-1 FUSED SILICA COLUMN  
NICOLET 7199 SYSTEM

VN 80-39 AROMATIC BLEND  
GRAM-SCHMIDT RECONSTRUCTION  
60 METER DB-5 FUSED SILICA COLUMN  
MODEL 36 IR CELL

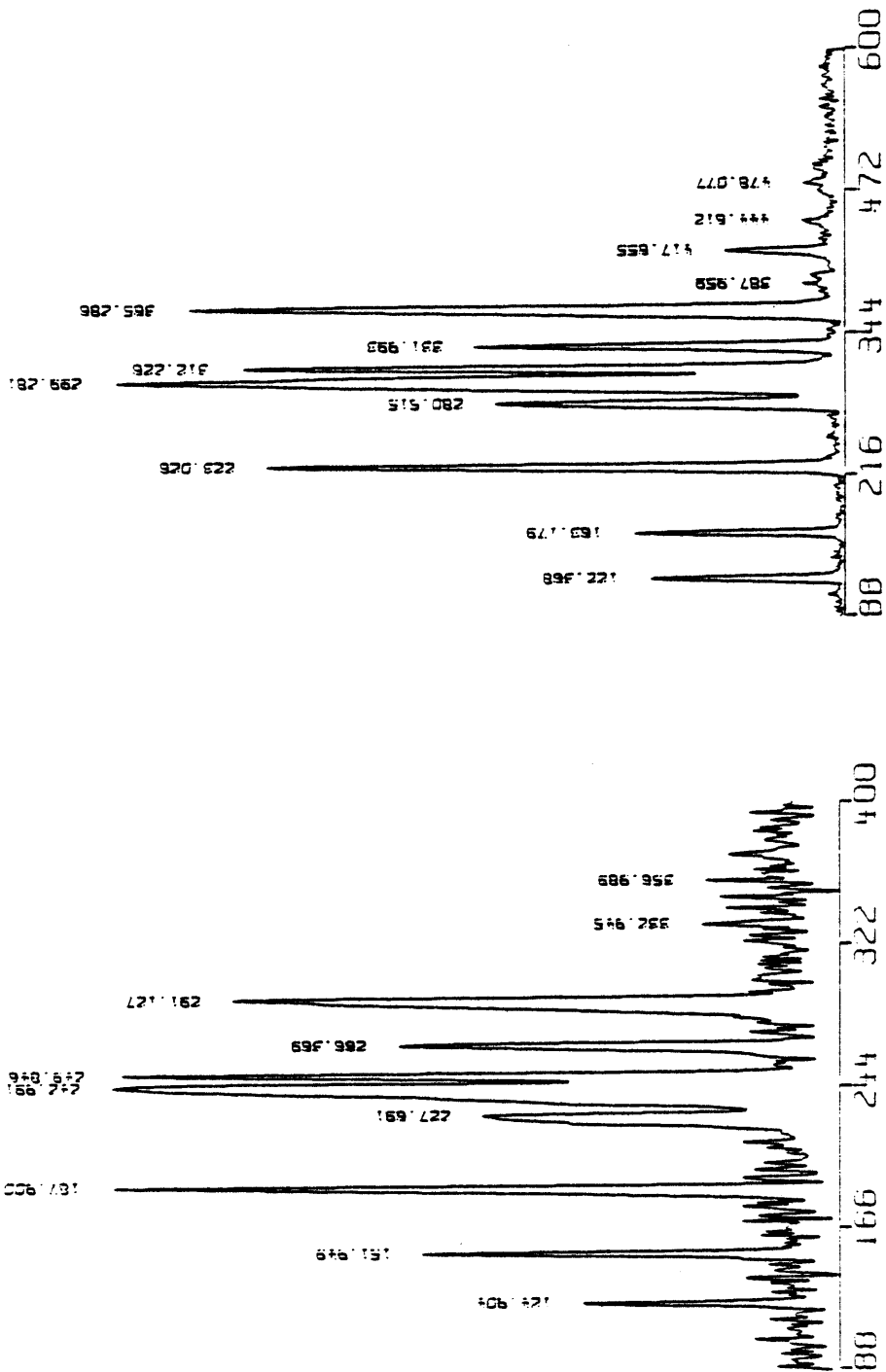


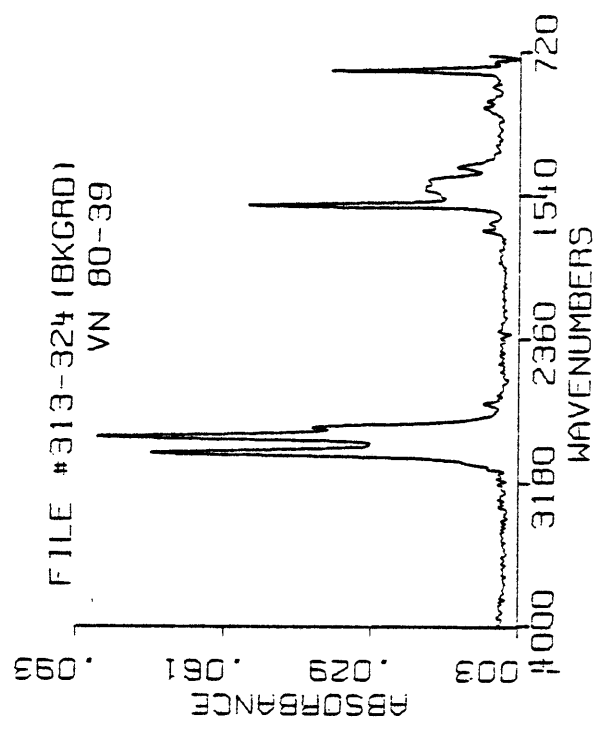
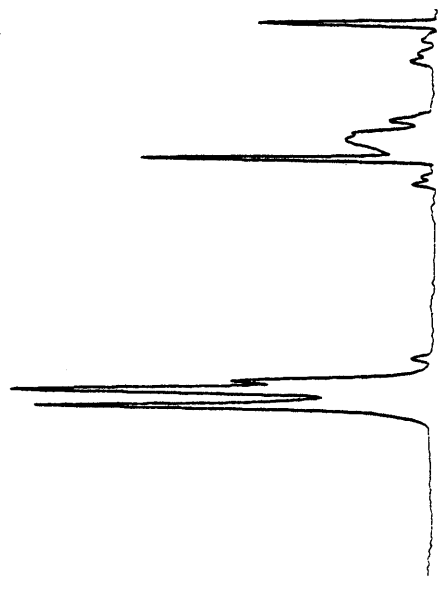
FIGURE 32

7199 run as compared to the 6000 run in which some components were lost in the more noisy baseline. Spectral searches of identical peaks as before revealed less noisier spectra. A noticeable improvement in spectral matching, however, was apparent only for the component of low concentration (Figures 33, 34, 15, 16). In any case, 1,3,5-trimethylbenzene and 1,2,3-trimethylbenzene were again identified for the major and minor peaks, respectively.

To gain more insight as to the actual sensitivity of the Nicolet 7199 GC-FTIR system, a standard mixture of aliphatics and aromatics (Table 2) at low concentration was separated chromatographically, spectrally searched and identified. For 0.5  $\mu$ l of actual injection, concentrations ranged from 65 ng to 440 ng per select component. Figure 35 illustrates the separation of this standard (complex) mixture.

When referring to detection limits and reporting such for GC-FTIR, one must keep in mind that 65 ng of an aromatic hydrocarbon species will have a total absorbance intensity different from an alkane hydrocarbon and certainly less than a component such as isobutylmethacrylate which is a very strong infrared absorber. It is not the purpose here of setting actual "detection limits" for classes of compounds but merely to correlate overall absorbance with an estimated amount of material. One might then, upon reviewing the spectrum of a complex jet fuel, estimate a range, for example, less than one microgram or even speculate low nanogram levels. For about 65 ng of p-xylene, Figure 36 indicates a total absorbance of less than

EPA VAPOR PHASE  
 BENZENE, 1,3,5-TRIMETHYL-,



FILE #313-324 (BKGRD)  
 VN 80-39

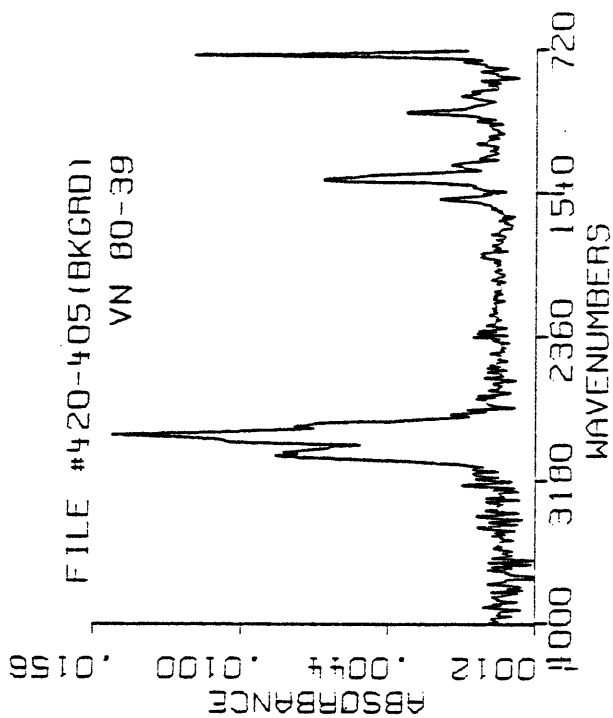
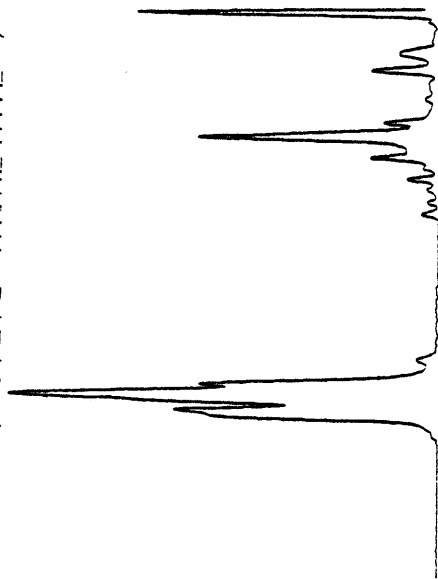
NICOLET 7199 SYSTEM

.SRQ  
 ENTER SKIP REGIONS, NEGATIVE NO. IF NONE  
 LOW LIMIT 400  
 HIGH LIMIT 730  
 LOW LIMIT 3700  
 HIGH LIMIT 4000  
 LOW LIMIT -1  
 MAX FOR SCALING, NEG IF AUTO -1

- EPA VAPOR PHASE  
 POSSIBLE HITS
- 799 BENZENE, 1,3,5-TRIMETHYL-, IR C E
  - 2498 BENZENE, 1,2,3,5-TETRAMETHYL-, IR B C E
  - 1311 BENZENE, 1,2,4-TRIMETHYL-, IR B D
  - 1771 2-BUTENE, 2,3-DIMETHYL-, 1Y&UY
  - 2042 BENZENE, 1,2,4,5-TETRAMETHYL-, IR B D E
  - 2149 3,5-LUTIDINE T6NJ C E
  - 2169 2,4-HEXADIENE, 2,5-DIMETHYL-, 1Y&UZUY
  - 2179 BENZENE, HEXAMETHYL-, U 6-R
  - 1190 BENZENE, 1,2,3,4-TETRAMETHYL-, IR B C D
  - 914 2-BUTENE, 2-METHYL-, YU2
  - 2279
  - 41
  - 2335

FIGURE 33

EPA VAPOR PHASE  
 BENZENE, 1,2,3-TRIMETHYL-,



NICOLET 7199 SYSTEM

.SRQ  
 ENTER SKIP REGIONS, NEGATIVE NO. IF NONE  
 LOW LIMIT 400  
 HIGH LIMIT 730  
 LOW LIMIT 2300  
 HIGH LIMIT 2400  
 LOW LIMIT 3700  
 HIGH LIMIT 4000  
 LOW LIMIT -1  
 MAX FOR SCALING, NEG IF AUTO -1

EPA VAPOR PHASE  
 POSSIBLE HITS  
 923 BENZENE, 1,2,3-TRIMETHYL-,  
 IR B C  
 304  
 2476 BENZENE, 1-ETHYL-3-METHYL-,  
 IR C  
 1863  
 914 BENZENE, 1,2,3,4-TETRAMETHYL-,  
 IR B C D  
 1886  
 2668 BUTANE, 1,3-DIPHENYL-, /PLUS/-,  
 2101 1YR&2R  
 78 M-XYLENE  
 2108 IR C  
 1190 BENZENE, HEXAMETHYL-,  
 2132 U 6-R  
 2610 HEXANE, 1,3,5-TRIPHENYL-,  
 2241 1YR&1Y&2R  
 2669 BUTANE, 1,3-DIPHENYL-, /MINUS/-,  
 2252 1YR&2R  
 2486 BENZENE, PROPYL-,  
 2300 3R  
 2666 OCTANE, 3,6-DIPHENYL-,  
 2340 2YR&2YR&2

FIGURE 34

MICROGRAM MIX      GRAM-SCHMIDT RECONSTRUCTION      PPK  
60 METER DB-1 FUSED SILICA  
NICOLET 7199 SYSTEM

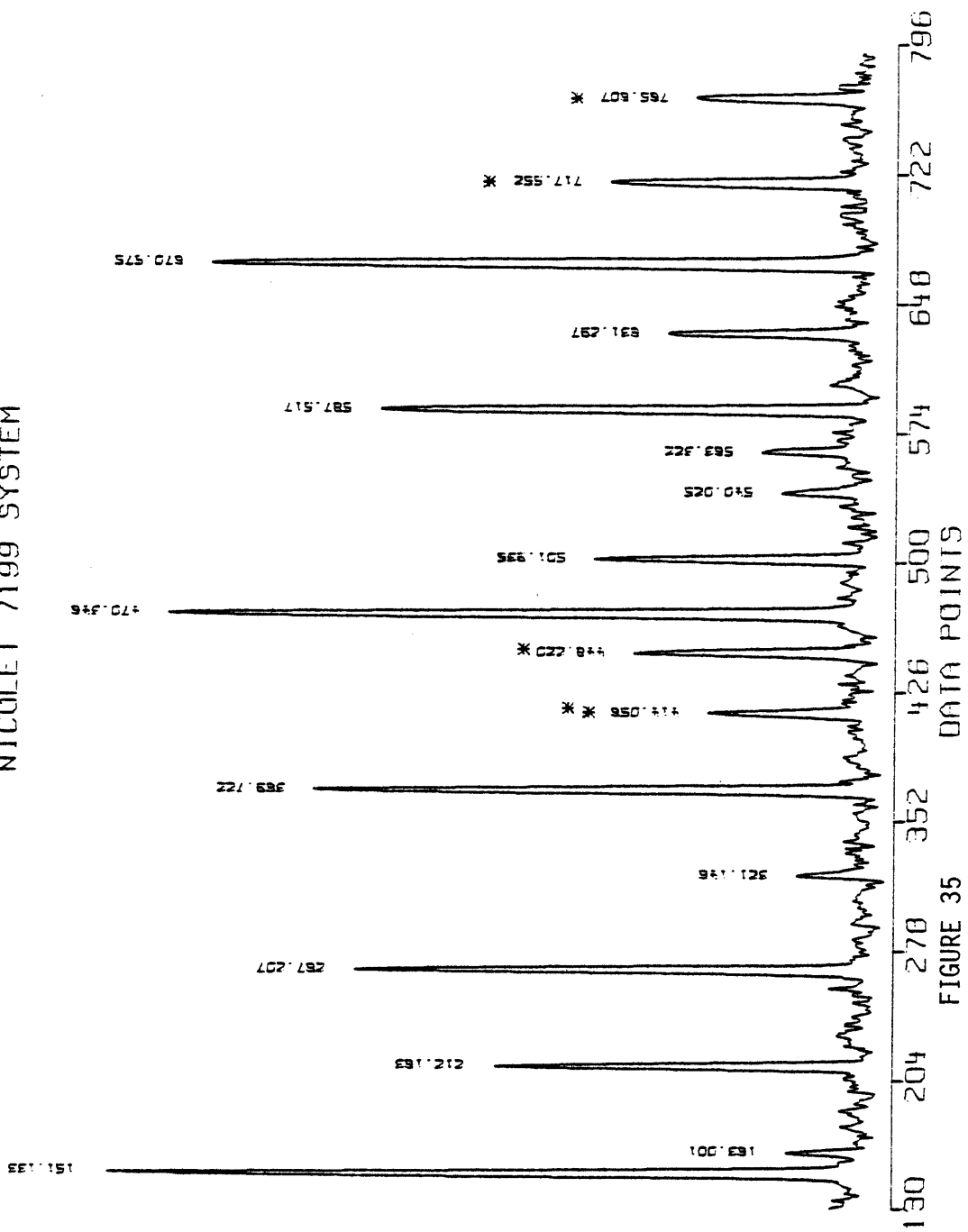
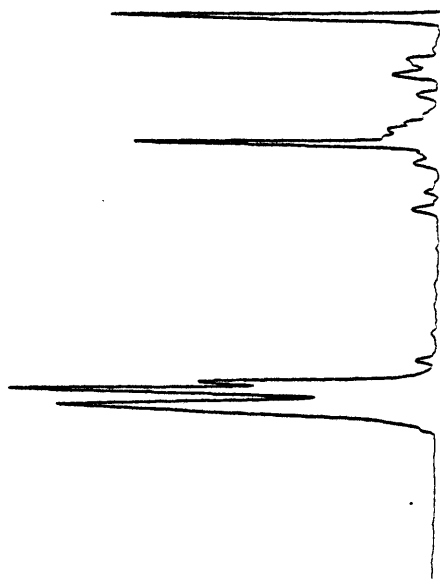


FIGURE 35

EPA VAPOR PHASE  
P-XYLENE



.SRO  
ENTER SKIP REGIONS, NEGATIVE NO. IF DONE  
LOW LIMIT 400  
HIGH LIMIT 730  
LOW LIMIT 2300  
HIGH LIMIT 2400  
LOW LIMIT 3600  
HIGH LIMIT 4000  
LOW LIMIT -1  
MAX FOR SCALING, NEG IF AUTO -1

- EPA VAPOR PHASE  
POSSIBLE HITS
- 871 P-XYLENE IR D
  - 495 IR D
  - 75 BENZENE, 1,2,4-TRIMETHYL-, IR B D
  - 1360 IR B D
  - 2222 BENZYLAMINE, 2,5-DIMETHYL-, ZIR B E
  - 2173 ZIR B E
  - 914 BENZENE, 1,2,3,4-TETRAMETHYL-, IR B C D
  - 2318 BIPHENYL, 4,4PR-DIMETHYL-, IR DR D
  - 2328 IR DR D
  - 2200 ETHANETHIOL, 2--BENZYLAMINOZ-, S2MIR
  - 2612 BENZENE, 1,2,3,5-TETRAMETHYL-, IR B C E
  - 2498 IR B C E
  - 2769 BENZENE, 1-ETHYL-3-METHYL-, IR B C
  - 2476 IR B C
  - 2905 IR B C
  - 1190 BENZENE, HEXAMETHYL-, U 6-R
  - 2915 U 6-R
  - 1107 BENZENE, 1,2,4,5-TETRAMETHYL-, IR B D E
  - 2951 IR B D E

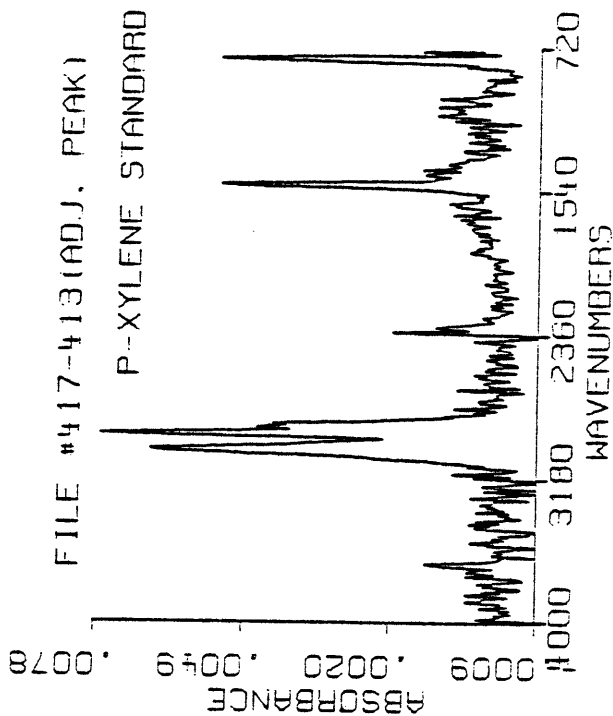


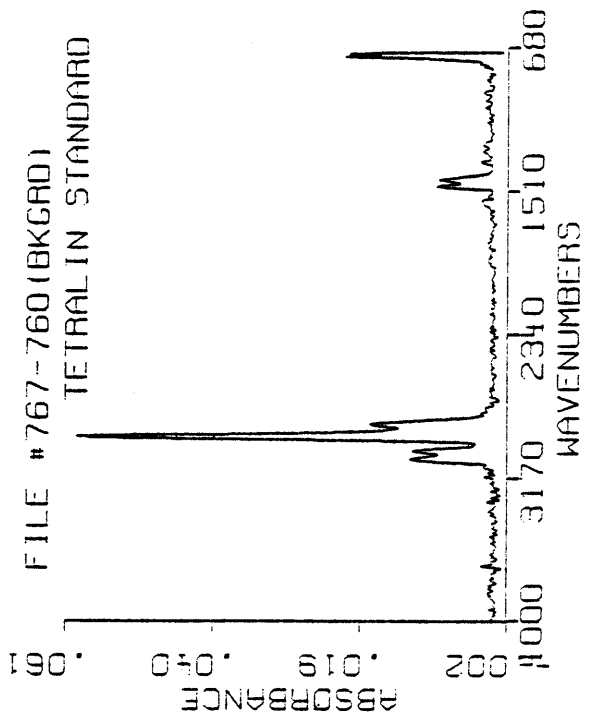
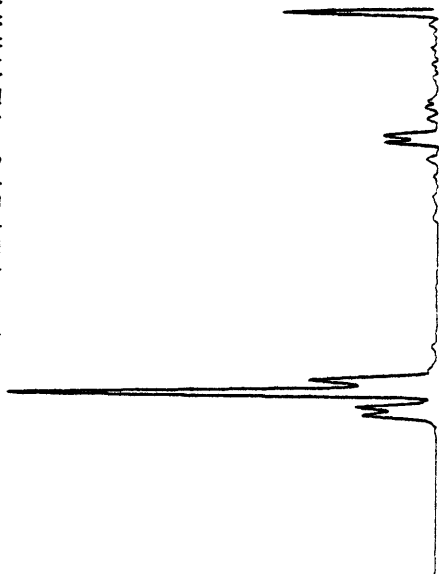
FIGURE 36

0.01 units. S/N, even at this concentration, appears quite good and the "match value" is reasonable considering the low S/N. For tetralin, 195 ng provides a substantial S/N; while 90 ng of cis-decalin is "virtually" noiseless (Figures 37, 38). The match value in each case is exceedingly low. In general, as aliphatic character increases, S/N ratio increases. However, information content can be reduced to the point where straight chain alkanes offer little individual IR distinction.

Probably one of the most significant advantages of infrared spectroscopy is its ability to distinguish between isomers, particularly substituted aromatics. Figure 39 illustrates these differences for two xylenes (o,m) chromatographed with the Nicolet 7199 system. Quantitatively these spectra represent 215 ng of m-xylene and 440 ng of o-xylene. Comparison of these spectra to the p-xylene isomer spectrum (Figure 37) again illustrates the differences in IR absorbance indicative of aromatic substitution. In checking the spectral match list (Table 6) for file spectrum #449 minus background, one notes that the para and meta isomers are not even listed in the top ten but o-xylene has the best match value. A similar situation is observed for file spectrum #414 minus background. Meta-xylene is the best match. O-xylene is not listed while p-xylene is an unlikely choice.

A more complex aromatic blend VN-80-40 was also analyzed using the Nicolet 7199 GC-FTIR system. For such a sample, even a slight column over-loading can lead to badly tailing chromatographic peaks, more so than for predominantly aliphatic samples. A reconstructed

EPA VAPOR PHASE  
 NAPHTHALENE, 1,2,3,4-TETRAHYDRO-



NICOLET 7199 SYSTEM

.SRQ  
 ENTER SKIP REGIONS, NEGATIVE NO. IF DONE  
 LOW LIMIT 400  
 HIGH LIMIT 710  
 LOW LIMIT -1  
 MAX FOR SCALING, NEG IF AUTO -1

- EPA VAPOR PHASE  
 POSSIBLE HITS
- 910 NAPHTHALENE, 1,2,3,4-TETRAHYDRO-, L6&TJ
  - 1008 TOLUENE, O-1-CYCLOHEXEN-1-YL-, L6UTJ AR B
  - 219 CYCLOHEXANOL, 1-O-TOLYL-, L6TJ AR AR B
  - 408 HEXANE, 1-PHENYL-, 6R
  - 1574 ACENAPHTHENE, 2A,3,4,5-TETRAHYDRO L566 1A LT&TJ
  - 336 OCTANE, 1-PHENYL-, 8R
  - 512 BENZENE, PENTYL-, 5R
  - 2510 NONANE, 1,9-DICHLORO-, 696
  - 516 DECAINE, 1,10-DICHLORO-, 6106
  - 917 BENZENE, TETRAHYDRO-, 14
  - 1222 BENZENE, TETRAHYDRO-, 555
  - 520 L607J

FIGURE 37

EPA VAPOR PHASE  
NAPHTHALENE, DECAHYDRO-, CIS-,

.SRQ  
ENTER SKIP REGIONS, NEGATIVE NO. IF DONE  
LOW LIMIT 400  
HIGH LIMIT 735  
LOW LIMIT -1  
MAX FOR SCALING, NEG IF AUTO -1

EPA VAPOR PHASE  
POSSIBLE HITS

1038	NAPHTHALENE, DECAHYDRO-, CIS-,
34	L66TJ
241	BICYCLO/4.4.0/DECANE
85	L66TJ
446	CYCLOOCTANE
115	L8TJ
169	CYCLOHEXANE, BUTYL-, C
120	L6TJ A4
982	CYCLODODECENE
120	L12 AUTJ
417	CYCLOHEXANE, ETHYL-,
124	L6TJ A2
137	CYCLOHEXANE, PENTYL-, C
128	L6TJ A5
3128	CYCLODODECANE
130	L-12-TJ
136	CYCLOHEXANE, PROPYL-, C
132	L6TJ A3
3253	FLUORENE, DODECAHYDRO-,
139	L636TJ

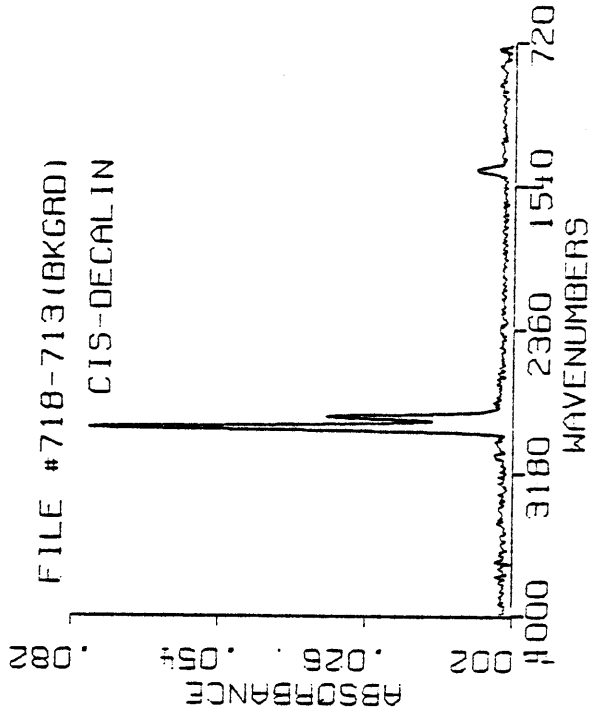
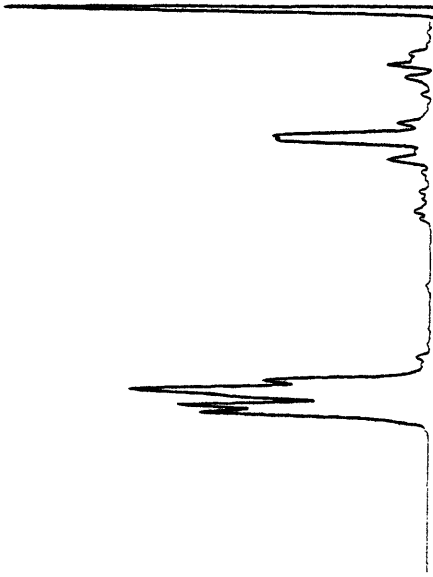
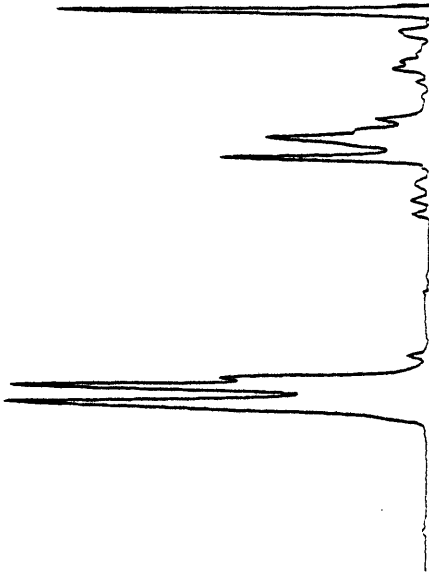


FIGURE 38

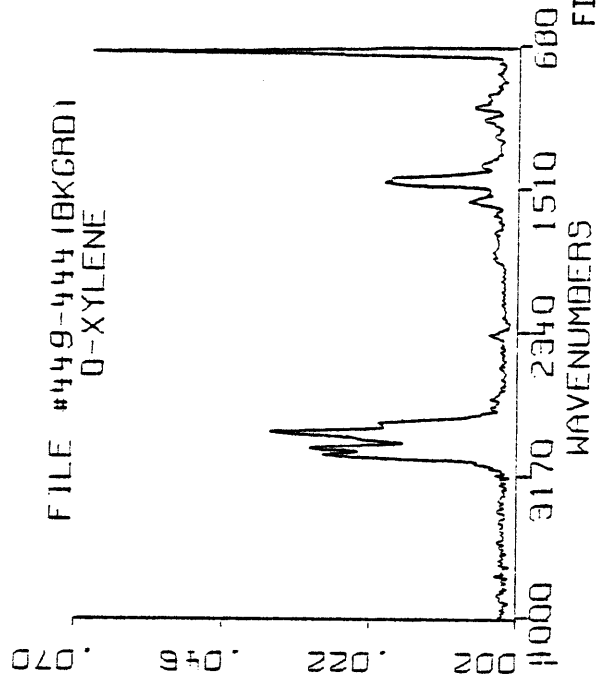
EPA VAPOR PHASE  
O-XYLENE



EPA VAPOR PHASE  
M-XYLENE

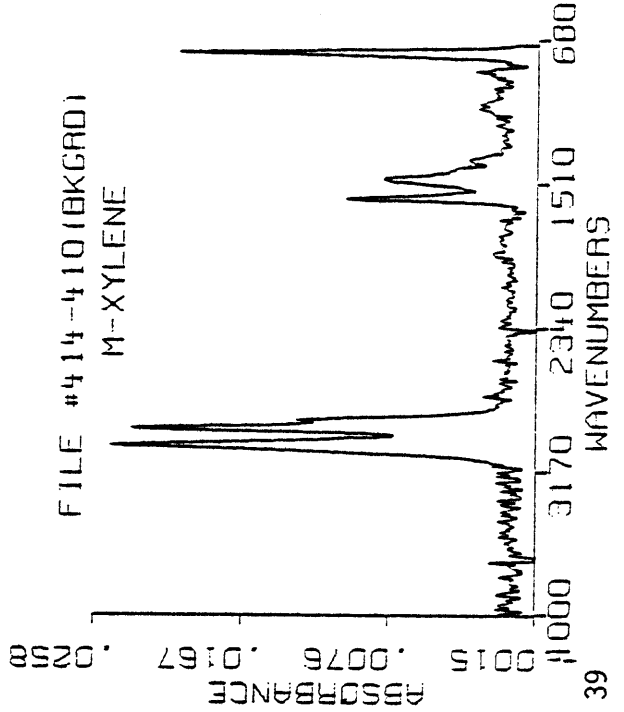


ABSORBANCE  
0.02  
.022  
.070



FILE #449-444 (BKGRD)  
O-XYLENE

ABSORBANCE  
0.015  
.0076  
.0167  
.0258



FILE #414-410 (BKGRD)  
M-XYLENE

FIGURE 39

TABLE 6

NICOLET 7199 FTIR SYSTEM

O-XYLENE STANDARD SEARCH LIST

.SRQ  
 ENTER SKIP REGIONS, NEGATIVE NO. IF DONE  
 LOW LIMIT 400  
 HIGH LIMIT 710  
 LOW LIMIT 2300  
 HIGH LIMIT 2400  
 LOW LIMIT -1  
 MAX FOR SCALING, NEG IF AUTO -1

M-XYLENE STANDARD SEARCH LIST

.SRQ  
 ENTER SKIP REGIONS, NEGATIVE NO. IF DONE  
 LOW LIMIT 400  
 HIGH LIMIT 712  
 LOW LIMIT -1  
 MAX FOR SCALING, NEG IF AUTO -1

EPA VAPOR PHASE  
 POSSIBLE HITS  
 806 O-XYLENE  
 106 IR B  
 795 SULFIDE, PHENYL 3-PHENYLPROPYL,  
 1232 RSSR  
 2609 BUTANE, 1-BROMO-2,4-DIPHENYL-,  
 1342 E1YR&R  
 2686 PROPANE, 1,3-DIPHENYL-,  
 1391 R3R  
 2610 HEXANE, 1,3,5-TRIPHENYL-,  
 1404 1YR&1YR&R  
 2489 TOLUENE, O-ETHYL-,  
 1522 2R B  
 26 BENZENE, METHYL-,  
 1557 IR  
 1938 ISODIQUINOLINE, 1,2,3,4-TETRAHYDRO-  
 1591 T&C CMT&J  
 2669 BUTANE, 1,3-DIPHENYL-, /MINUS/-,  
 1593 1YR&R  
 2668 BUTANE, 1,3-DIPHENYL-, /PLUS/-,  
 1658 1YR&R

EPA VAPOR PHASE  
 POSSIBLE HITS  
 78 M-XYLENE  
 220 IR C  
 923 BENZENE, 1,2,3-TRIMETHYL-,  
 1805 IR B C  
 342 BITOLYL, M,MPR-,  
 1874 IR CR C  
 2476 BENZENE, 1-ETHYL-3-METHYL-,  
 2304 2R C  
 2610 HEXANE, 1,3,5-TRIPHENYL-,  
 2350 1YR&1YR&R  
 871 P-XYLENE  
 2423 IR D  
 799 BENZENE, 1,3,5-TRIMETHYL-,  
 2525 IR C E  
 75 BENZENE, 1,2,4-TRIMETHYL-,  
 2594 IR B D  
 2668 BUTANE, 1,3-DIPHENYL-, /PLUS/-,  
 2735 1YR&R  
 2669 BUTANE, 1,3-DIPHENYL-, /MINUS/-,  
 2751 1YR&R

chromatogram of the region characteristic of aromatics, 3020-3200  $\text{cm}^{-1}$ , accurately illustrates the wide range of aromatic components (both mono- and polyaromatic) detected for 0.025  $\mu\text{L}$  of sample injected (Figure 40). The transformed spectrum for a minor monoaromatic component, file #322, gives reasonable S/N and a good match with 1,2,4-trimethylbenzene (Figure 41). Although VN-80-40 is highly complex, three polyaromatics make up the bulk of this sample. One of these compounds has been tentatively identified as 1-methylnaphthalene. Figure 42 (file spectrum #892 minus background) shows the excellent match achieved by the search system from both visual and numerical comparisons.

The fuel product (VN-80-40) was also run on our Nicolet 6000 system with the Model 26 cell. Lack of sensitivity resulted in badly tailing peaks from the column overloading needed to detect the minor constituents. The three polyaromatics were, however, identified as a result of their high concentration and high corresponding S/N. They were found to be naphthalene, 2-methylnaphthalene and 1-methylnaphthalene. These findings agree with spectral matches using the more sensitive 7199 system (Figures 43-45). It should be noted, however, that considerably less sample was used in the 7199 case. Although these polyaromatics differ in structure by only one methyl group, infrared absorbance spectra of each are dissimilar both visually and spectroscopically. This observation points out the unique advantages of FTIR detection in the gas phase.

VN 80-40 AROMATIC BLEND  
3020-3200 CM-1 RCN  
NICOLET 7199 SYSTEM  
60 METER DB-1 FUSED SILICA

PPK

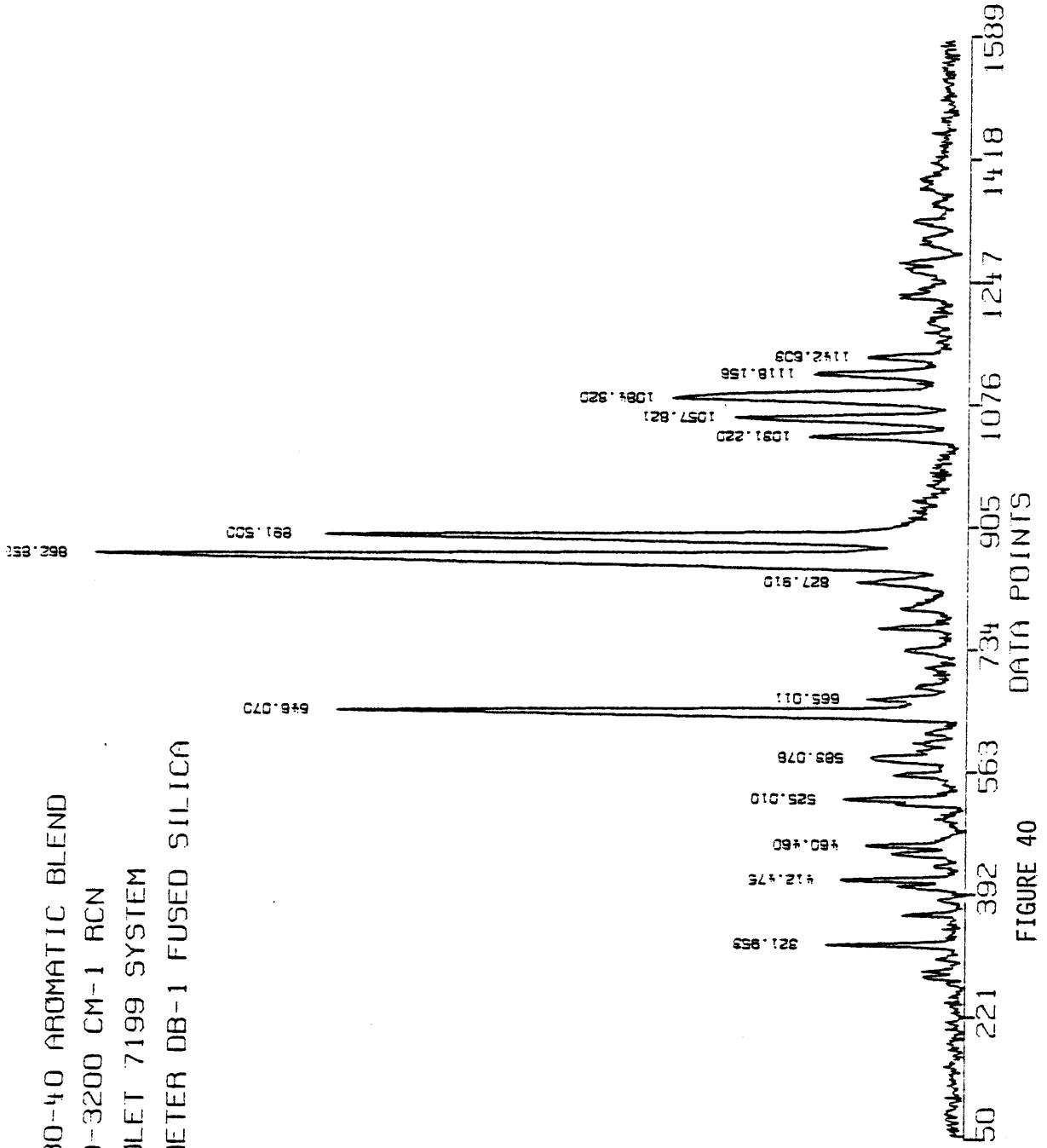
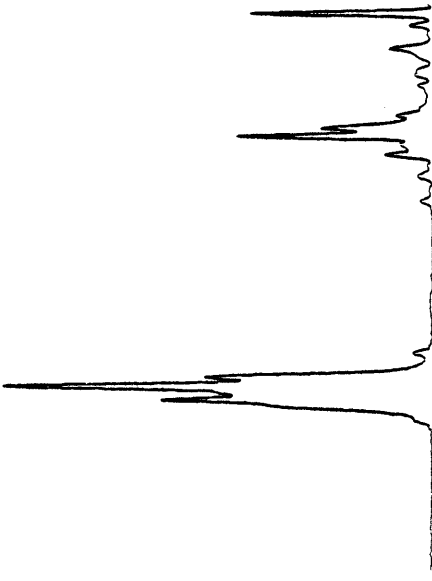


FIGURE 40

NICOLET 7199 SYSTEM

EPA VAPOR PHASE  
BENZENE, 1,2,4-TRIMETHYL-



.SR0  
ENTER SKIP REGIONS, NEGATIVE NO. IF DONE  
LOW LIMIT 400  
HIGH LIMIT 740  
LOW LIMIT 2300  
HIGH LIMIT 2400  
LOW LIMIT -1  
MAX FOR SCALING, NEG IF AUTO -1

EPA VAPOR PHASE  
POSSIBLE HITS

75	BENZENE, 1,2,4-TRIMETHYL-, IR B D
156	
914	BENZENE, 1,2,3,4-TETRAMETHYL-, IR B C D
635	
2498	BENZENE, 1,2,3,5-TETRAMETHYL-, IR B C E
653	
1107	BENZENE, 1,2,4,5-TETRAMETHYL-, IR B D E
754	
41	2-BUTENE, 2-METHYL-, YU2
1044	
1190	BENZENE, HEXAMETHYL-, U 6-R
1115	
103	2,4-HEXADIENE, 2,5-DIMETHYL-, 1Y&U2UY
1398	
2308	PROPANE, 2,2-BIS(3,4-XYLYL)-, IR B EXR C D
1448	
457	2-BUTENE, 2,3-DIMETHYL-, 1Y&UY
1454	
2222	BENZYLAMINE, 2,5-DIMETHYL-, Z1R B E
1563	

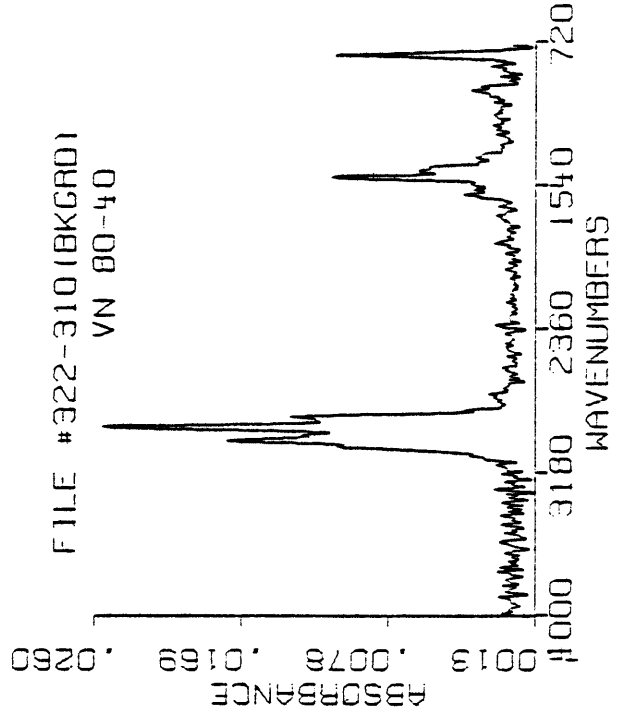
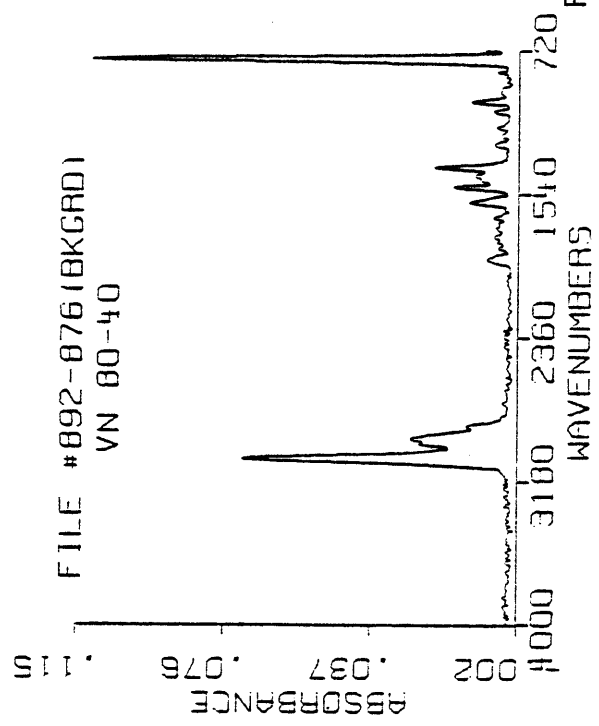
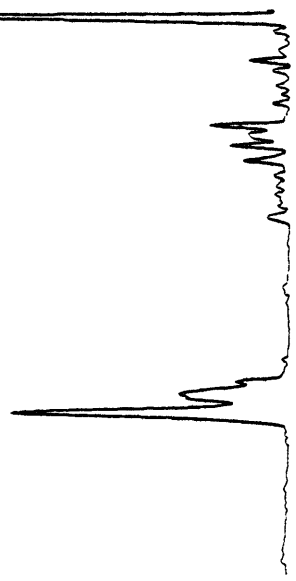


FIGURE 41

EPA VAPOR PHASE  
NAPHTHALENE, 1-METHYL-

NICOLET 7199 SYSTEM



FILE #892-876(BKGRD)  
VN 80-40

.SR0  
ENTER SKIP REGIONS, NEGATIVE NO. IF DONE  
LOW LIMIT 400  
HIGH LIMIT 720  
LOW LIMIT -1  
MAX FOR SCALING, NEG IF AUTO -1

- EPA VAPOR PHASE  
POSSIBLE HITS
- 798 NAPHTHALENE, 1-METHYL--  
76 L66J B
  - 175 NAPHTHALENE, 1-ETHYL--  
701 L66J B2
  - 1357 NAPHTHALENE  
737 L66J
  - 1493 1-NAPHTHALENESULFONIC ACID, DIHYD  
981 L66J BSMQ &GH &OH
  - 1254 NAPHTHALENE, 1,5-DIMETHYL--  
1012 L66J B G
  - 330 NAPHTHALENE, 1-CHLOROMETHYL--  
1090 L66J B16
  - 2518 1-NAPHTHALENECARBONITRILE  
1179 L66J BCN
  - 1331 AZOBENZENE  
1613 RAVNR
  - 172 QUINOLINE, 8-METHYL--  
1745 T66 BHJ J
  - 876 M-TOLUNITRILE  
1774 NCR C

FIGURE 42

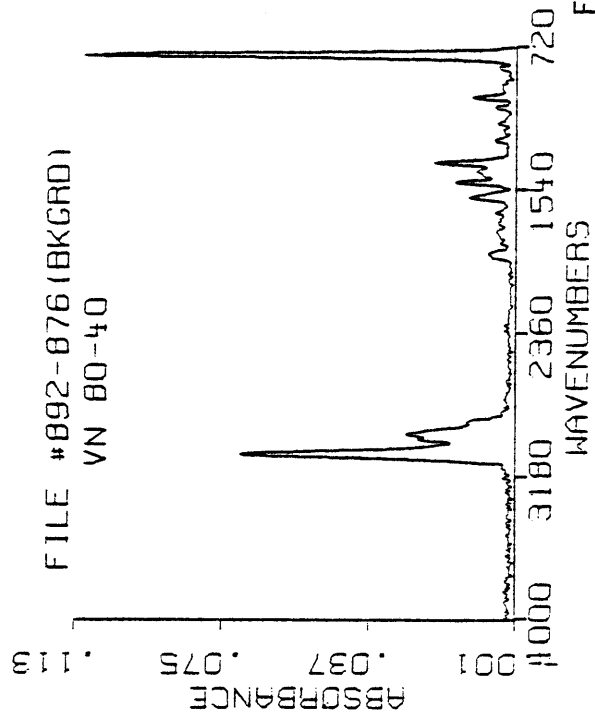
EPA VAPOR PHASE  
NAPHTHALENE, 1-METHYL-



EPA VAPOR PHASE  
NAPHTHALENE, 2-METHYL-



FILE #892-876 (BKGRD)  
VN 80-40



FILE #862-813 (BKGRD)  
VN 80-40

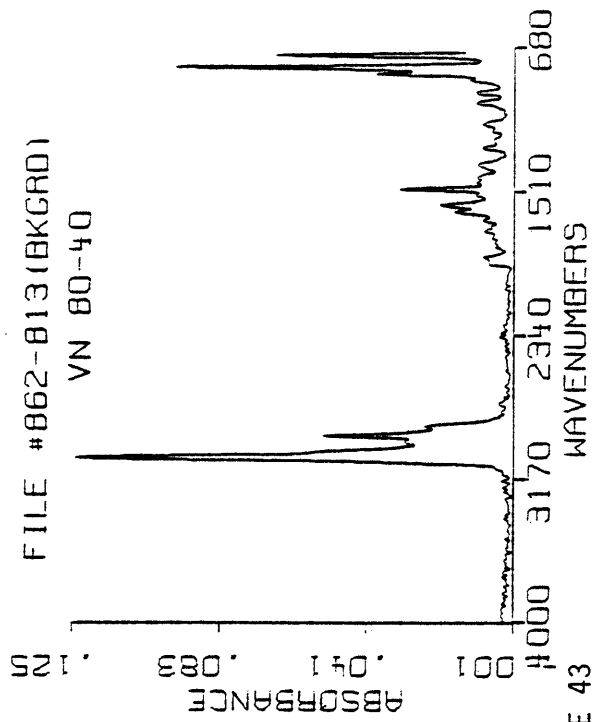


FIGURE 43

EPA VAPOR PHASE  
NAPHTHALENE, 2-METHYL-

NICOLET 7199 SYSTEM

.SRQ  
ENTER SKIP REGIONS, NEGATIVE NO. IF DONE  
LOW LIMIT 400  
HIGH LIMIT 712  
LOW LIMIT 2300  
HIGH LIMIT 2400  
LOW LIMIT -1  
MAX FOR SCALING, NEG IF AUTO -1

EPA VAPOR PHASE  
POSSIBLE HITS  
2514 NAPHTHALENE, 2-METHYL-,  
185 L66J C  
2201 NAPHTHALENE, 1-CHLORO-2-METHYL-,  
1764 L66J B6 C  
2513 NAPHTHALENE, 2-ETHYL-,  
1796 L66J C2  
334 NAPHTHALENE, 1-BROMO-2-METHYL-,  
1845 L66J BE C  
1713 ISOQUINOLINE  
1951 T66 CNJ  
1264 PHENANTHRENE, 3-METHYL-,  
2109 L B666J D  
1101 PHENANTHRENE  
2413 L B666J  
172 QUINOLINE, 8-METHYL-,  
2430 T66 BNJ J  
1852 ETHYLAMINE, 1,2-DIPHENYL-,  
2450 ZYR&IR  
855 1-BENZAZINE  
2456 T66 BNJ

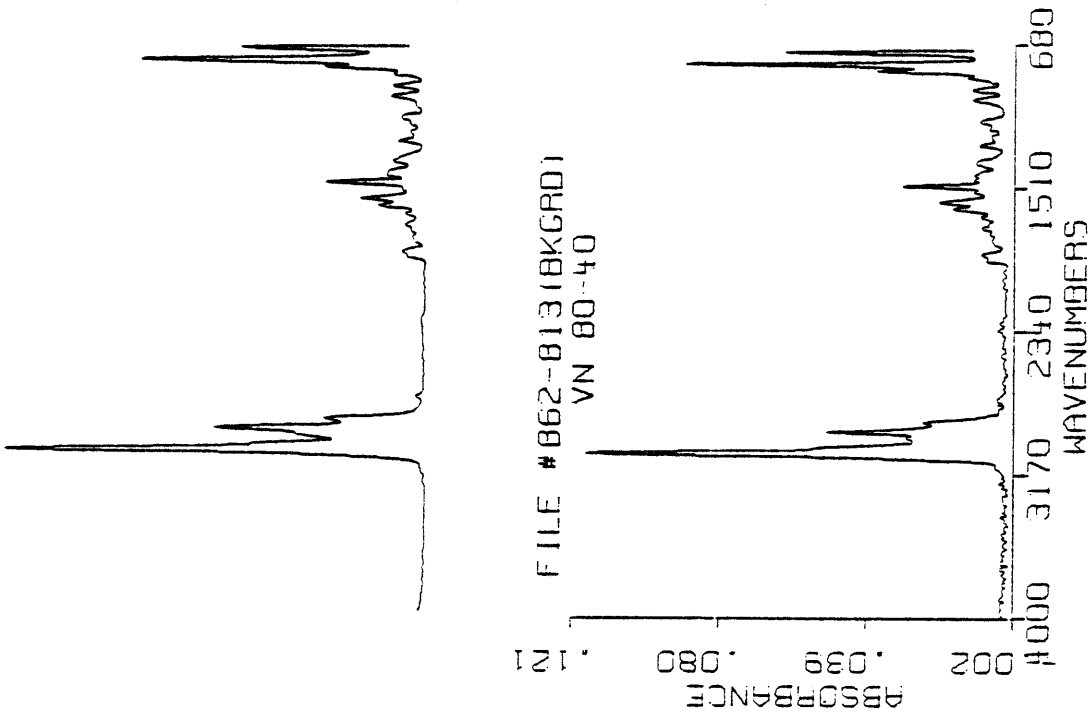


FIGURE 44

EPA VAPOR PHASE  
NAPHTHALENE

NICOLET 7199 SYSTEM

.SRQ  
ENTER SKIP REGIONS, NEGATIVE NO. IF DONE  
LOW LIMIT 400  
HIGH LIMIT 725  
LOW LIMIT -1  
MAX FOR SCALING, NEG IF AUTO -1

EPA VAPOR PHASE  
POSSIBLE HITS

1357	49	NAPHTHALENE
	L66J	
1493	467	1-NAPHTHALENESULFONIC ACID, DIHYD
	L66J BSMQ &OH &OH	
330	494	NAPHTHALENE, 1-CHLOROMETHYL-
	L66J B1G	
798	596	NAPHTHALENE, 1-METHYL-
	L66J B	
2518	1006	1-NAPHTHALENECARBONITRILE
	L66J BCI	
1254	1262	NAPHTHALENE, 1,5-DIMETHYL-
	L66J B 6	
1331	1264	AZOBENZENE
	ANVHR	
175	1532	NAPHTHALENE, 1-ETHYL-
	L66J B2	
325	1732	PROPANE, 1,1,2-TRICHLORO-, GY6YG
837	1743	METHANE, BROMOTRICHLORO-, GXEGG

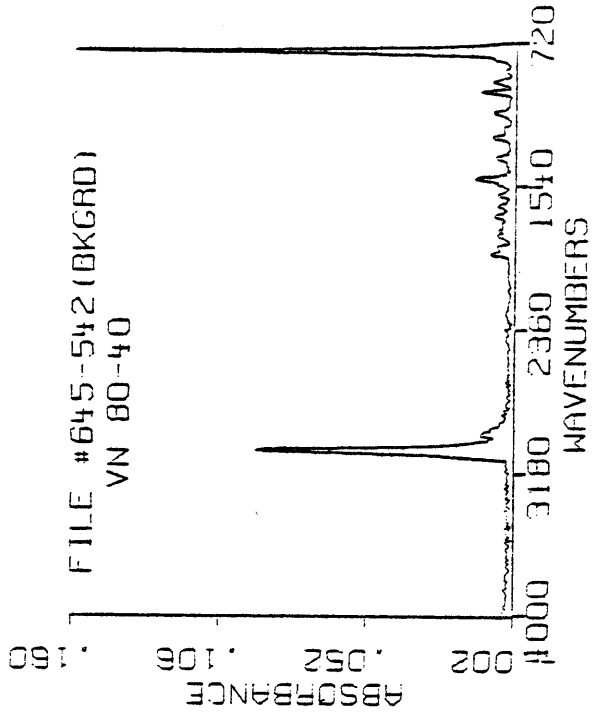


FIGURE 45

## GAS CHROMATOGRAPHY-MASS SPECTROMETRY

### COMPARISONS

Comparison of GC-FTIR to GC-MS was conducted by analysis of test fuel VN-77-11, aromatic blend VN-80-40, and a standard mixture. The Accuspec GC with DB-5 fused silica column was interfaced to a Varian MAT 112 electron impact mass spectrometer by a short, heated transfer line. The same or very similar injection volumes as used for the 7199 GC-FTIR analysis were approximated. Since on-column injection was used in the GC-MS experiment, a dilution of the sample was necessary since sample volumes of less than 0.1  $\mu\text{l}$  were not possible.

The VN-77-11 test fuel was run with the source pressure at about  $1.5 \times 10^{-5}$  torr. The GC effluent was directed into the mass spectrometer without a separator. A 2 ml/min linear flow rate of helium carrier gas accounts for the relatively high source pressure. All fittings in the interface were tested with argon gas to detect leaks prior to using the mass spectrometer. With knowledge to the total alkane character of this fuel and estimated molecular weight maximum, a mass/charge scan range of 50-180 was used. This scan range resulted in approximately 1 (130 m/e total) scan per second. The sample was diluted ten-fold in tetradecane to avoid solvent interferences. One consequence of using a lower boiling solvent would have been loss of volatile sample data. In addition, the relatively large amount of diluting solvent was found to cause the ionization source pressure to exceed  $10^{-4}$  torr, thus causing a temporary system shutdown. The large  $\text{C}_{14}$  peak is, however, not as sharp due to retention band broadening and

causes no problems. A listing of the temperature program and associated parameters are given on the total ion reconstructed chromatogram (Figure 46). For clarity, Figure 46 shows only half of the total sample detected. For 0.02  $\mu\text{L}$  of actual sample injected, the MS trace shows a response for some trace components not adequately detected by the 7199 GC-FTIR system. In reference to detection limit comparisons, about twice as much sample was injected into the GC-MS as was injected into the GC-FTIR (0.02  $\mu\text{L}$  vs.  $\sim$ 0.013  $\mu\text{L}$ ), although the amount associated with the FTIR may be more or less, since quantitation using the injection splitter is not as certain as on-column injection.

The mass/charge versus ion intensity plot for spectrum #1756 confirms the earlier FTIR peak identification as methylcyclopentane (Figure 47a). Recalling earlier FTIR analyses, the component eluting and giving rise to spectrum #1921 had been identified as methylcyclohexane (7199 system) or 1,1-dimethylcyclohexane (Model 36). Mass spectral data indicate a molecular ion of 98 for this peak component and a splitting pattern similar to methylcyclohexane (Figure 47b). In this example, mass spectrometry is very useful in defining the overall molecular weight of the molecule.

Due to the difference in column bonded phases used for the 7199 FTIR and GC-MS analyses, confirmation of m-xylene found earlier by FTIR was more elusive. The m/e versus intensity plot for spectrum #2266 does not indicate the expected strong intensity at m/e=91 for m-xylene (Figure 48). As was mentioned earlier, because jet fuel VN-77-11 was of mainly aliphatic character (85%) only "minimal" differences in retention

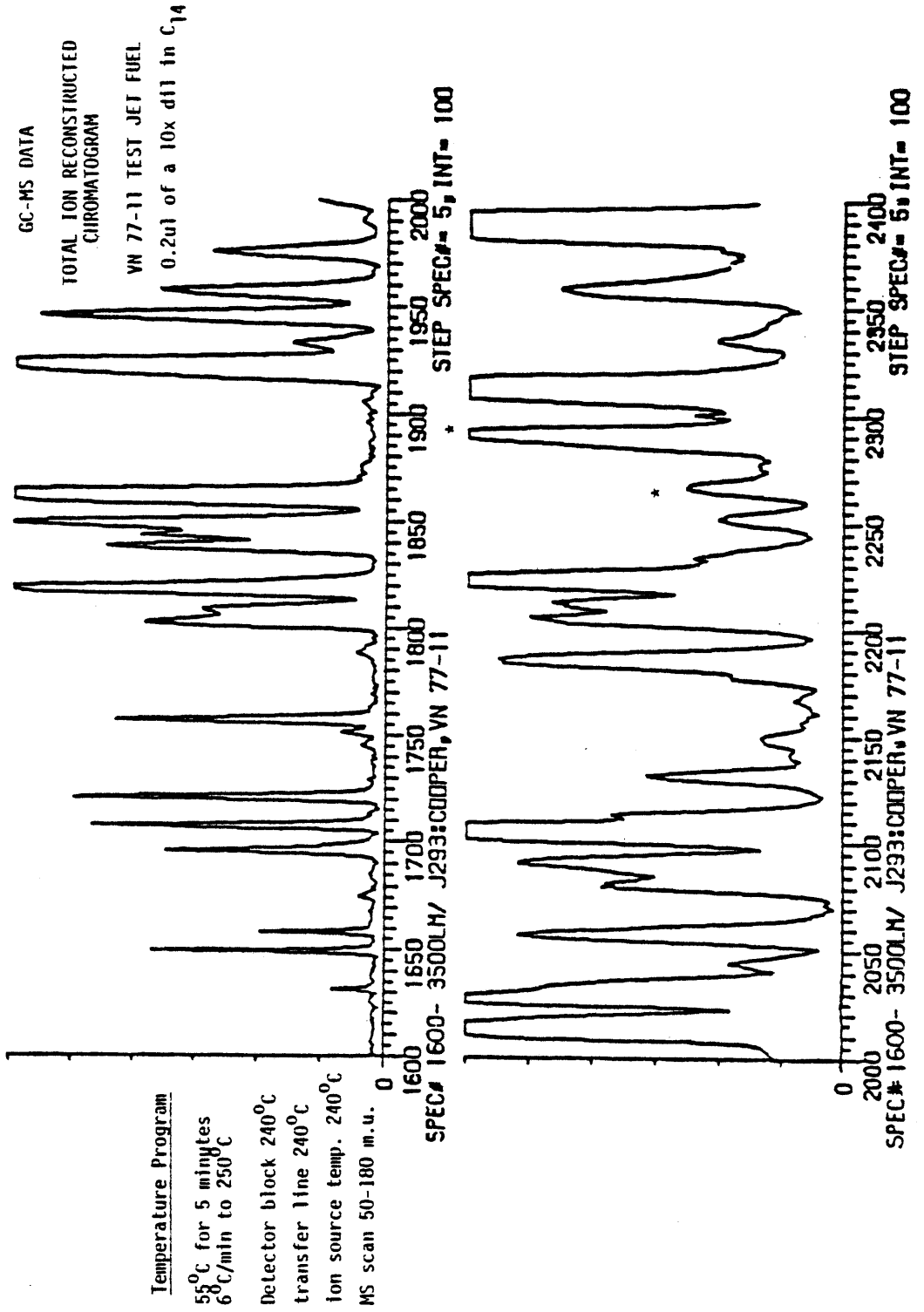


FIGURE 46

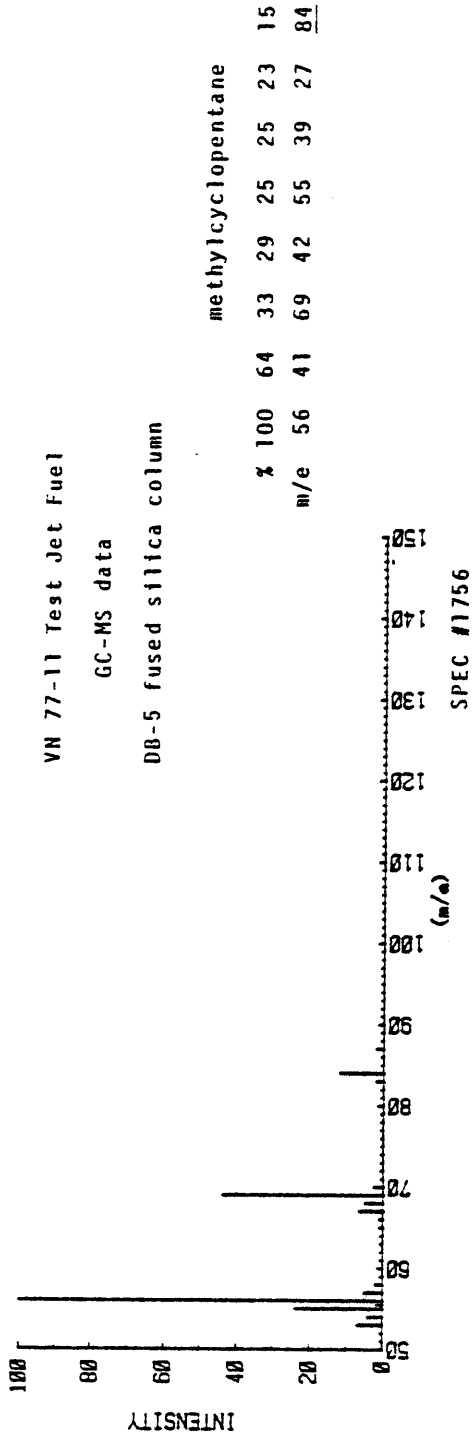


FIGURE 47a

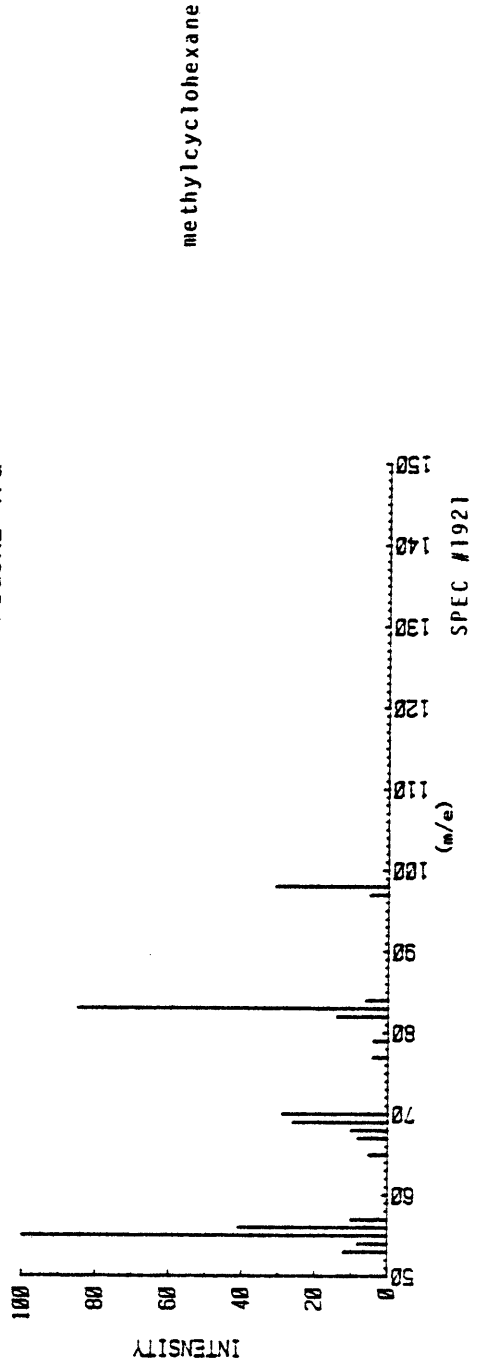


FIGURE 47b

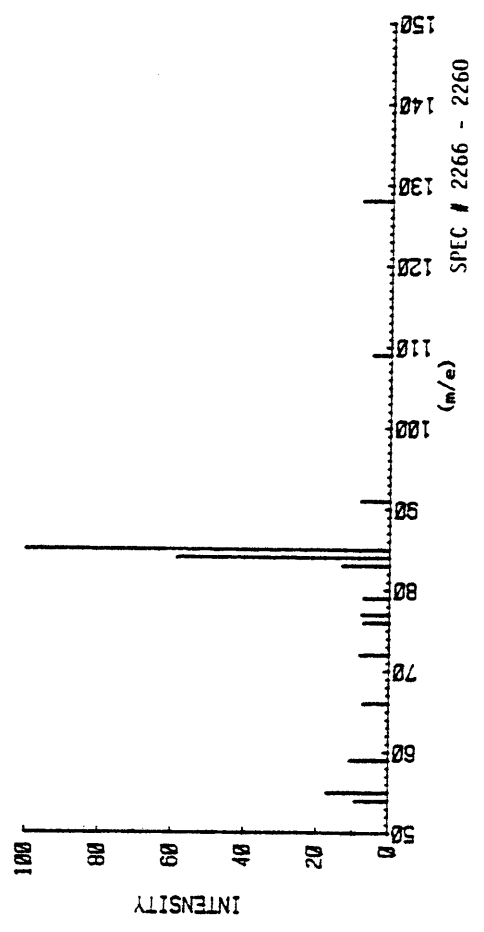
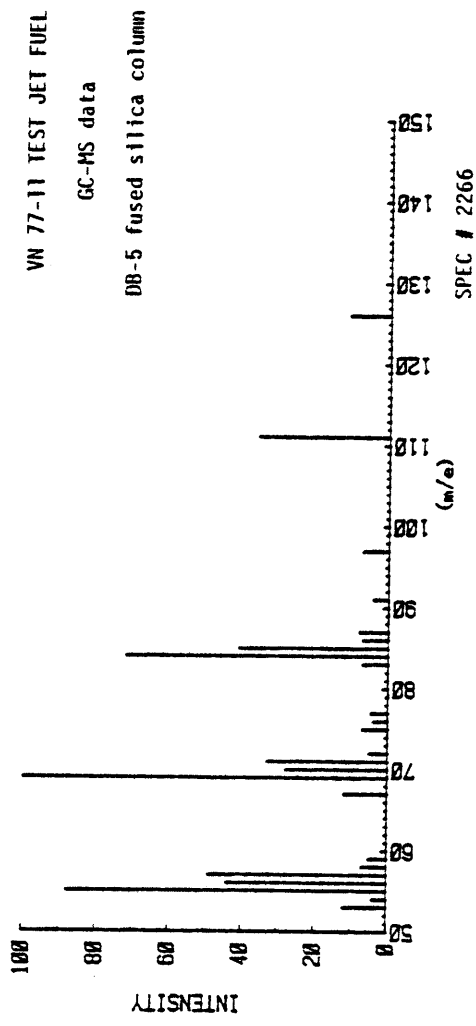


FIGURE 48

times were to be expected. In looking for the m-xylene component, however, by GC-MS (using the DB-5 column) significant retention time shifts were observed, particularly for the aromatic m-xylene. In Figure 49 sections of the GC-FTIR Gram-Schmidt reconstruction for VN-77-11 near the m-xylene location are presented to illustrate these retention time differences for chromatography on the DB-1 and DB-5 capillary columns. The starred peaks for each section of the respective chromatogram correspond to the tentatively identified m-xylene. These sections originate from FTIR chromatograms previously run using the Model 36 IR cell and for the Nicolet 7199 IR system. The GC-MS data for the corresponding section of chromatogram added more uncertainty in locating the m-xylene since two individual peaks showed mass spectra indicative of a xylene compound (Figure 50). These peaks are located at mass spectrum #2291 and #2315 in the GC-MS total ion reconstructed chromatogram (Figure 46). The starred peaks indicate the component peaks of interest in the first half of the total ion chromatogram (presented for clarity). Since the splitting patterns and molecular ion masses for all three isomers of xylene (o, m, p) are nearly identical, an identification by GC-MS alone could not be made. An exhaustive file by file search of each FTIR run could find no other xylene near the m-xylene peak. Due to the fact that the mass spectrometer is more sensitive to aromatics than is FTIR, no confirmation could be made concerning the second aromatic "xylene-type" component. In the mass spectrum, because of the relative chemical stability of the aromatic xylene molecule (compared to an alkane),

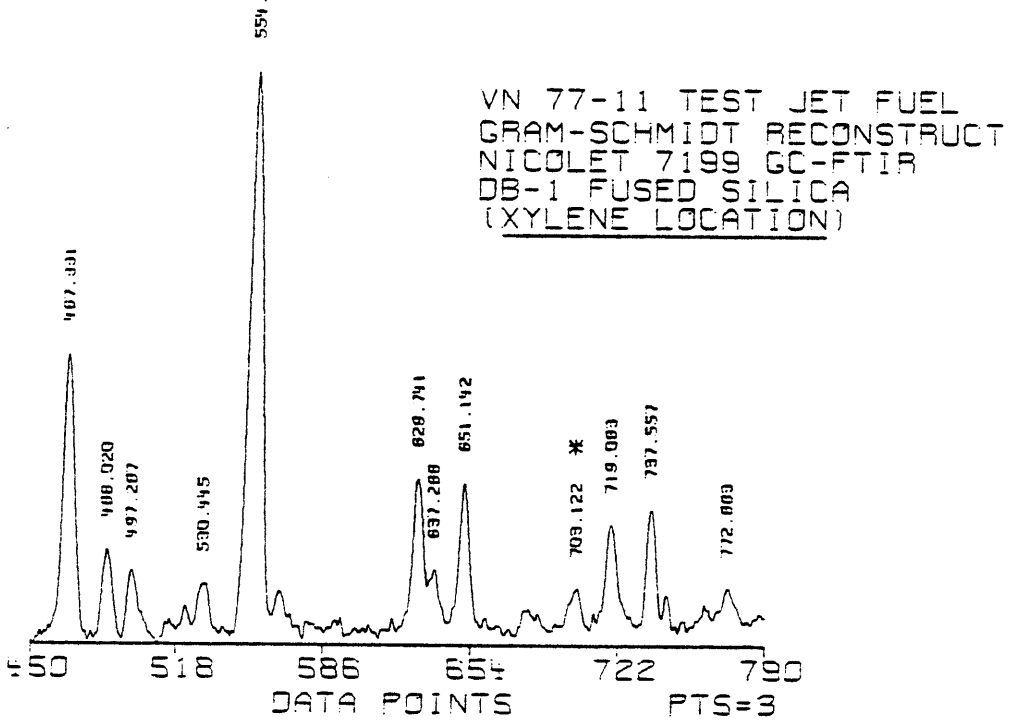
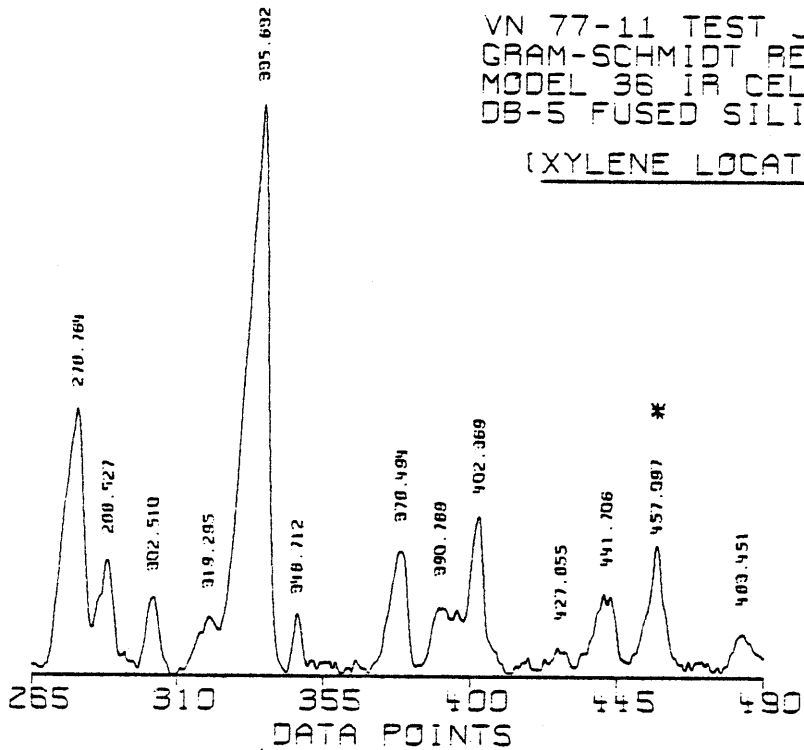
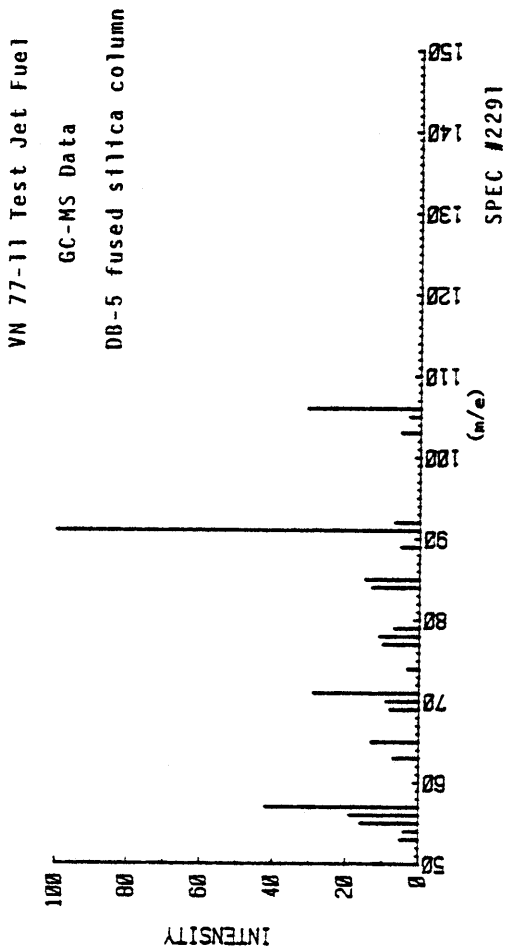


FIGURE 49



m-xylene

%	100	62	29	11	9	8	7	6
m/e	91	106	105	77	51	92	39	79

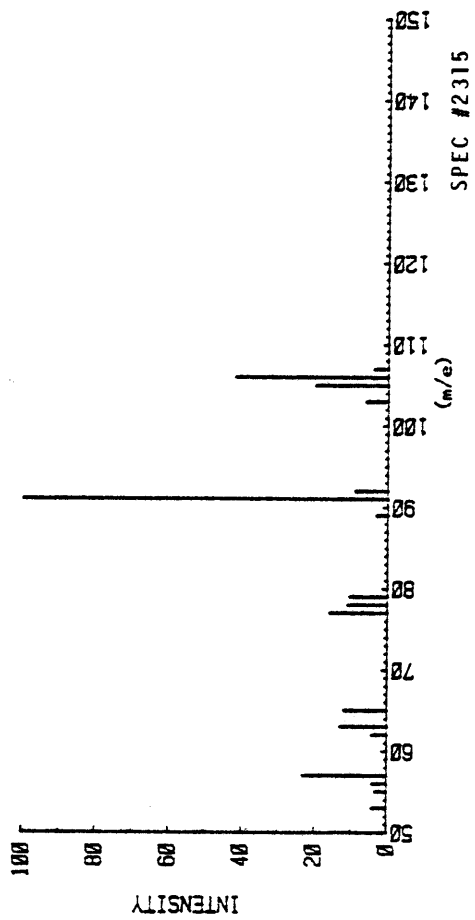


FIGURE 50

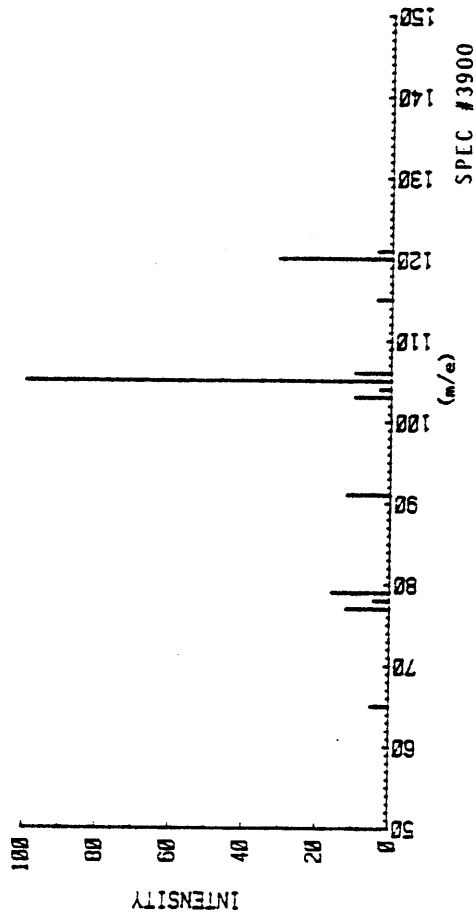
co-elution of a xylene with an alkane would still give an intense aromatic molecular ion intensity. Although a combination of GC-MS and GC-FTIR data may appear incomprehensible, the information which is discernable should not go without some merit. By having access to both sets of data one can surmise that an aromatic xylene is present according to the mass spectrum, and further, that this xylene can be distinguished from other xylene isomers by its characteristic infrared absorbance spectrum.

Another illustration of the mass spectrometer's sensitivity toward aromatics can be seen for spectrum #3900 (Figure 51) which corresponds to the starred component in VN-80-40 (Figure 52). Using a sample dilution of 10x in THF, a 0.02  $\mu\text{L}$  equivalent was injected onto the GC-MS as compared to 0.023  $\mu\text{L}$  (calculated) for the GC-FTIR Nicolet 7199 experiment. A good total ion intensity can be seen for this very low concentration component (Figure 52, starred peak). The splitting pattern and a molecular ion of 120 indicate that this compound is a substituted benzene, possibly o-ethyltoluene or isopropylbenzene. An FTIR library search of file spectrum #286, the corresponding peak, from VN-80-40 yielded uncertain results due to the poor S/N and baseline inconsistencies (Figure 53). Neither o-ethyltoluene nor isopropylbenzene are listed for the FTIR search although toluene-3,5-diisopropyl is listed as the second match using the AB algorithm. The spectrum of this match is, however, not very similar at all to the sample spectrum. Visually, however, the compound resembles 1,3,5-trimethylbenzene. Quite possibly, the two

VN 80-40 Aromatic Blend

GC-MS data

DB-5 fused silica column



o-ethyl toluene

% 100 31 10 10 9 9 7 6  
m/e 105 120 77 91 106.. 79 44 103

isopropyl benzene

% 100 27 13 11 9 9 8 5  
m/e 105 120 77 79 106 51 103 91

FIGURE 51

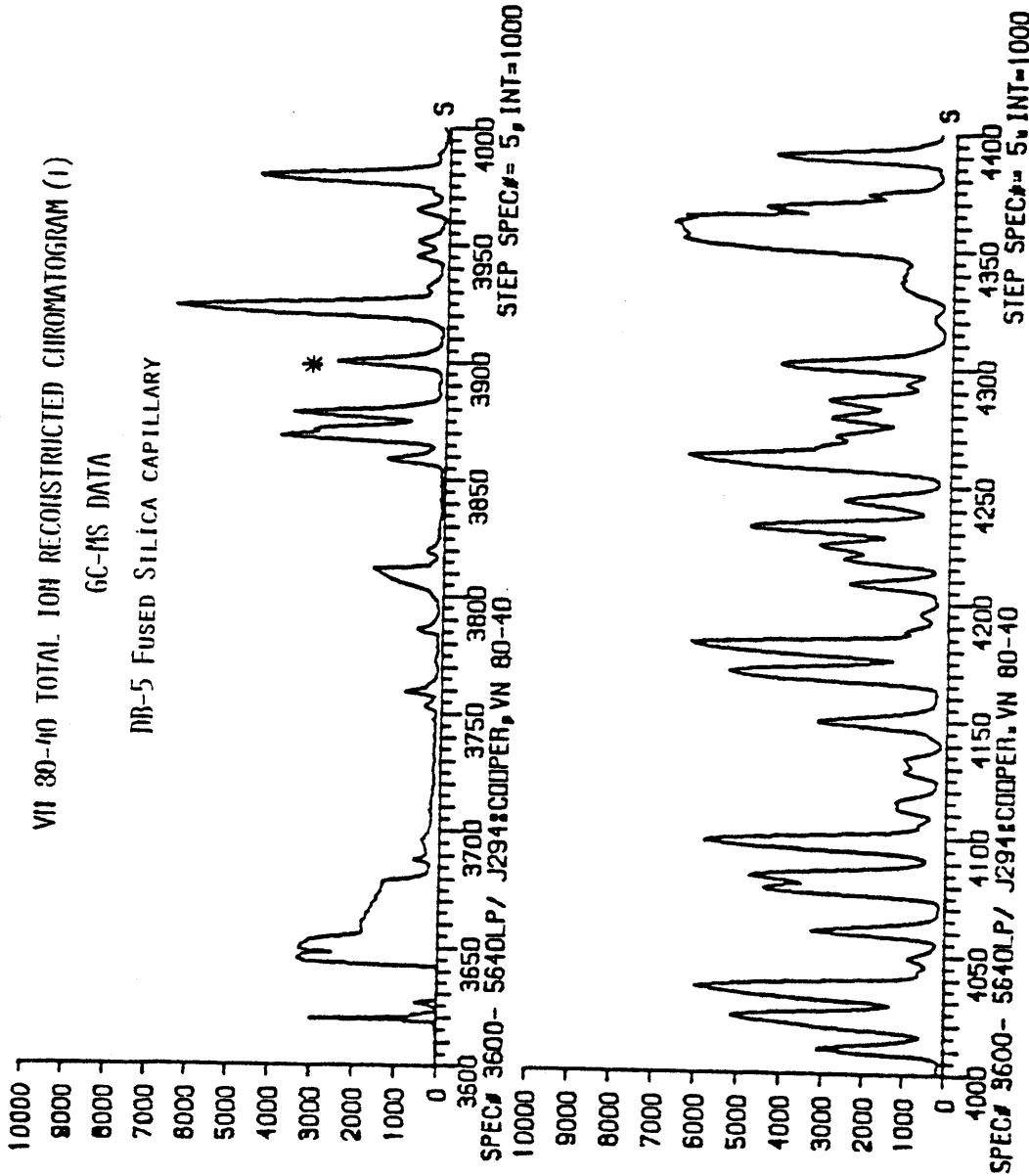


FIGURE 52a

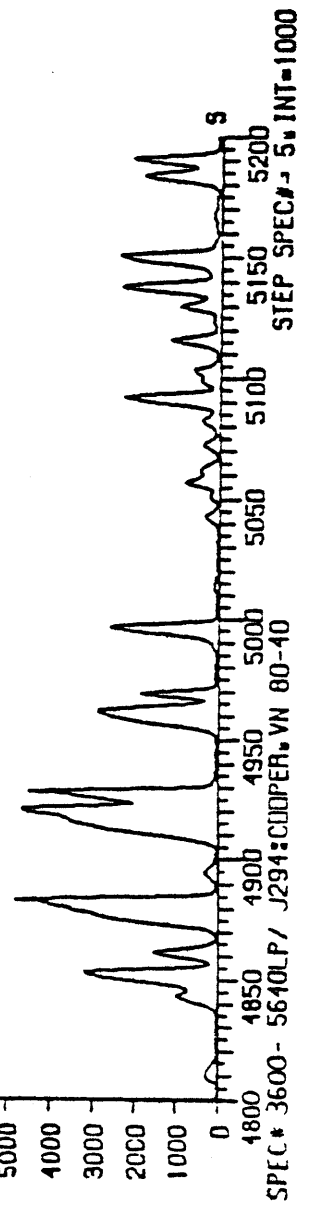
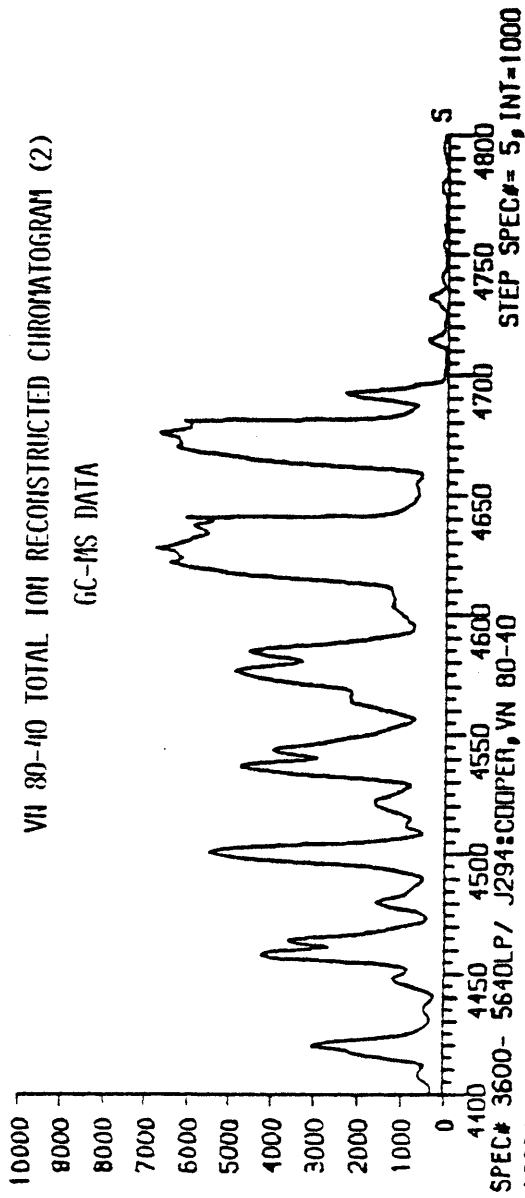
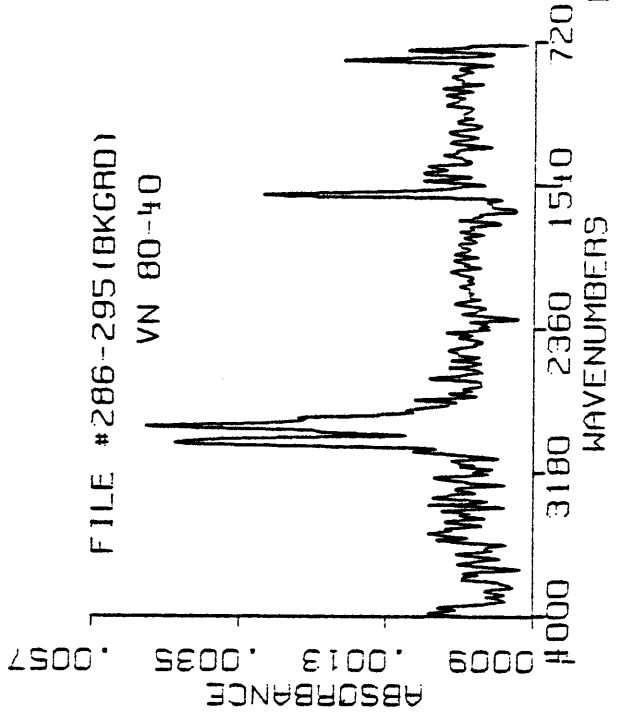
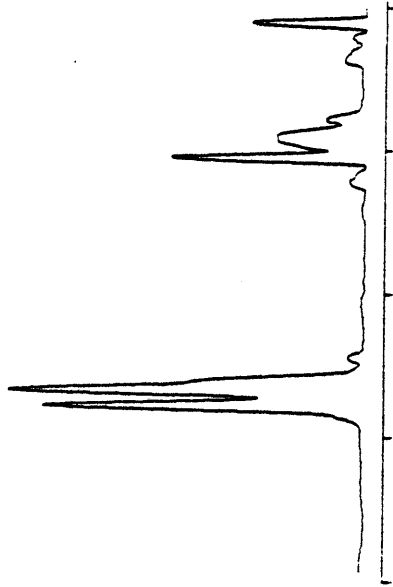


FIGURE 52b

EPA VAPOR PHASE  
 BENZENE, 1,3,5-TRIMETHYL-



NICOLET 7199 GC-FTIR

SPA = AB  
 .SRQ  
 ENTER SKIP REGIONS, NEGATIVE NO. IF DONE  
 LOW LIMIT 400  
 HIGH LIMIT 740  
 LOW LIMIT 3600  
 HIGH LIMIT 4000  
 LOW LIMIT -1  
 MAX FOR SCALING, NEG IF AUTO -1

EPA VAPOR PHASE POSSIBLE HITS	
371	BROMOFORM
201	EYEE
1026	TOLUENE, 3,5-DIISOPROPYL-, YR CY E
907	BENZENE, CYCLOHEXYL-, L6TJ AR
1960	METHANOL, TRI-2-NORBORNYL-, L55 ATJ 3/CX0
374	ETHANE, 1,2-DICHLORO-, G25
219	ETHANE, 1,1,1-TRICHLORO-, GX66
222	BICYCLO/6.1.0/INDANE, 9,9-DIBROMO L38TJ BE BE
2654	BICYCLO/6.1.0/INDANE, 9,9-DIBROMO L38TJ BE BE
402	BICYCLOHEXYL
224	L6TJ A-2
2708	CYCLOHEXANECARBONITRILE, 1-PHENYL L6TJ ACH AR
224	HEXADECANE, 1,2-EPOXY-, T30TJ B14
2759	TETRACOSANE 24H
1176	CYCLOHEXANECARBONITRILE, L6TJ ACH AR D
2655	CYCLOHEXANECARBONITRILE, L6TJ ACH AR D
225	CYCLOHEXANETHIOL L6TJ ASH
668	1-OCTADECANETHIOL SH18
226	CYCLOHEXANE, /2-BROMOETHYL-/-, L6TJ A2E
2721	
420	
227	

FIGURE 53

aforementioned compounds are simply not in the FTIR library search file.

On the positive side of GC-FTIR methodology, Figure 54 confirms the presence of a trisubstituted benzene, although the corresponding GC-MS information cannot be certain as to which one. GC-FTIR has previously identified the VN-80-40 component as 1,2,4-trimethylbenzene (Figure 41) because of the difference in infrared absorbance patterns of trisubstituted benzenes. Figure 55 shows that the mass spectral data for two substituted polyaromatic hydrocarbons are indistinguishable by GC-MS. The assignment of spectrum #4670 to 1-methylnaphthalene and spectrum #4620 to 2-methylnaphthalene was only possible after reviewing previous GC-FTIR data for VN-80-40. The distinction between these two isomers in their infrared absorbance patterns has already been established and need not be repeated (Figure 43). Herein lies a significant advantage of GC-FTIR over GC-MS. While isomer analysis using GC-MS is often ambiguous, the often profound differences in absorbance spectra for a series of very similar isomers usually lead to a confident identification by GC-FTIR.

Since the Varian MAT mass spectrometer did not have available a library file, a 20 component standard mixture similar to the one used with the GC-FTIR experiments was separated by gas chromatography and individual mass spectra analyzed. The standards were used to check the calibration and accuracy of GC-MS data. For each component in the mixture an accurate  $m/e$  vs. intensity plot was observed which

VN 80-40 Aromatic Blend  
GC-MS data  
DB-5 fused silica column

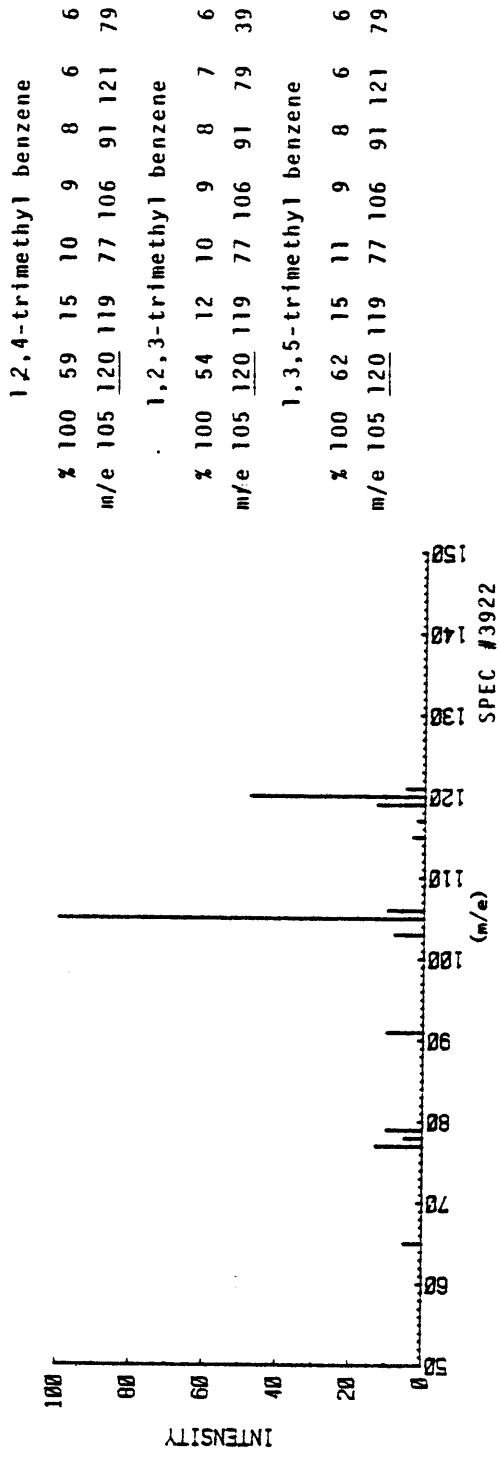


FIGURE 54

VN 80-40 Aromatic Blend

GC-MS data

DB-5 fused silica column

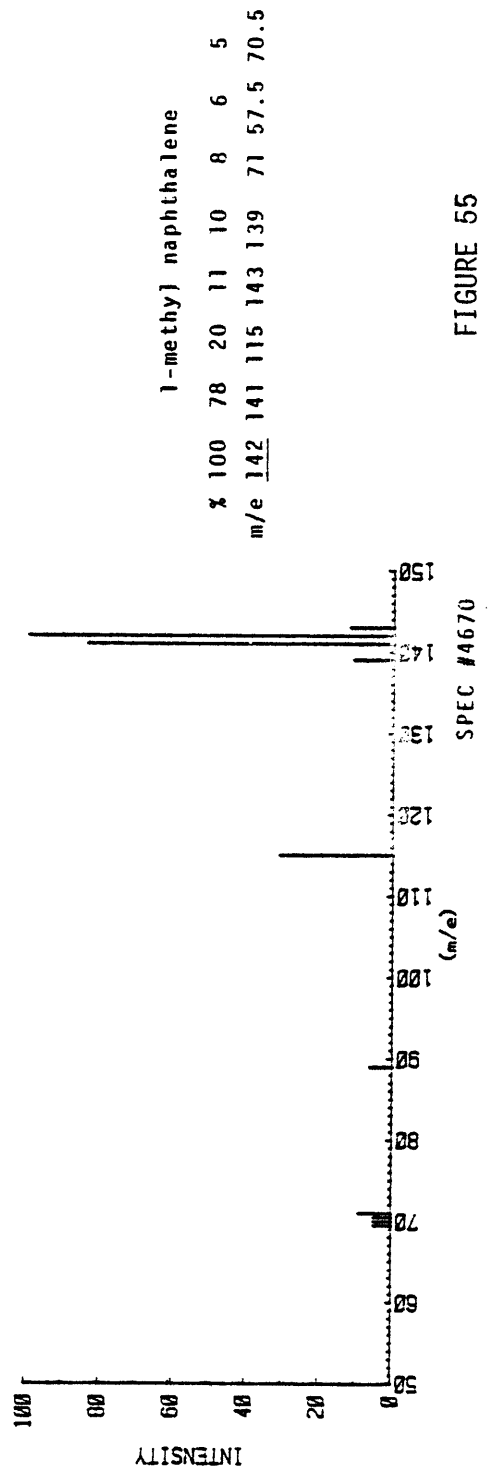
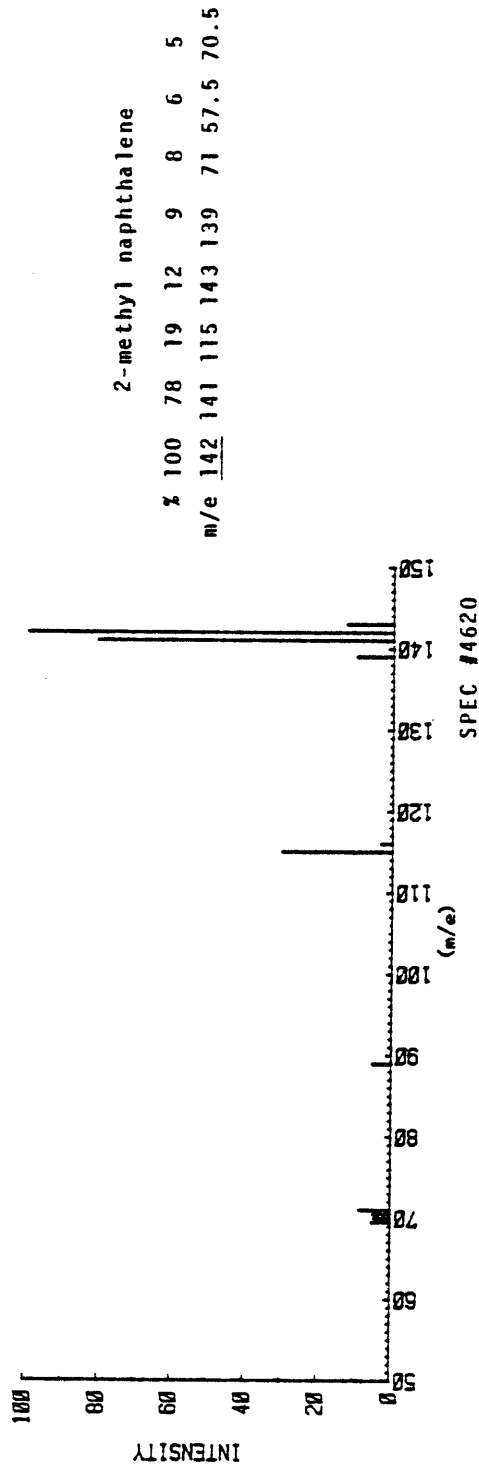


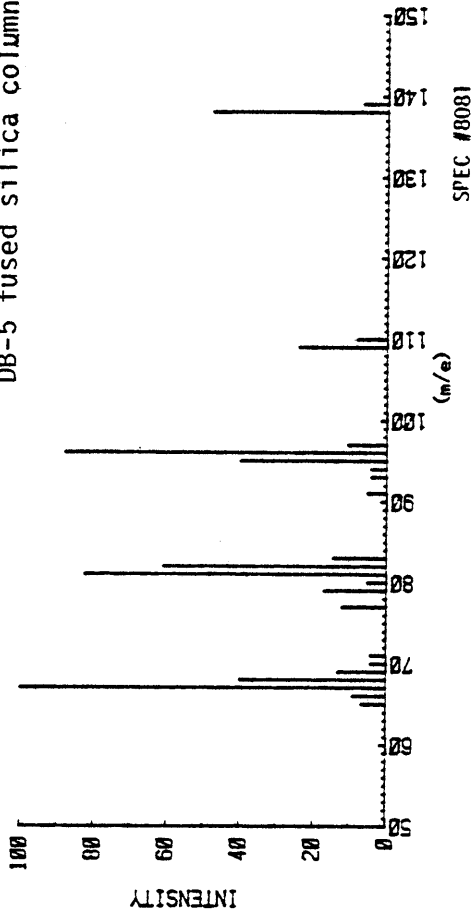
FIGURE 55

corresponded well to values listed in the Eight Peak Index of Mass Spectra tables<sup>25</sup>. Although relative m/e intensities did not generally match up perfectly, acceptable matches were possible taking into consideration the probable differences in instrument parameters such as source current, internal pressure and mode of ionization used to generate the reference data. It is quite common to see several mass spectral listings for the same compound, although the experimental conditions are not given. Two examples of standards that were run are given in Figure 56 with respective index entries. The mass spectra represent 25 ng of cis-decalin and 65 ng of o-ethyl-toluene. The listings to the right of each spectrum are the tabulated m/e intensities as referenced in Eight Peak Index of Mass Spectra<sup>25</sup>. The m-ethyltoluene listing (1-methyl-3-ethylbenzene) is included to illustrate the near identical spectral data obtainable for these isomers using GC-MS.

STANDARD MIXTURE

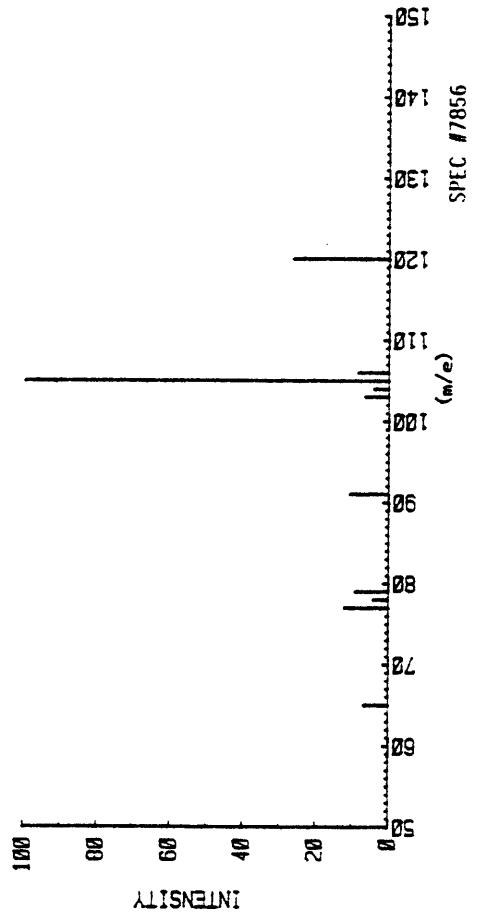
GC-MS data

DB-5 fused silica column



cis-decalin

%	100	91	87	86	60	56	48	47
m/e	67	41	81	96	82	95	39	138



o-ethyl toluene

%	100	29	9	9	9	8	6	6
m/e	105	120	77	91	106	79	39	103

m-ethyl toluene

%	100	29	9	9	9	8	6	6
m/e	105	120	91	77	106	79	39	51

FIGURE 56

## CONCLUSIONS

The research accomplished thus far has shown that given optimum conditions and state-of-the-art equipment high quality infrared data can be generated from the separation of complex mixtures. While the focus has been on characterizing and identifying relatively non-polar compounds in jet fuel products, progress is anticipated in the detection of trace intermediate and/or polar compounds by GC-FTIR. Since fused silica capillary efficiency can be fully utilized, maximum resolution can, again, be achieved with more polar heteroatom containing compounds.

When designing and assembling the hardware necessary for GC-FTIR, attention should be focused on several aspects. Proper matching of lightpipe and MCT detector can give sensitivity in the low nanogram range. Shorter lightpipes with less dead volume may limit band broadening and increase throughput, but the loss in sensitivity may be more critical. While the Model 36 has 420  $\mu\text{L}$  of dead volume and the 40 cm x 1 mm gold lightpipe has  $\sim 310 \mu\text{L}$ , band broadening appears to be minimal for both when a make-up gas of 4 to 5 mL/min is used. For use with gas chromatography, the MCT-B detector is generally not sensitive enough. No doubt with a longer, narrower lightpipe than the Model 36 (6 cm x 3 mm i.d.) throughput for an MCT-B would be unrealistically limited. A wider spectral range (4000-400  $\text{cm}^{-1}$ ) in the MCT-B case is however, certainly one advantage over the more narrow range MCT-A<sup>+</sup> (4000-700  $\text{cm}^{-1}$ ) when infrared information is available below 700  $\text{cm}^{-1}$ .

For less ambiguous and/or confusing infrared data, several FTIR scans per component peak should be attempted. The use of a rapid-scan mode which allows coadding of data in a time frame approaching fractions of a second is necessary when separating multicomponent mixtures on capillary columns. For best S/N, as many scans as possible should be coadded and ratioed against a background file. At a VEL of 50 (rapid-scan), 10 scans coadded and ratioed to 40 coadded background scans takes close to 1 second for real time "on-the-fly" data acquisitions. A one second per data file time frame is very useful for interpreting coeluting components although data storage space can be used up rapidly.

Interferences from atmospheric gases plague the FTIR experimental results either from masking essential IR regions or from creating an unstable, changing baseline throughout the experiment. Standing vibrations whether caused from the interferometer itself or externally can lead to erratic baselines and ruined data. The process of subtracting out such anomalies is many times a source of irreproducible errors and may change the actual spectral results. Base-line correcting of spectra can also lead to confusing "match results" when using the spectral search routines.

FTIR as a selective detector is very powerful in elucidating functionality, often by simply monitoring the real time on-the-fly CHEMIGRAM. User specified infrared windows can be used to selectively assemble chromatograms based solely on functional group infrared

absorbance. In comparing capillary GC-FTIR with GC-MS, one realizes the respective advantages of each as a separate analytical tool. Together, one method can fill the information void left by the other. For analysis of jet fuel type samples, molecular weight and splitting patterns from MS analysis can be an asset when extremely low quantities of unknown make FTIR detection difficult. In the analysis of aliphatic hydrocarbons, limited GC-FTIR spectral information can sometimes lead to ambiguous identifications. The mass information of GC-MS can be invaluable here also. When concerned with isomer analysis, whether for aliphatic or aromatic species, infrared absorbance differences are as varied as substitution patterns. Gas phase FTIR can readily distinguish most isomers whereas, mass spectral information is often ambiguous.

In reference to possible detection limits with the FTIR systems used, the 7199 system is at least 20 or more times as sensitive as the Nicolet 6000 (Model 36) system. The combination of a longer, narrower lightpipe and a detector giving better S/N account for this difference in performance. While the dual-beam characteristics of the 7199 do not add to this difference, use of a properly designed effluent transfer system from GC to lightpipe is very important. Use of an external lightpipe and detector bench is convenient to use and temperature control of the transfer system can be more adequately managed. For an optimized GC-FTIR system, tens of nanograms of a weakly absorbing aromatic component can be readily detected. Generally, the GC-MS

sensitivities are related to stability of the parent (molecular) ion. Aromatics can, therefore, be detected at much lower concentrations than FTIR because of the benzene ring stability. Roughly an order of magnitude can separate MS sensitivity from FTIR for these weak absorbers. For other compounds this discrepancy will close rapidly depending on the intensity and stability of molecular bending and stretching infrared absorbing vibrations.

## REFERENCES

1. Katlafsky, B. and M. W. Dietrich, "On-Line Infrared Identification of Gas Chromatographic Effluents", Appl. Spectros. 29, 24 (1975).
2. Golay, M. J. E. in Gas Chromatography (1957 Lansing Symposium) Coates, V. J., H. J. Noebels and I. S. Fagerson, Eds., Academic Press, New York, 1958.
3. Desty, D. H., Goldup, A., and Whyman, B. H. F., J. Inst. Petrol., 45:287 (1959).
4. Holasz and Horvath, Nature 197, 71 (1963).
5. Azarraga, L. V. Paper presented at the 5th Annual Symposium on Recent Advances in Analytical Chemistry of Pollutants, Jekyll Is., GA, May, 1975.
6. Azarraga, L. V. and C. A. Potter (EPA) An Integrated GC/FT-IR System for the Analysis of Environmental Pollutants, Journal HRC & CC Vol. 4, Feb. 1981, p. 60-68.
7. Shafer, K. H., A. Bjorseth, "Advancing the Chromatography of GC/FT-IR To WCOT Capillary Columns", J. HRC & CC, Vol. 3, 1980, p. 87.
8. Shafer, K. H. and M. Cooke, "WCOT Capillary Column GC/FTIR and GC-MS for Identifying Toxic Organic Pollutants" Applied Spectros. Vol. 35, No. 5, 1981, p. 469.
9. Azarraga, L. V., Paper presented at the Pittsburgh Conference on Analytical Chemistry and Applied Spectros, Cleveland, OH, 1976.
10. Dandevau, R. D. and E. H. Zerenner, "An Investigation of Glasses for Capillary Chromatography", J. HRC & CC, Vol. 1, June, 1979, p. 351-356.
11. Hembree, D. M., et al. "Matrix Isolation Fourier Transform Infrared Spectrometric Detection in the Open Tubular Column Gas Chromatography of Polycyclic Aromatic Hydrocarbons", Anal. Chem., 53, (1981) 1783-88.
12. Rossiter, V., "Capillary GC/FTIR", Am. Lab., June, 1982, p. 71.
13. Desty, D. H. and J. N. Haresnip, Anal. Chem. 32, 302 (1960).

14. Griffiths, Peter R., "The Present State-of-the-art of GC/FTIR and HPLC/FTIR" Paper given at 1982 Pittsburgh Conference, No. 240 March 8-13, 1982. (Dept. of Chem., Ohio University).
15. Garlock, Sue E., S. L. Smith, G. E. Adams, "High Resolution Capillary GC/FTIR" (IBM Instruments, Danburg, CT) Paper given at 1982 Pittsburgh Conference No. 031, March 8-13, 1982.
16. Shafer, Kenneth H. and Robert J. Jakobsen (Battelle, Columbus Laboratories) "Application of GC/FTIR-MS to Environmental Pollution Sample Analysis", Paper given at 1982 Pittsburgh Conference No. 029, March 8-13, 1982.
17. Azarraga, L. V., "Gold Coating of Glass Tubes for Gas Chromatography/Fourier Transform Infrared Spectroscopy 'Lightpipe' Gas Cells", Applied Spectroscopy, Vol. 34, No. 2, 1980, p. 224.
18. Dorn, Harry C., "<sup>1</sup>H and <sup>13</sup>C Fourier Transform NMR Characterization of Jet Fuels Derived From Alternate Energy Sources" (Final Progress Report for the period March 1978-Sept 1981) Virginia Polytechnic Institute and State University.
19. Lowry, Stephan R. and David H. Huppler, "Infrared Spectral Search System for Gas Chromatography/Fourier Transform Infrared Spectros." Anal. Chem., 53 (1981) p. 889-93.
20. Trestianu, S., "Possibilities and Limitations of Non-Vaporizing, Cold, On-Column Injection Technique in High Resolution Gas Chromatography" Paper given at 1982 Pittsburgh Conference, No. 633 March 8-13, 1982.
21. Hanna, D. A., G. Hangoc, B. A. Hohne, R. C. Wieboldt, "A GC/FTIR Compound Identification System", J. Chromatogr. Sci., 17, 423, (1979).
22. Grob K. and K. Grob, Jr. "On-Column Injection on to Glass Capillary Columns", J. Chromat., 151 (1978) 311-320.
23. Grob, K. and K. Grob, Jr. "Splitless Injection and the Solvent Effect", J. High Resolution Chrom. and Chromat. Commun., July, 1978, p. 57-64.
24. Hohne, B. A., G. Hangoc, et al. "An On-line Class Specific GC/FTIR Reconstruction from Interferometric Data", J. Chromatogr. Sci., Vol. 19, June 1981, p. 283-289.
25. Eight Peak Index of Mass Spectra, Vol. 1 and 2, 1970, United Kingdom, Atomic Energy Authority.

26. Gas Chromatography with Glass Capillary Columns, 2nd ed. Jennings, Walter, Academic Press, Inc., 1980.
27. Applications of Glass Capillary Gas Chromatography, Edited by Jennings, Walter G., Marcel Dekker, Inc., NY, 1981.
28. Silverstein, Bassler and Morrill, Spectrometric Identification of Organic Compounds, 4th ed. John Wiley and Sons, Inc., 1981, Chapter 3.

## VITA

John R. Cooper was born on the 3rd day of July, 1957 in District Heights, Maryland. He received his high school diploma from Suitland Senior High School in 1975 and a Bachelor of Science degree from Lynchburg College, Lynchburg, Virginia in 1979 with a major in chemistry. After working for a small analytical laboratory in Silver Spring, Maryland for 15 months, he came to Virginia Polytechnic Institute and State University to pursue an advanced degree in Chemistry. Completion of the requirements for the degree of Master of Science was accomplished in September, 1982.

*John R. Cooper*

OPTIMIZATION OF CAPILLARY GC/FTIR  
FOR  
COMPLEX SAMPLE ANALYSIS

by

John R. Cooper

(ABSTRACT)

Optimization of capillary gas chromatography-Fourier Transform Infrared (GC-FTIR) spectrometry has been accomplished by studying various columns, lightpipe designs, FTIR detectors and spectroscopic parameters. For adequate separation of complex samples the efficiency of WCOT (Wall Coated Open Tubular) fused silica capillary columns was found to be unmatched by packed columns or wide bore glass capillaries. A consequence of using more narrow bore columns, however, is lower sample capacity and less IR detectability. Two 6 cm lightpipes and a more narrow 40 cm lightpipe were compared with respect to both optical throughput and eluent band broadening. FTIR spectroscopic parameters such as mirror velocity and number of scans coadded were examined in order to achieve an optimum signal to noise ratio. The complexity of a particular sample has been shown to dictate certain spectroscopic parameters. The sensitivity differences of two liquid-nitrogen cooled FTIR detectors used in the GC-FTIR experiments have been determined with reference to using them with either a long or short lightpipe.

The capability of optimized capillary GC-FTIR has been demonstrated in the analysis of model compound mixtures and complex petroleum products including test aviation jet fuels. Major attention

was given to the detection and identification of aliphatic and aromatic components in the highly complex samples. Computerized library search routines have been used to tentatively identify eluting components by infrared spectral matching to quality vapor phase library file spectra. Gas chromatography-mass spectrometry (GC-MS) data are also included for the same jet fuel samples to directly compare extent of information provided and relative spectroscopic sensitivities.